

UNCLASSIFIED

# THE SEATED SOLDIER STUDY: POSTURE AND BODY SHAPE IN VEHICLE SEATS



Matthew P. Reed  
Sheila M. Ebert

Biosciences Group  
University of Michigan Transportation Research Institute

*October 2013*



UNCLASSIFIED

The Seated Soldier Study: Posture and Body Shape in Vehicle Seats

Final Report

UMTRI-2013-13

by

Matthew P. Reed

Sheila M. Ebert

University of Michigan Transportation Research Institute

October 2013

UNCLASSIFIED

## UNCLASSIFIED

<b>REPORT DOCUMENTATION PAGE</b>			<i>Form Approved</i> <i>OMB No. 0704-0188</i>		
Public reporting burden for this collection of information is estimated to average 1 hour per response, including the time for reviewing instructions, searching existing data sources, gathering and maintaining the data needed, and completing and reviewing this collection of information. Send comments regarding this burden estimate or any other aspect of this collection of information, including suggestions for reducing this burden to Department of Defense, Washington Headquarters Services, Directorate for Information Operations and Reports (0704-0188), 1215 Jefferson Davis Highway, Suite 1204, Arlington, VA 22202-4302. Respondents should be aware that notwithstanding any other provision of law, no person shall be subject to any penalty for failing to comply with a collection of information if it does not display a currently valid OMB control number. <b>PLEASE DO NOT RETURN YOUR FORM TO THE ABOVE ADDRESS.</b>					
<b>1. REPORT DATE (DD-MM-YYYY)</b> October 31, 2013		<b>2. REPORT TYPE</b> Final Report		<b>3. DATES COVERED (From - To)</b> September 2011- October 2013	
<b>4. TITLE AND SUBTITLE</b>  The Seated Soldier Study: Posture and Body Shape in Vehicle Seats			<b>5a. CONTRACT NUMBER</b> W56HZV-04-2-0001 P00038		
			<b>5b. GRANT NUMBER</b>		
			<b>5c. PROGRAM ELEMENT NUMBER</b>		
<b>6. AUTHOR(S)</b>  Reed, Matthew P. and Ebert, Sheila M.			<b>5d. PROJECT NUMBER</b>		
			<b>5e. TASK NUMBER</b>		
			<b>5f. WORK UNIT NUMBER</b>		
<b>7. PERFORMING ORGANIZATION NAME(S) AND ADDRESS(ES)</b>  University of Michigan Transportation Research Institute			<b>8. PERFORMING ORGANIZATION REPORT</b>  UMTRI-2013-13		
<b>9. SPONSORING / MONITORING AGENCY NAME(S) AND ADDRESS(ES)</b>  US Army Tank Automotive Research, Development, and Engineering Center  Warren, MI 48397-5000			<b>10. SPONSOR/MONITOR'S ACRONYM(S)</b>		
			<b>11. SPONSOR/MONITOR'S REPORT NUMBER(S)</b> Issued Upon Submission		
<b>12. DISTRIBUTION / AVAILABILITY STATEMENT</b>					
<b>13. SUPPLEMENTARY NOTES</b>					
<b>14. ABSTRACT</b> Designing vehicles for the safety and comfort of occupants requires detailed information on posture, position, and body shape. This report presents the methods and results of a study of soldiers as drivers and passengers in vehicle seats. A total of 257 male and 53 female soldiers were measured at three Army posts while minimally clad, wearing the Advanced Combat Uniform (ACU), with the addition of personal protective equipment (PPE), composed of the Improved Outer Tactical Vest (IOTV) and Advanced Combat Helmet (ACH), and with encumbrance (ENC) simulating the gear of either a rifleman or SAW-gunner. Standard anthropometric data, such as stature and body weight, were recorded. Participants were measured as either drivers or crew. Five driver workstation configurations (packages) were produced in a vehicle mockup by varying the steering wheel position relative to the pedals. The participants adjusted the seat to obtain a comfortable driving posture. The three-dimensional locations of body landmarks were measured using a FARO Arm coordinate digitizer. In the crew conditions, the experimenters varied the seat height and back angle and conditions included a simulated protective footrest. A whole-body laser scanner was used to record body shape at each garb level. A statistical analysis of the body landmark data was conducted to obtain models to predict soldier posture as a function of vehicle factors, such as seat height, and soldier attributes, such as stature, and garb level (ACU, PPE, or ENC). Driver posture was strongly affected by steering wheel position and crew posture by seat back angle. Adding PPE and ENC resulted in more-upright postures, but the effects on spine posture were small. Statistical models of both seated and standing body shape were developed from the scan data, including the effects of PPE and ENC on space claim. The effects of ENC on space claim were largely independent of body size. The results of this study have broad applicability for the design and assessment of military vehicles. Approved for public release.					
<b>15. SUBJECT TERMS</b> Anthropometry, Posture, Vehicle Occupants, Statistical Shape Analysis, Safety					
<b>16. SECURITY CLASSIFICATION OF:</b>			<b>17. LIMITATION OF ABSTRACT</b>	<b>18. NUMBER OF PAGES</b>	<b>19a. NAME OF RESPONSIBLE PERSON</b> M.P. Reed
<b>a. REPORT</b> TBD	<b>b. ABSTRACT</b> TBD	<b>c. THIS PAGE</b> TBD			<b>19b. TELEPHONE NUMBER (include area code)</b> (734)936-1111

Standard Form 298 (Rev. 8-98)  
Prescribed by ANSI Std. Z39.18

UNCLASSIFIED

## ACKNOWLEDGMENTS

This work was supported by the Automotive Research Center, a U.S. Army Center of Excellence for Modeling and Simulation of Ground Vehicles led by the University of Michigan.

This research would not have been possible without the contributions of a large number of people. We would like to thank the soldiers who participated in the study, providing valuable data that will improve safety and accommodation for the next generation of soldiers. The project was conducted in close collaboration with personnel from the U.S. Army Tank Automotive Research, Development and Engineering Center (TARDEC). Katrina Harris was the primary technical point of contact throughout the study and helped to guide the formulation and execution of the study plan. We are also grateful to the following TARDEC personnel who provided valuable assistance: Risa Scherer, Holly Howard, Harry Zywiol, Stacy Budzik, and Jennifer Ammori. Special thanks to the points of contact at the Army posts, whose efforts were critical in obtaining access to facilities: John MacArthur (Joint Base Lewis-McChord), Fred Corbin (Fort Hood), and Jim Parks (Fort Campbell). Valuable input on the study plan was received from Brian Corner, Steve Paquette, and Todd Garlie of NSRDEC, and from Joe McEntire of USAARL.

At UMTRI, important contributions were made by Jingwen Hu, Jonathan Rupp, Carl Miller, Nathaniel Madura, Brian Eby, Quentin Weir, Charlie Bradley, and Laura Malik. The Anthrotech team who gathered the data in the field were led by Bruce Bradtmiller and Belva Hodge. The outstanding data collection personnel were Mike Mucher, Mark Breza, Lisa Ann Piercy, Travis Hotaling, Tatiana Lurie, and Christina Smith. We also thank the student research assistants who worked tirelessly to process and extract data from the laser scans, including Alexis Baker, Christian Calyore, Olivia DeTroyer, Tiffany Fredrick, David Hayashi, Danielle Hedden, Huibin Hu, Jordan MacDonald, Mollie Pozolo, Rachel Palmer, Sarah Scholten, Ryan Warner, Mikhail Wise, and Lindsay Youngren.

Finally, we thank Anna Stefanopoulou, Director of the ARC, for her support of this project.

**CONTENTS**

ACKNOWLEDGMENTS ..... v

EXECUTIVE SUMMARY ..... 2

INTRODUCTION ..... 3

METHODS ..... 6

RESULTS ..... 42

APPLICATIONS ..... 77

DISCUSSION ..... 79

REFERENCES ..... 82

APPENDIX A. Consent Form. .... 85

APPENDIX B. Demographics Form ..... 87

APPENDIX C. Subject Interaction Scripts..... 89

APPENDIX D. Points Digitized on Scans..... 93

APPENDIX E. Techniques for Measuring and Representing Posture ..... 101

APPENDIX F. Standard Anthropometry: Summary of Measures ..... 113

## EXECUTIVE SUMMARY

This report presents the methods and results of a study of soldiers as drivers and passengers in vehicle seats. A total of 257 male and 53 female soldiers were measured at three Army posts while minimally clad, wearing the Advanced Combat Uniform (ACU), with the addition of personal protective equipment (PPE), composed of the Improved Outer Tactical Vest (IOTV) and Advanced Combat Helmet (ACH), and with encumbrance (ENC) simulating the gear of either a rifleman or SAW-gunner.

Standard anthropometric data, such as stature and body weight, were recorded. Participants were measured as either drivers or crew. Five driver workstation configurations (packages) were produced in a vehicle mockup by varying the steering wheel position relative to the pedals. The participants adjusted the seat to obtain a comfortable driving posture. The three-dimensional locations of body landmarks were measured using a FARO Arm coordinate digitizer. In the crew conditions, the experimenters varied the seat height and back angle, and conditions included a simulated protective footrest. A whole-body laser scanner was used to record body shape at each garb level in both seated and standing postures.

A statistical analysis of the body landmark data was conducted to obtain models to predict the posture of any soldier as a function of vehicle factors, such as seat height, soldier attributes, such as stature, and garb level (ACU, PPE, or ENC). Driver posture was strongly affected by steering wheel position and crew posture by seat back angle. Adding PPE and ENC resulted in more-upright postures, but the effects on spine posture were small. Statistical models of both seated and standing body shape were developed from the scan data, including the effects of PPE and ENC on space claim. The two ENC kits added essentially constant offsets to dimensions measured at the ACU level, indicating that the effects of new kits on space claim can be assessed using measurements on relatively few subjects. The results of this study have broad applicability for the design and assessment of military vehicles. Near-term uses include the layout of driver workstations, development of safer and more accommodating squad seating, and the development of new physical and computational surrogates to represent soldiers for ergonomics and safety assessments.

## INTRODUCTION

The design of seats and interiors for a wide variety of vehicles has benefited from detailed data on the sizes, shapes, and postures of the intended occupants. Beginning in the 1950s, data on overall body dimensions, such as stature (erect standing height) and body segment lengths were used to create design tools (Dempster, 1955). Beginning in the early 1960s, the Society of Automotive Engineers (now SAE International) standardized a two-dimensional template and a three-dimensional, weighted manikin (known as the H-point machine) for measurement and layout of seats and interiors. These tools in SAE Recommended Practice J826 have been only slightly modified in the intervening years and are still used globally as a central component of automotive design for occupant accommodation and comfort.

The mid-1960s saw the introduction of the first statistical, population-based model of occupant accommodation, the *eyellipse*. The *eyellipse* describes the distribution of driver eye locations in a vehicle as an ellipse (or ellipsoid in three dimensions) based on an underlying multivariate normal approximation (Meldrum 1965). The *eyellipse* is notable because it encapsulates three important influences on occupant posture: body size (the eyes of taller people tend to be higher and more rearward in the vehicle), vehicle layout (package variables such as seat height), and driver posture preference unrelated to body size. Since the 1960s, *population accommodation models* with these characteristics have been introduced in SAE Recommended Practices for driver-selected seat position, head location, maximum reach, truck driver shin/knee clearance, and truck driver abdomen clearance (SAE International 2012).

With the widespread introduction of computer-aided design (CAD) software in the 1980s and 90s, digital human figure models (DHMs) began to be used for ergonomic assessments and design of vehicle interiors and seats, particularly for driver workstation layout (Chaffin 2001). DHM software represents humans by an anthropomorphic, three-dimensional figure that can be adjusted via manual or automated means to replicate a wide range of human postures. Early models used simple ellipsoids to represent body segments, but more recent software versions include smooth-skinned figures for both men and women with a range of appearance options. DHM software packages widely used in industry include RAMSIS and Jack. Many CAD and integrated engineering analysis packages now include human figures, such as CATIA and Pro/Engineer.

The development of computer manikins for vehicle interior design and assessment exposed two important knowledge gaps. First, human body shape varies widely, and representing the scope of body shape variability across the range of feasible postures has been challenging. Most widely used manikins rely on relatively simple anthropometric scaling, in part because methods for predicting and representing three-dimensional (3D) body shape on manikins have not been widely available. Second, use of a manikin requires the generation or specification of a particular static posture or motion appropriate to the task to be analyzed. For example, accurate prediction of driving posture for a particular manikin is needed to ensure that the resulting analysis of clearance, vision, or reach is meaningfully accurate.

Laser scanning technology has made available large datasets on human body shape. The Civilian American and European Surface Anthropometric Resource (CAESAR) study was the first large-scale dataset that has been widely available (Robinette et al. 2002), but many other

datasets are now available based on national samples, e.g., SizeGermany, SizeUK, SizeChina, etc. Three important barriers have limited the application of these data to commercial manikins. First, many of the datasets have been constrained by restrictive licenses that have limited commercial application. Second, although the technology to generate figure models based on single scans has been available for at least a decade, statistical models allowing a wide range of body sizes to be generated have not been available. The first such model was presented in 2003 (Allen et al. 2003), but widespread applications have lagged due both to technical hurdles and licensing issues. Third, the large anthropometric surveys, such as CAESAR, have typically gathered data in only a few postures, none of which are directly related to vehicle interior design. Some studies have gathered data only on standing postures, while others have included one or a few unsupported seated postures. Applying such data or statistical models based on such data to vehicle environments requires extrapolation to predict body shape change in seating situations with back support. Moreover, although many previous studies have been motivated by apparel design issues (e.g., SizeUSA), few have examined the effects of apparel on posture and body shape.

Driving posture prediction has been part of human modeling software for at least 25 years, reflecting the early DHM adoption in vehicle design. RAMSIS was introduced with a data-based model for predicting driving posture using an optimization algorithm (Seidl 1997). The occupant packaging toolkit in the Jack software uses posture prediction algorithms developed at the University of Michigan, as does the vehicle occupant accommodation module in CATIA. These algorithms are based on measurements of hundreds of drivers with widely varying body size in a wide range of vehicle packages, ranging from low-seat-height sports cars to the largest commercial trucks. Both the RAMSIS and University of Michigan approaches use different models for different vehicle classes, such as passenger cars or heavy trucks, reflecting the fact that the dimensions, constraints, and user populations are different.

In some ways, the tools and technology available for automotive development have moved ahead of those used for military vehicle development. In the past two decades, new seating accommodation (Flannagan et al. 1998) and eyellipse (Manary et al. 1998, Reed 2011) models were developed at UMTRI and implemented in SAE Recommended Practices. These new models for driver accommodation modeling (such as SAE J941 and J4002) have not been widely used for military vehicles, in part because the military occupant population differs meaningfully from the civilian populations for which the SAE models are intended. In the past decade, new methods for optimizing passenger car and truck layout for driver accommodation have been developed (Parkinson et al. 2005; Parkinson and Reed 2006; Parkinson et al. 2007) but soldier-specific data are needed to apply these methods to Army vehicles.

Occupant package layout in military vehicles has been primarily based on the simple dimensional guidelines presented in MILSTD-1472, which recommend a set of linear clearance dimensions. These guidelines are difficult to interpret or to apply in an environment with adjustable seats. Importantly, the currently available guidelines and tools do not take into account the effects of body armor or other body-borne gear on occupant posture, position, or preference. That is, no current tools provide quantitative information on the distributions of postures or clearance requirements that can be expected for diverse population of occupants wearing battle gear.



## UNCLASSIFIED

Based on this assessment of the current state of the art, the present study was developed with the following objectives:

1. Gather detailed data on the postures of soldiers with a wide range of body sizes sitting in military vehicle seats as drivers and passengers with and without protective equipment and with and without protective footrests.
2. Gather detailed data on the position and space requirements for body armor and other gear in both standing and seated postures.
3. Develop data-based tools to represent the postures, positions, and body size (space claim) for soldiers as drivers and passengers in tactical vehicles as a function of occupant and vehicle characteristics.
4. Provide quantitative data on the locations of protective equipment relative to the soldier and vehicle seat for use in human modeling and blast event simulation.

To accomplish these objectives, a detailed study plan was developed with coordination among U-M, the Army, and Anthrotech, Inc., a company specializing in anthropometric data collection and analysis. Adjustable mockups of driver and crew (squad) seating environments were created. A team of six staff trained in anthropometry methods traveled to three Army bases to recruit and measure soldiers. Body landmark locations were measured as the soldiers sat in the two mockups, and three-dimensional body shape was captured in both standing and seated postures using a whole-body laser scanner capable of high-resolution surface measurement. Body shape data were obtained with the soldiers minimally clad, and both seated posture and body shape data were obtained at three levels of garb: combat uniform, uniform plus body armor vest and helmet, and with the addition of a body borne equipment ensemble including simulated ammunition and a hydration pack. The data were analyzed to develop a new suite of tools for the human-centered design and assessment of military vehicles.

UNCLASSIFIED

## METHODS

### Human Research Approval

The study protocol was approved by the University of Michigan Institutional Review Board for Health Behavior and Health Sciences (IRB # HUM00055446) and by the USAMRMC Office of Research Protections, Human Research Protection Office (HRPO # Log Number A-17186). Written informed consent was obtained using the language in Appendix A.

### Data Collection Sites

The Army provided access to facilities at three Army bases listed in Table 1. Figure 1 shows the general data collection activities and Figures 2-4 show the facilities at each base. The equipment, which was developed and fitted at UMTRI, was shipped to each base via truck and set up by the Anthrotech staff with assistance from UMTRI. Data collection was conducted January through April 2012. Soldiers were invited to participate by local personnel at each base. By design, the subject pool was not recruited to match a particular profile. Rather, this convenience sample was intended to provide a broad range of human variability that is not necessarily representative of any particular part of the Army.

Table 1  
Soldiers Measured at Each Base

Base	Location	Women	Men
Joint Base Lewis McChord	Washington	16	38
Fort Hood	Texas	6	67
Fort Campbell	Kentucky	31	152
Totals		53	257
Total Participants			310

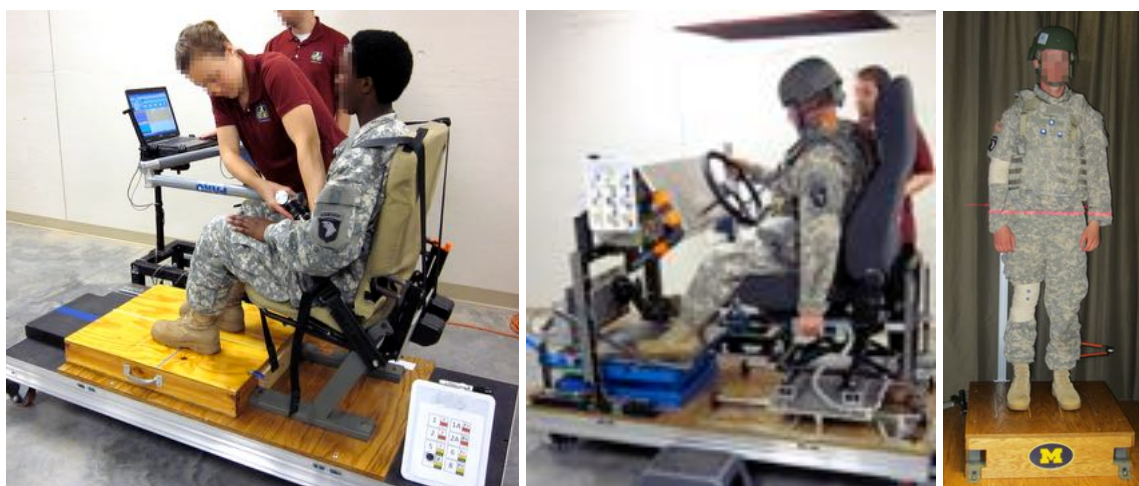


Figure 1. An investigator recording landmark locations on soldier in crew mockup (left); soldier adjusting the seat position in the driver mockup (center), and soldier being scanned.



Figure 2. Joint Base Lewis McChord building and study area.



Figure 3. Fort Hood building and study area.

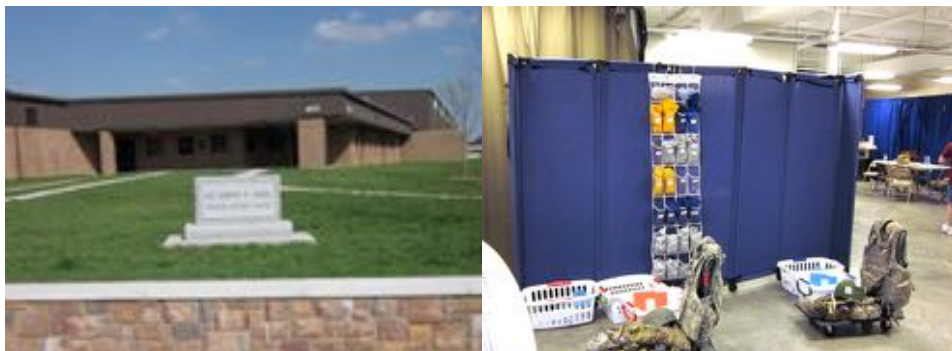


Figure 4. Fort Campbell building and study area.

### Garb Levels and Fitting

Figure 5 shows the four garb levels used in the study. Scanning was conducted with the participants minimally clad, wearing close-fitting shorts and, for women, a sports bra. At the ACU level, soldiers wore their own advanced combat uniform consisting of a jacket, trousers,

moisture wicking shirt and brown combat boots. All items were removed from the pockets, extra padding removed from the knees, and any cap or helmet removed. At the PPE (personal protective equipment) level, soldiers wore an Improved Outer Tactical Vest (IOTV) with Enhanced Small Arms Protective Insert (ESAPI) plates, Enhanced Side Ballistic Inserts (ESBI), and an Advanced Combat Helmet (ACH) over their ACU ensemble. Five sizes of IOTV were available at the study site. Examples are shown in Figure 6. The soldiers were given their self-reported sizes of helmet and IOTV with front, back and side plates. The investigator helped the soldier don the PPE and checked the fit. The fit was considered acceptable if (1) the elastic waistband of the IOTV was snug with the Velcro closure fully overlapped and (2) the bottom of the IOTV was located below the navel and above the belt. The soldiers wore the smallest size helmet in which the soldier's head was in contact with the padding on the inside of the top of the helmet.

The third level of gear was referred to as encumbered (ENC), which consisted of ACU, PPE, a hydration pack, and a Tactical Assault Panel (TAP). Figure 5 shows a soldier in the three levels of gear, including both versions of ENC (rifleman and SAW gunner).



Figure 5. Three levels of military garb worn during measurement: ACU, PPE and two types of ENC (left to right).



Figure 6. IOTV used in the study (sizes small to 2X large) and helmet (medium to extra-large) worn by soldiers as PPE level of gear.

The TAP is an adaptable platform intended to replace the Fighting Load Carrier (FLC) vest to allow for quick-release of equipment in emergency situations. It is designed to carry a variety of basic Modular Lightweight Load-Carrying Equipment (MOLLE) fighting load pouches. The TAP is attached to the front panel of the IOTV with clips at the shoulders and sides. A CamelBak-style hydration system (Figure 7), filled with 2.5 L of water, was attached to the back of the IOTV.

Two infantry TAP configurations were used. The SAW (Squad Automatic Weapon) gunner TAP shown in Figure 8 represents the heavy ammunition load of a soldier who carries the light machine gun. The rifleman's TAP shown in Figure 9 represents the load of a rifleman or driver of a transport vehicle. This ensemble includes a communications radio. Table 2 and 3 list the equipment or equipment replicas carried in the TAPs.



Figure 7. CamelBak hydration system filled with 2.5 L of water worn by all subjects as part of the ENC level of gear.





Figure 8. SAW gunner TAP worn by subjects as ENC level of gear in crew mockup

Table 2  
Inventory of Equipment in SAW gunner ENC

Item	Count
200 Round SAW Drum	2
100 Round SAW Drum	2
Replica fragmentation grenade (on IOTV)	1
Canteen case with weight of night vision goggles added	1
Improved first aid kit (IFAK)	1
TAP with pouches	1



Figure 9. Rifleman TAP worn by subjects as ENC level of gear in driver mock-up.

Table 3  
Inventory of Equipment in Rifleman ENC

Item	Count
Replica M16 magazine clips	8
Replica Multiband Inter/Intra Team Radio (MBITR)	1
Replica fragmentation grenade	2
Multipliers	1
Canteen case with weight of night vision goggles added	1
Improved first aid kit (IFAK)	1
TAP with pouches	1

## Standard Anthropometry

Anthropometric data were gathered from each soldier to characterize overall body size and shape following the procedures in Hotzman et al. (2009). Standard anthropometric measures were obtained using manual measurements. The measurements included the core subset of dimensions gathered in Anthropometry Survey (ANSUR) II, a large-scale data Army anthropometry study. Table 4 lists the dimensions, which are described in detail in Appendix F. All measurements were obtained minimally clad, except that stature was measured with and without boots to characterize heel height. The form in Appendix B was used to gather subject-reported demographic data, including race/ethnicity, rank, and military occupational specialty (MOS).

Table 4  
List of Standard Anthropometric Variables

	Measurement	Posture	ANSUR II
1	Weight		6.4.92
2	Tragion to Top of Head	Sitting	6.4.83
3	Head Length	Sitting	6.4.48
4	Head Breadth	Sitting	6.4.46
5	Erect Sitting Height	Sitting	6.4.72
6	Eye Height	Sitting	6.4.35
7	Acromial Height	Sitting	6.4.2 (standing)
8	Knee Height	Sitting	6.4.58
9	Popliteal Height	Sitting	6.4.67
10	Acromial Breadth	Sitting	6.4.9
11	Bideltoid Breadth	Sitting	6.4.12
12	Maximum Hip Breadth	Sitting	6.4.52
13	Buttock-Knee Length	Sitting	6.4.20
14	Buttock-Popliteal Length	Sitting	6.4.21
15	Acromion - Radiale Length	Sitting	6.4.3 (standing)
16	Radiale - Stylium Length	Sitting	6.4.68 (standing)
17	Forearm - Hand Length	Sitting	6.4.41 (standing)
18	Forearm - Forearm Breadth	Sitting	6.4.40 (standing)
19	Stature Without Boots	Standing	6.4.76
20	Stature With Boots	Standing	
21	Cervicale Height	Standing	6.4.23
22	Chest Breadth (max anterior pt)	Standing	6.4.24
23	Chest Circumference (max anterior pt)	Standing	6.4.25
24	Chest Depth (flat blades, max anterior pt)*	Standing	6.4.26
25	Chest Depth (curved blades, on spine, max anterior pt)*	Standing	
26	Height of Chest (max anterior pt)	Standing	6.4.27
27	Waist Circumference at Omphalion	Standing	6.4.88
28	Waist Height at Omphalion	Standing	6.4.91
29	Bispinous Breadth	Standing	
30	Bicristal Breadth	Standing	6.4.11
31	Hip Circumference at Buttocks	Standing	6.4.17
32	Height of Hip Circumference	Standing	6.4.19
33	Hand Length	Sitting	6.4.45
34	Hand Breadth	Sitting	6.4.43
35	Foot Breadth, Horizontal	Standing	6.4.36
36	Foot Length	Standing	6.4.37



## Driver Mockup

Figure 10 shows the driver mockup. A commercial truck seat was mounted to a motorized platform that allowed a large range of vertical and horizontal travel. The steering wheel was fixed in place for all trials. Nine package conditions were produced by varying the height and fore-aft position of the pedal assembly, which was mounted on a hydraulic lift table. The pedal assembly pivoted at the accelerator heel point, so that the pedal plane angle could be varied with seat height according to SAE J1516.

Table 5 lists the driver mockup conditions. The conditions were selected to bridge the gap between typical light truck packages (SAE H30 seat height values of 350 to 400 mm) and commercial trucks (SAE H30 values of 450 to 550 mm). These conditions will allow the results to be merged with previous UMTRI studies of driving posture in passenger cars, light trucks, and commercial trucks to form an integrated model.

Figure 11 shows a soldier in each of the driver conditions after adjusting the seat. Figure 12 shows a soldier in each of the three levels of gear in driver condition D5 after adjusting the seat. Table 6 lists the mockup, body, and gear landmarks measured in each condition.

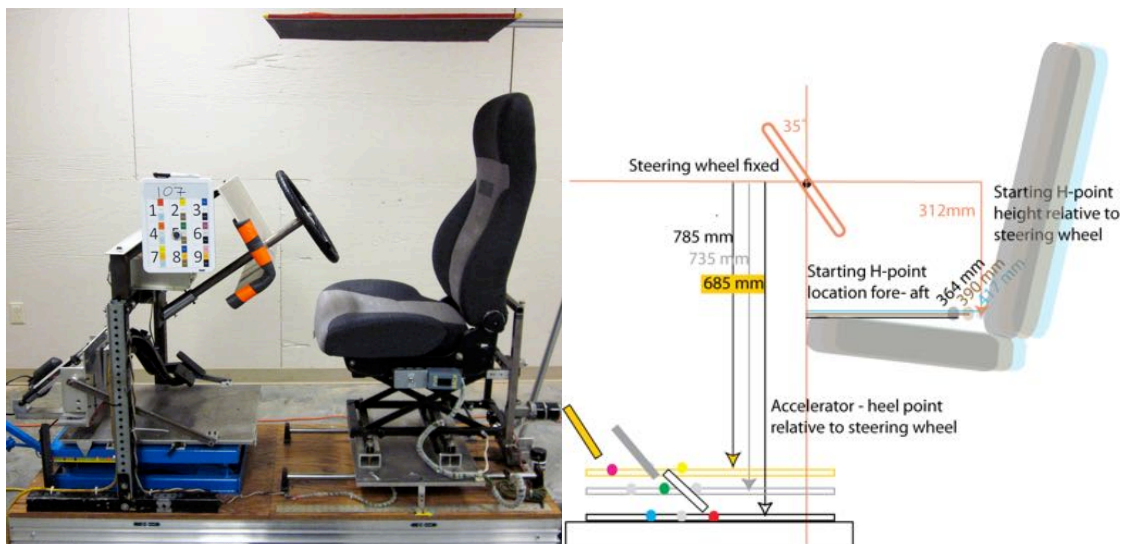


Figure 10. Driver mockup (left) set to condition D5 and illustration of driver conditions (right).

UNCLASSIFIED

Table 5  
Condition Matrix for Driver Mockup

Package	Accelerator Heel Point Relative to Steering Wheel		Accelerator Pedal Angle  Degrees from horizontal	Initial Seat H-point Relative to Steering Wheel  Fore-Aft (mm)	Seat Height SAE H30 (mm)
	SAE L11, Fore-Aft (mm)	SAE H17, Vertical (mm)			
1	225	785	47	417	473
<i>2†</i>	300	785	47	390	473
3	375	785	47	364	473
4	262.5	735	40	417	423
5*	337.5	735	40	390	423
6	412.5	735	40	364	423
7	300	685	33	417	373
8	375	685	33	390	373
9	450	685	33	364	373

\*Repeated with PPE and ENC

† Conditions in italics were dropped after the first few sessions due to time constraints.

UNCLASSIFIED

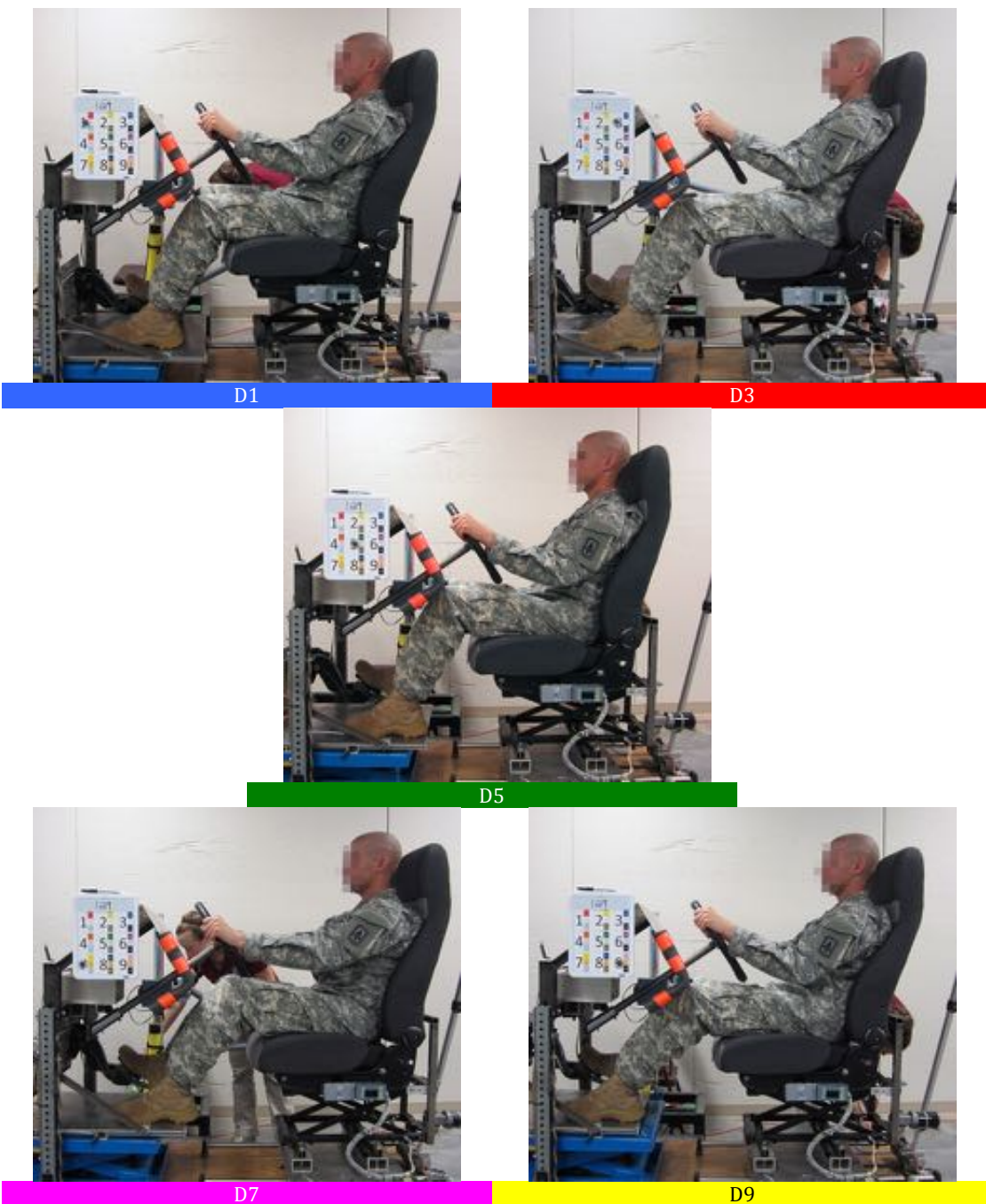


Figure 11. Soldier in ACU being measured in each of the driver mockup conditions.



D5 - ACU



D5 - PPE



D5 - ENC

Figure 12. Soldier in the three levels of gear being measured in the D5 driver mockup condition after he selected the seat fore-aft and vertical positions and the seat back recline angle.

Table 6  
Landmarks and Reference Points Recorded in Driver Mockup

Cart (3)	Suprasternale*
Platform (3)	Substernale*
Pedal	ASIS, Right and Left*
Floor	Suprapatella, Right and Left
Seat Cushion (2)	Infrapatella, Right
Seat Back (2)	Knee, Right (Lateral Femoral Condyle)
C7 (Cervicale)	Toe Right (Bottom edge of sole, longest shoe pt)
Back Of Head/Helmet Max Rearward	Ball of Foot Lateral Right
Top Of Head/Helmet Max Height	Ankle, Right (Lateral Malleolus)
Tragion, Right (Near side)	Heel, Right (Bottom edge of sole at midline)
Ectoorbitale, Right	Helmet (3)
Infraorbitale at Pupil Center, Right	IOTV (3)
Glabella	TAPS (3)
Wrist, Right (Ulnar Styloid Process, Lateral)	CamelBak (3)
Elbow, Right (Lateral Humeral Epicondyle)	
Acromion, Right (Anterior)	

\* Not recorded in PPE or ENC.

## Crew Mockup

Figure 13 shows the crew position mockup. A Mastercraft troop seat was chosen from among those available because it was minimally featured and could readily be modified to suit the project needs. The pan length was 380 mm and the pan and back angles were modified to be adjustable. A five-point harness system with automatic retractors for the shoulder belts and quick-release buckle (supplied by IMMI) was also added to the seat. The seat height (SAE H30) was decreased by adding a foot platform on top of the floor of the mockup. A foot protection system was simulated by the addition of a 60-mm-high block underneath the subject's feet. The participants did not adjust the seat, which was set by the investigator to each condition shown in Table 7. In each condition, the posture was recorded by digitizing with the CMM the points listed Table 8. Figure 14 shows a soldier in each of the conditions listed in Table 7. Figure 15 shows a soldier in the three levels of gear in the crew seat.

The soldier stepped onto the mockup platform, sat down, donned the five-point harness, and tightened the lower portion of the harness. Conditions were blocked on seat back angle and cushion angle, and the order of the blocks was randomized. Within each block, the two floor heights were presented in random order, with the foot-protection condition always following the no-foot-protection condition. The soldiers' feet were positioned on floor or platform with their toes up to a line 575 mm in front of the seat H-point or on the foot protection block with their heels 425 mm in front of H-point. If arriving at the crew station in ACU, the soldier completed all conditions and then repeated a subset of the conditions in the PPE and ENC levels of gear. If arriving at the crew station in ENC, the soldier was measured in only the subset of conditions in all levels of gear.



Figure 13. Crew mockup with adjustable cushion and back angles.

UNCLASSIFIED

Table 7  
Condition Matrix for Soldiers in Crew Mockup

Block†	Conditions†	Back Angle	Cushion Angle	H30: Seat Height (mm)	Foot ** Protection H30 -60 mm	Foot Position Forward of Seat H-point	
						Toe	Heel
1	<b>1*</b>	0°	0°	450 (floor)	No	575	
	<b>1A*</b>	0°	0°	450 (floor)	Yes (Block)		425
	2	0°	0°	350 (platform)	No	575	
	2A	0°	0°	350 (platform)	Yes (Block)		425
3	5	10°	5°	450 (floor)	No	575	
	6	10°	5°	450 (floor)	Yes (Block)		425
	7	10°	5°	350 (platform)	No	575	
	8	10°	5°	350 (platform)	Yes (Block)		425

†Block 2 and associated conditions (3, 4) were deleted after pilot measurements due to time constraints.

\*Repeated with PPE and ENC

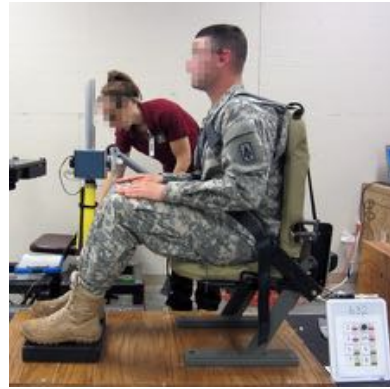
\*\*Foot protection 380 x 280 x 60 mm

UNCLASSIFIED





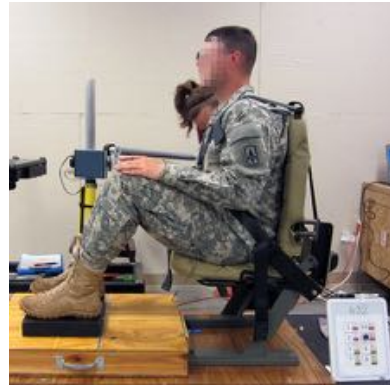
C1



C1A



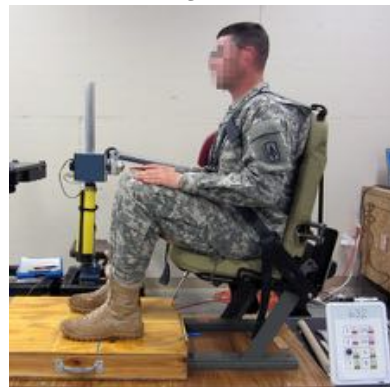
C2



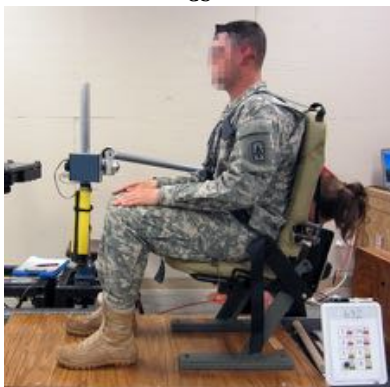
C2A



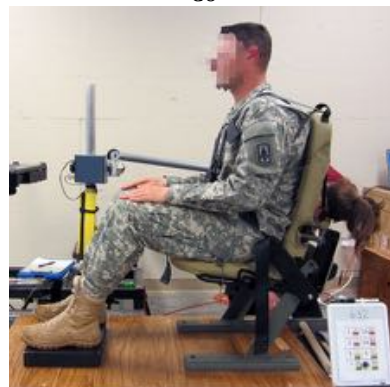
C5



C6



C7



C8

Figure 14. Soldier seat in each of the crew mockup conditions in which the back angle, cushion angle and seat height was varied.



C1 - ACU



C1A - ACU



C1 - PPE



C1A - PPE



C1 - ENC




C1A - ENC

Figure 15. Soldier in three levels of gear in crew mockup conditions C1 and C1A.



Table 8  
Landmarks Recorded in Crew Mockup

	Foot Support Level
	Seat Cushion (2)
	Seat Back (2)
	C7 (Cervicale)
	Back Of Head/Helmet Max Rearward
	Top Of Head/Helmet Max Height
	Tragion, Right
	Ectoorbitale, Right
	Infraorbitale at Pupil Center, Right
	Glabella
	Wrist, Right (Ulnar Styloid Process, Lateral)
	Elbow, Right (Lateral Humeral Epicondyle)
	Acromion, Right (Anterior)
	Harness on Right Clavicle (2)
	Harness at Lateral Position of Right ASIS (2)
	Buckle Center
	Suprasternale*
	Substernale*
	ASIS, Right*
	ASIS, Left*
	Suprapatella, Right
Infrapatella, Right	
Knee, Right (Lateral Femoral Epicondyle)	
Toe, Right (Bottom edge of sole, longest shoe pt)	
Ball of Foot Lateral, Right	
Ankle, Right (Lateral Malleolus)	
Heel, Right (Bottom edge of sole at midline)	
Helmet (3)	
IOTV (3)	
Taps (3)	
CamelBak (3)	

\* Not recorded in PPE or ENC levels of gear

### Whole-Body Scanning

Body shapes were recorded using a Vitronic Vitus XXL full-body laser scanner and AnthroScan software by Human Solutions. The Vitus XXL records hundreds of thousands of data points on the surface of the body in about 12 seconds. Red lasers in four towers arranged in a square create a line on the subject as they move synchronously from top to bottom. Two cameras on each of the four scanning heads pick up the contour projected on the subject and translate the images into accurate three-dimensional data. Figure 16 shows the columns of the scanner being assembled and the scanner draped with curtains to control light and provide privacy.



Figure 16. Investigators setting up the four columns of the Human Solutions Vitus SSL scanner (left), and the scanner set up at Fort Hood (right).

### Scanning Materials

Custom fixtures were created to enable rapid and accurate positioning of the soldiers for scanning. Figure 17 shows the platforms, repositionable and removable seat, and handles constructed to facilitate the positioning of the soldiers in standing and seated postures. The soldiers were scanned in the four levels of clothing and gear shown in Figure 18.

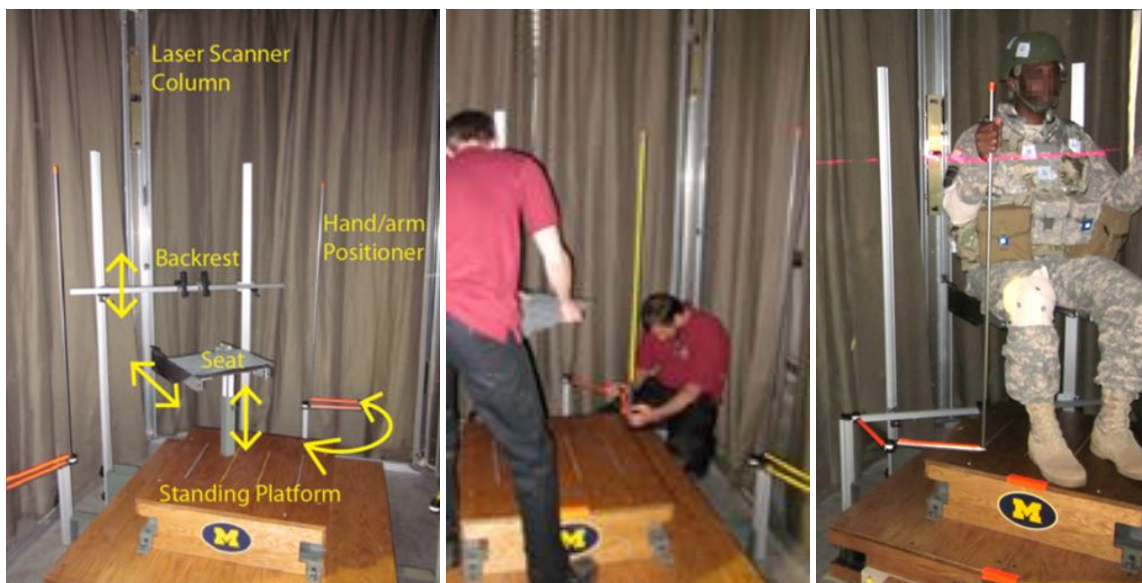


Figure 17. Reconfigurable platform, hand positioners, and seat built for positioning soldiers inside the scanner.

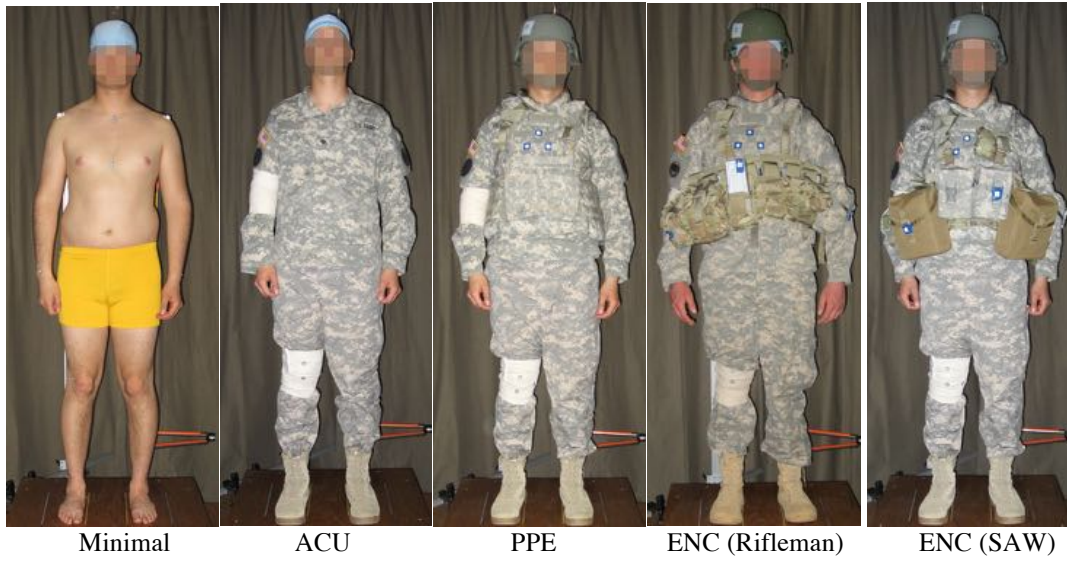


Figure 18. Four levels of gear worn during scanning (from left to right): scanwear (minimally clad), ACU, PPE, and ENC (SAW gunner and Rifleman).

## Marking Landmarks

The scanner records gray scale images that can be projected onto the 3D surface scan as shown in Figure 19. Landmarks on the soldiers were tracked via skin targets stamped on the skin using the process shown in Figure 20. The complete list of skin markers is shown in Figure 21 and Table 9. Small hemispheres were taped to the shoulders of the soldiers to track the location of the acromion landmark (Figure 22). When the participants were dressed in ACU, many of the skin stamps were not visible. To improve measurement of the skeleton location, the right elbow and knee of the soldiers were wrapped with elastic bandages to compress the fabric of the ACU, then in each posture scanned the investigators palpated for the landmarks in Table 10 and attached targets to the bandage as shown in Figure 23. Tape targets were used to track the PPE and ENC.

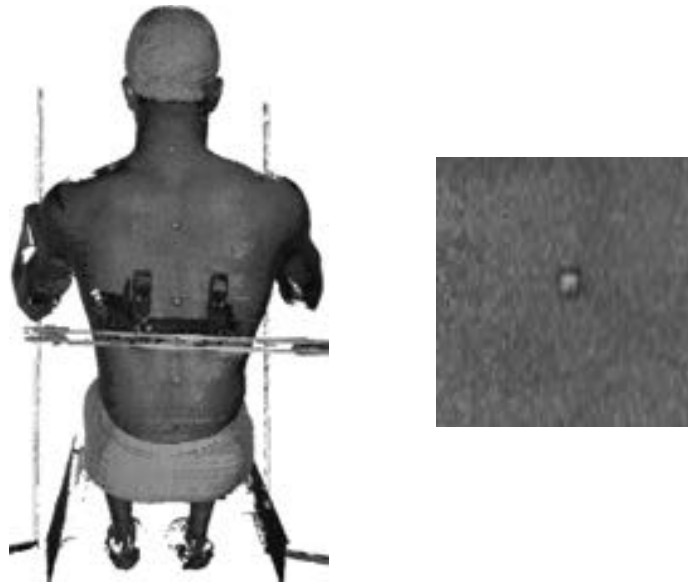


Figure 19. Gray-scale image of scan (left) and close-up of stamp used to track landmarks (right).

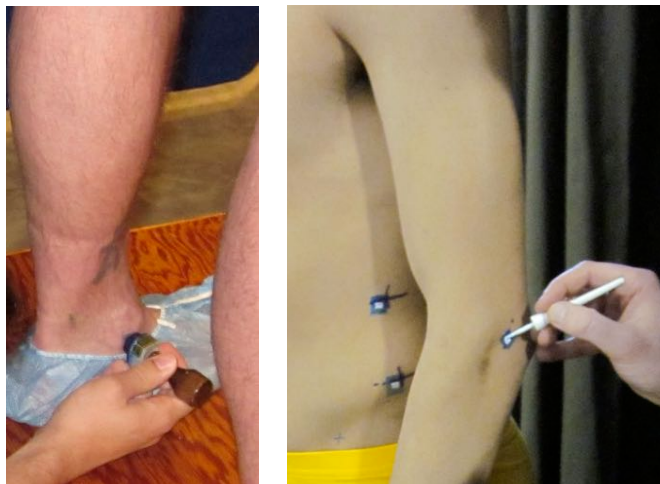


Figure 20. Stamp and paint marking system.

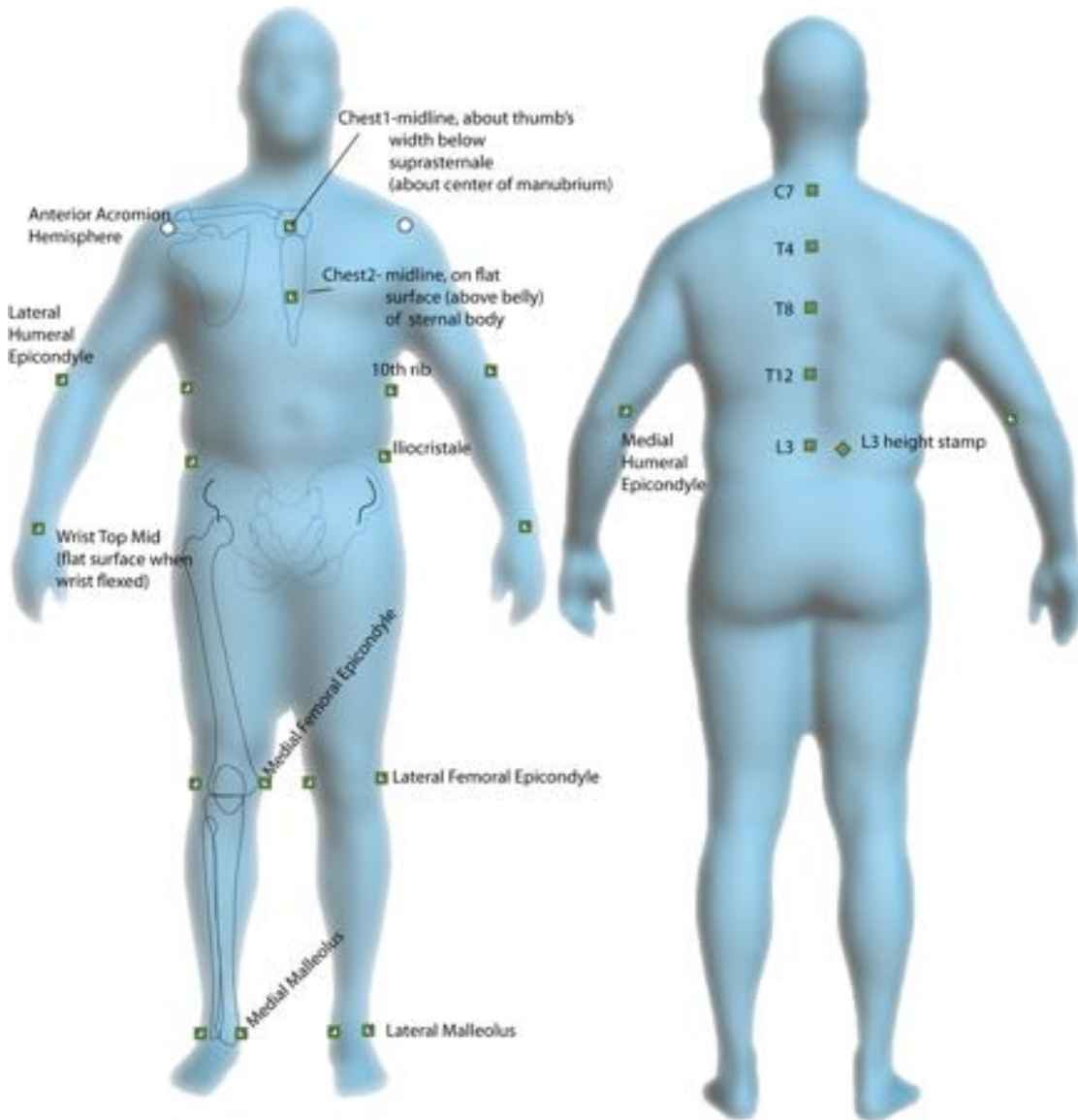


Figure 21. Position of stamped landmarks.



UNCLASSIFIED

Table 9  
Landmarks Stamped on Skin Surface

<b>Stamp Name</b>	<b>Stamp Position</b>	<b>Posture When Stamped</b>	<b>Corner to digitize with FARO Arm</b>
Chest 1	Body midline, about one thumb's width down from suprasternal, (or about mid-manubrium)	Sitting	Superior, Soldier's Left
Chest 2	Body midline, first flat, boney surface on sternum body above belly	Sitting	Superior, Soldier's Left
Acromion	Hemisphere centered on most anterior point of acromion	Arms hanging at sides	Center of hemisphere
Elbow, Lateral	Humeral epicondyle, lateral	Elbow 90° Flexion	Proximal, extensor surface
Elbow, Medial	Humeral epicondyle, medial	Elbow 90° Flexion	Proximal, extensor surface
Wrist Top	On the back of the wrist slightly proximal to the cross section plane of the ulnar styloid. Skin should not move much when wrist flexes and extends.	Any	Proximal, nearest ulnar styloid
Knee, Lateral	Femoral epicondyle, lateral	Sitting	Proximal, flexor surface
Knee, Medial	Femoral epicondyle, medial	Sitting	Proximal, flexor surface
Ankle, Lateral	Malleolous Lateral	Any	Proximal, plantar flexion surface side
Ankle, Medial	Malleolous Medial	Any	Proximal, plantar flexion surface side
Hip Top	Iliocristale	Standing	Superior-Posterior
Rib 10, Lateral	Tenth rib, lateral	Standing	Superior-Posterior
C7	Cervicale	Sitting Erect	Center
T4	Spinous process of 4 <sup>th</sup> thoracic vertebra	Sitting Erect	Center
T8	Spinous process of 8 <sup>th</sup> thoracic vertebra	Sitting Erect	Center
T12	Spinous process of 12 <sup>th</sup> thoracic vertebra	Sitting Erect	Center
L3	Spinous process of 3 <sup>rd</sup> lumbar vertebra	Sitting Erect	Center
L3Height	At the same height as the L3 stamp, about 2 inches to the soldier's left.	Sitting Erect	Not Digitized

UNCLASSIFIED

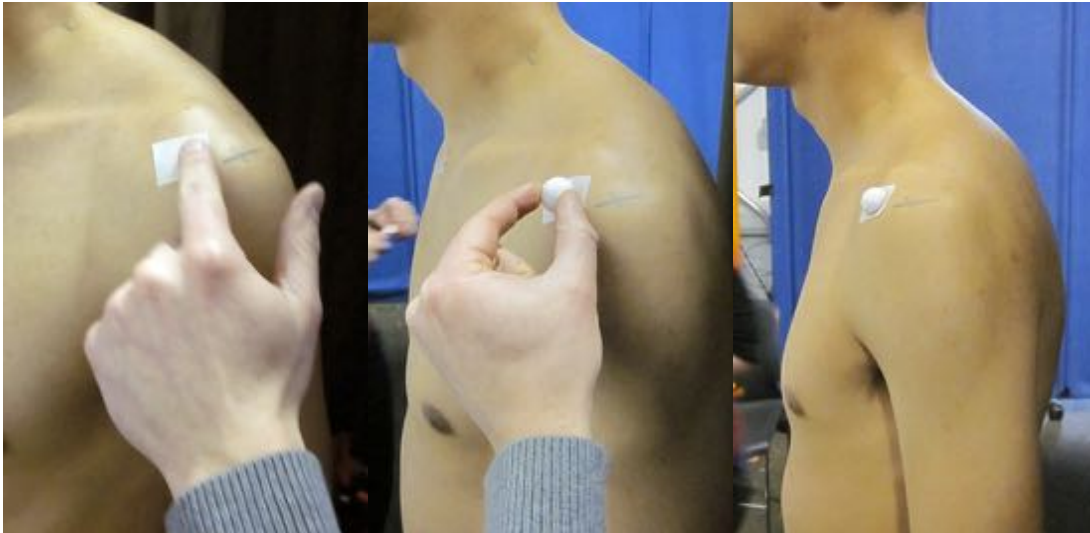


Figure 22. Placing a hemisphere on the anterior-superior aspect of the acromion. The cross on the shoulder is the superior lateral acromion landmark.



Figure 23. Right knee and elbow wrapped with an elastic bandage while the soldier was standing. Each time the soldier changed posture, Velcro targets were centered on the landmarks.

Table 10  
Landmarks Marked on Right Side in ACU

1	Humeral Epicondyle, Lateral
2	Humeral Epicondyle, Medial
3	Femoral Condyle, Lateral
4	Femoral Condyle, Medial
5	Suprapatella
6	Infrapatella

## Scan Postures

Table 11 lists the 18 postures scanned. All soldiers were scanned in the Sitting Lap and Standing Abduction postures at all garb levels. The remaining postures were scanned with those driver and crew soldiers randomized to scanner priority.

Table 11  
Scan Postures

Posture	Code	Scanwear	ACU	PPE	ENC	Seat Back	Lower Limbs	Spine	Shoulders
Recline 1 (min)	R1	X	X	X	X	15°		Erect	Handles*
Recline 2 (mid)	R2	X	X	X				Slump1	
Recline 3 (max)	R3	X	X	X				Slump2	
Sitting Lap**	L1	X	X	X	X	NA	Legs and feet symmetrical with thighs parallel, ankles under the knees, and feet parallel	Erect	Handle
Sitting ISO	L2	X				NA		Erect	Elbow 90°
Arm Flexion 90°	A1	X				NA		Erect	Flexion 90°
Arm Flexion Max	A2	X				NA		Erect	Max Flexion
Arm Abduction 90°	A3	X				NA		Erect	Abduction 90°
Arm Abduction Max	A4	X	X	X		NA		Erect	Max Abduct
Arm Extension Max	A5	X		X		NA		Erect	Max Extension
Spine Flexion Min/Nat	V1	X				NA		Natural	Handle
Spine Flexion Max	V2	X				NA		Max Flexion	Handle, lower
Spine Flexion Mid	V3	X	X			NA		Mid Flexion	Handle, lower
Spine Extension Max	V4	X	X	X		NA	Ext max	Handle	
Standing Natural	T1	X	X	X	X		15cm	Natural	Natural
Standing Abduction**	T2	X	X	X	X		15cm	Natural	Abduction 40°
Standing Erect	T3	X					15 cm	Erect	Abduction 40°
Standing T-pose	T4	X	X	X	X		30 cm	Natural	Abduction 90°

\*Handles= Palm at height of suprasternale, shoulders as if arms were hanging at sides with elbows 45° out from body in coronal view and the shoulder-elbow-wrist angle at 120°

\*\*All soldiers at all levels of garb

The “recline” scans were a series of three postures in which the subject’s posture went from very erect to very slumped, while maintaining a knee angle slightly greater (less flexed) than 90 degrees with legs and feet parallel. The seat surface above the floor was set to the same height as the top of the knee. To increase the amounts of recline, the seat pan was moved forward, away from the backrest resulting in the soldier’s hips moving forward. The backrest supports pivoted to accommodate the resulting reclined postures. To achieve scan coverage of the sides of the



torso, the soldier's arms were moved away from the body, but the shoulder position was kept in a relaxed seat position. The investigator set the elbow angle to  $120^\circ$ , the angle of the arm relative to the midline of the torso in the transverse plane to  $45^\circ$ , and the hand height to the suprasternale height in the erect posture. The soldier was instructed to sit looking forward with relaxed shoulders with the weight of the arms supported by gripping an upright rod and with a relaxed spine in the two more recline postures.

Figure 24 shows the two unsupported sitting postures. In L1, the subject sat with an erect and unsupported torso, with the arms in the same posture as was used for the recline postures. L2 was selected to be similar to the standard anthropometric sitting posture with the arms vertical and forearms horizontal. Figure 25 shows the three supported, reclined postures R1 through R3, each progressively more reclined.

Figure 26 shows a set of postures designed to document the torso shape across the lumbar spine range of motion, from maximally extended to maximally flexed. Figure 27 shows postures that demonstrated shoulder range of motion in flexion, extension, and abduction. The primary goal of these postures was to quantify the changes in shoulder and torso shape associated with these motions, rather than to make accurate measurements of shoulder range of motion. Figure 28 shows the four standing postures, which included a relaxed standing pose and one with the arms and legs slightly abducted to improve laser coverage. A T-pose was included, since data from this pose is often used in the creation of digital human figure models, but the forearms and hands were outside the scan volume in this pose.

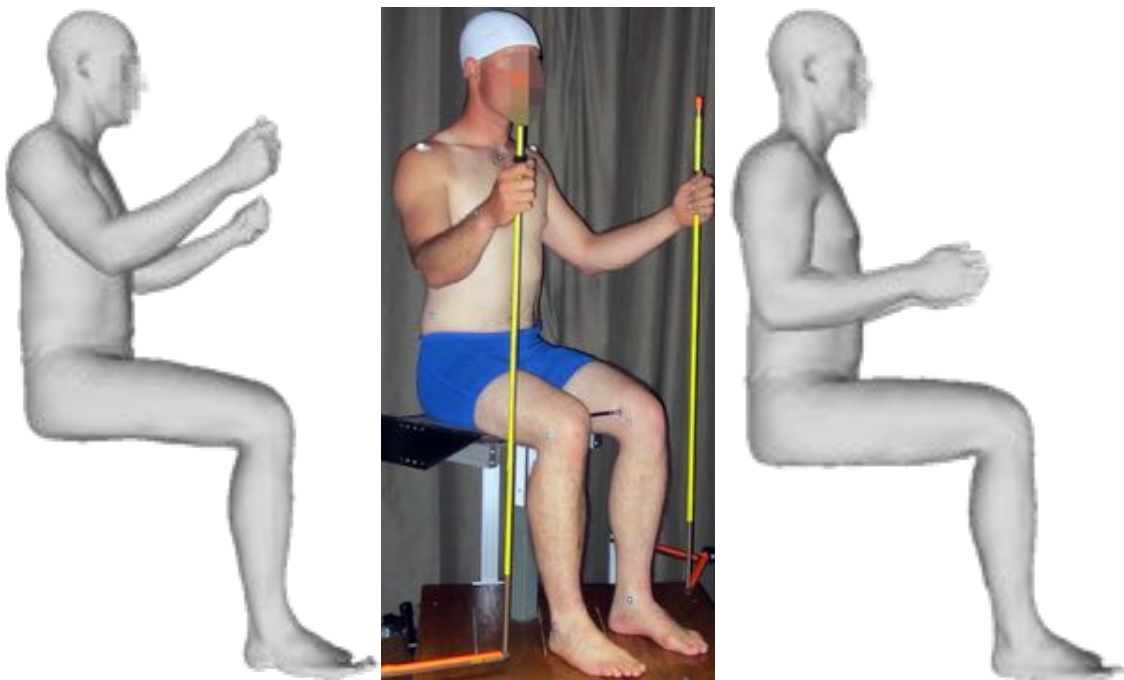


Figure 24. Sitting Postures L1 (left) and L2 (right).



Figure 25. Recline posture 1 through 3 (left to right).



Figure 26. Spine range of motion postures.



Figure 27. Shoulder range of motion postures.

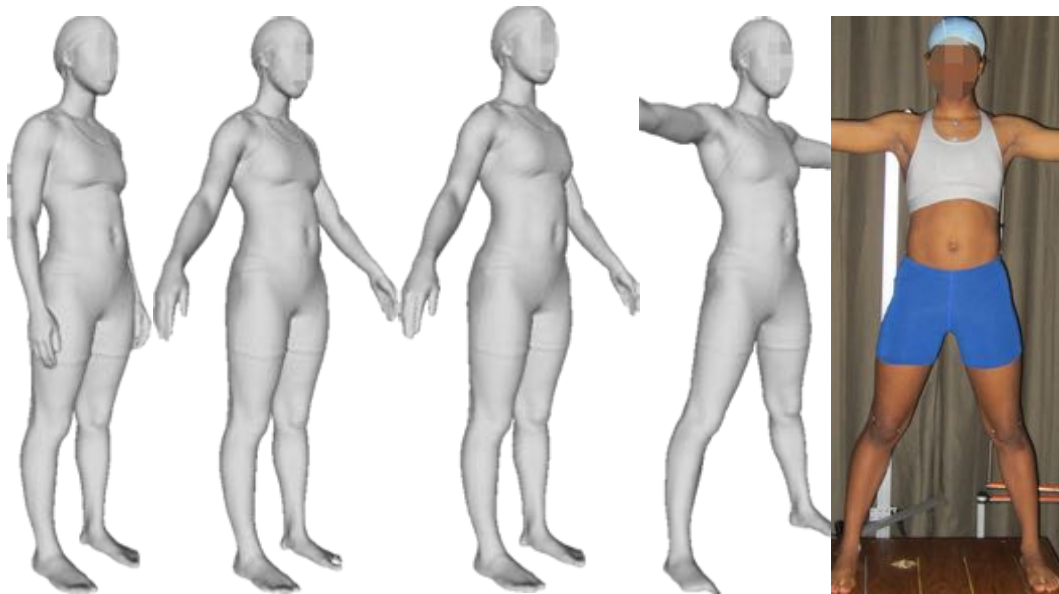


Figure 28. Standing postures: natural, natural with arms raised, spine erect with arms raised and T-pose (left to right).

## Laboratory Hardseat

Each soldier was measured in scanwear (minimally clad) in the laboratory hardseat shown in Figure 29. The hardseat allows the locations of posterior landmarks on the spine and pelvis that are not accessible in the vehicle mockups to be recorded. This information was used to estimate torso joint locations and to characterize each individual's skeletal linkage. Table 12 lists the landmarks recorded in the hardseat.

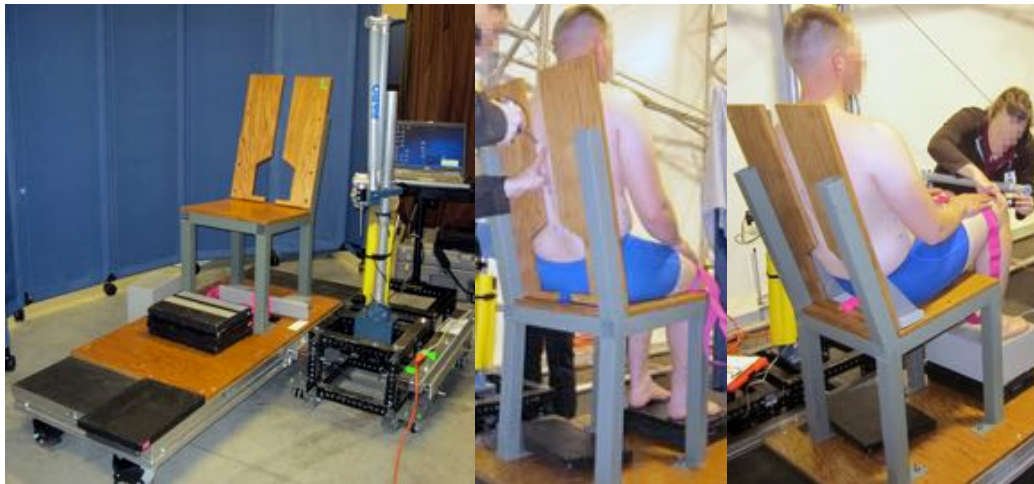


Figure 29. The hardseat with back cutaway to enable measurement of spine and back of the pelvis.

Table 12  
Landmarks and Reference Points and **Markers** Digitized in Hard Seat

C7 (Cervicale)	C7	Lateral Femoral Epicondyle, Right
Back Of Head (Opistion)	<b>C7 Marker</b>	<b>Lateral Femoral Epicondyle, Right Marker</b>
Top Of Head (Vertex)	T4	Medial Femoral Epicondyle, Right
Tragion, Left	<b>T4 Marker</b>	<b>Medial Femoral Epicondyle, Right Marker</b>
Ectoorbitale, Left	T8	Suprapatella, Right
Infraorbitale at Pupil Center, Left	<b>T8 Marker</b>	Infrapatella, Right
Glabella	T12	Medial Femoral Epicondyle Left
Suprasternale	<b>T12 Marker</b>	<b>Medial Femoral Epicondyle, Left Marker</b>
<b>Chest 1 Marker</b>	L1	Lateral Femoral Epicondyle, Left
Substernale	L2	<b>Lateral Femoral Epicondyle, Left Marker</b>
<b>Chest 2 Marker</b>	L3	Suprapatella, Left
Acromion, Right	<b>L3 Marker</b>	Infrapatella, Left
Acromion, Left	L4	Lateral Malleolus, Left
Lateral Humeral Epicondyle, Left	L5	<b>Lateral Malleolus, Left Marker</b>
<b>Lateral Humeral Epicondyle, Left Marker</b>	PSIS Right	Medial Malleolus, Left
Medial Humeral Epicondyle Left	PSIS Left	<b>Medial Malleolus, Left Marker</b>
<b>Medial Humeral Epicondyle, Left Marker</b>	ASIS Right	Ball of Foot Medial, Left
Ulnar Styloid Process, Left	ASIS Left	Toe, Left (Longest Tibiale)
Radial Styloid Process, Left		Ball of Foot Lateral, Left
<b>Wrist Top, Left Marker</b>		Heel, Left
<b>Hip Top, Left Marker</b>		ASIS, Right
<b>Rib10, Left Marker</b>		ASIS, Left

## Study Flow

Appendix C contains the scripts used for subject interaction. Due to time constraints, not all soldiers could be measured in all conditions. Soldiers were randomly assigned as “crew” or “drivers.” Crew soldiers wore the SAW gunner TAP and were measured in the crew mockup. Driver soldiers wore the rifleman’s TAP and were measured in the driver mockup. Crew and driver groups were further divided into two subgroups: either scan-priority or mockup-priority. If assigned scan-priority, the soldier would be run through the entire scanning matrix, but then through a shortened vehicle mockup matrix (either driver or crew). Conversely, if assigned mockup-first, the soldier would be run through the entire vehicle mockup matrix (either driver or crew) and then through a shortened scanning matrix.

## Dependent Measures: Posture

The posture analysis followed the methods described in Reed et al. (2002) to develop a Cascade prediction model (CPM) applicable to tactical vehicles. The CPM prioritizes the dependent measures that are most important for vehicle layout and seat design, while other posture variables are “cascaded”, i.e., predicted from the first set or via inverse kinematics.

The surface body landmark location data were used to estimate internal joint center locations using methods based on Reed et al. (1999). Appendix E provides complete details. In brief, scaling relationships based on previous anatomical studies, particularly x-ray and computed tomography analyses, were used to establish relationships between surface landmarks and underlying skeletal structures. The Reed et al. (1999) procedures use hardseat data to establish relationships between anterior and posterior landmarks on the chest and pelvis so that the spine posture can be measured for subjects in vehicle seats that do not allow access to posterior landmarks. In the current study, these methods were adapted to address the PPE and ENC conditions in which anterior torso landmarks were unavailable. As described in Appendix E, the hardseat data were used to establish a subject-specific torso linkage that was then fit to the available data from the vehicle seats. Information from the ACU condition, in which the anterior pelvis landmarks were available, was also used. As a result of these calculations, the same dependent measures describing the torso posture are available for all seated conditions.

Table 13 lists the dependent measures that are of primary importance. Hip location (HipX, HipZ), the mean of the right and left hip joint centers, is predicted with respect to seat H-point as well as with respect to accelerator heel point (AHP) for driver conditions. For driver conditions, the reference is the translated (i.e., driver-selected) H-point location. Eye locations (EyeX, EyeZ) are also predicted with respect to H-point locations. Driver-selected H-point location (i.e., seat position) is predicted with respect to AHP. Torso posture is characterized by the angles of kinematic segments with respect to vertical. Head angle is calculated as the orientation of the Frankfurt plane with respect to horizontal, with positive values associated with rearward head rotation (eyes higher than ears).

Table 13  
Posture Dependent Measures (mm, deg)

HipX	Side-view fore-aft location of mean hip joint center with respect to seat H-point or AHP
HipZ	Side-view vertical location of mean hip joint center with respect to seat H-point or AHP
EyeX	Side-view fore-aft location of the eye center* with respect to seat H-point or AHP
EyeZ	Side-view vertical location of the eye center* with respect to seat H-point or AHP
HPtX (driver only)	Fore-aft location of driver-selected H-point (seat position) with respect to accelerator heel point (AHP)
HPtZ (driver only)	Vertical location of driver-selected H-point (seat position) with respect to accelerator heel point (AHP)
PelvisSegmentAngle	Angle in side view with respect to vertical of vector from mean hip joint center to L5/S1 joint, positive rearward of vertical.
LumbarSegmentAngle	Angle in side view with respect to vertical of vector from L5/S1 joint to T12/L1 joint, positive rearward of vertical
ThoraxSegmentAngle	Angle in side view with respect to vertical of vector from T12/L1 to C7/T1 joint, positive rearward of vertical
NeckSegmentAngle	Angle in side view with respect to vertical of vector from C7/T1 to AO joint, positive rearward of vertical
HeadAngle	Angle in side view with respect to horizontal of vector from mean tragion to mean infraorbitale, positive with infraorbitale above tragion; equivalent to Frankfurt plane angle with respect to horizontal

\* Eye center is estimated at the vertical location of the corner-eye landmark (ectocanthus) and fore-aft location of infraorbitale.

### Scan data processing

Figure 30 describes the information flow during processing of the scan data. Many steps were needed to bring the scan data to the point that statistical analysis could be conducted. Following data collection, an extensive processing and extraction effort was necessary. Scans were manually cleaned in ScanWorX 2.9.9b (Human Solutions, GmbH) to remove light artifacts and to delete the props and fixtures. Research assistants used Meshlab software version 1.31 (meshlab.org) to extract landmark locations using a version of the scan data that included grayscale vertex coloring. Some landmarks were digitized on an “avatar” model generated in ScanWorX. The avatar has been processed to fill holes that can interfere with the digitizing process. Figures 31-33 show screenshots of the landmarks extracted in Meshlab for representative scans. The complete list of landmarks is found in Appendix D, which also contains an analysis of the repeatability and reproducibility of the landmark digitizing process.

After landmark extraction, a statistical analysis on the combined landmark and body shape data was conducted using methods developed at UMTRI. To conduct statistical analyses of the scan data, it is necessary to express each scan using a consistent set of mesh vertices, such that each vertex is *homologous* across scans, meaning that it lies in the same location with respect to the anatomy. For the current project, this was accomplished by fitting a template to each scan. For seated trials, a template was created manually using a model of a seated driver (Figure 34) derived from the seated body shell of a midsize male created in the Anthropometry of Motor Vehicle Occupants (AMVO) project (Schneider et al. 1983). The AMVO-based template had 34038 vertices and 68072 polygons and was laterally symmetric. Landmark locations were digitized on the template using the same procedures applied to the scan data.

Template fitting employed a two-stage process using custom software developed at UMTRI. Figure 35 shows these steps. First, a non-rigid registration procedure based on radial basis functions was applied to morph the template to match the target data at a set of 70 landmarks. This procedure used a morphing methodology based on radial-basis-function interpolation methods (Bennink et al. 2006). Second, an implicit-surface fitting procedure similar to Carr et al. (2001) was used to move each template vertex into correspondence with a mathematical surface defined by the scan data. The fitting process required several minutes per scan, but was accelerated through the use of the University's high-performance computing facility. Template for fitting standing scans, shown in Figure 36, was derived from the Jack version 7 human figure model (Siemens) to facilitate application of the model to the Jack software, which is widely used by the Army and its contractors and suppliers. Figure 36 illustrates the results of fitting the template to a scan.

At the conclusion of the fitting process, each seated or standing scan was represented by a consistent set of landmarks and mesh vertices, enabling a statistical analysis to proceed. A small number of landmarks (approximately 2% of the total) were missing due to poor scan quality or errors in digitizing. Because a complete landmark set is needed for analysis, a systematic imputation method was employed. In brief, a least-squares prediction of each landmark location as a function of all other landmarks was computed. This method takes advantage of the fact that landmark locations are highly correlated across subjects and trials because of their locations on anatomical structures. Missing landmarks were then predicted and added to the trial records.

Body shape models were computed using the methods described in Reed and Parkinson (2008). Landmark and mesh vertex coordinate data were flattened so that each scan was represented by a 1D vector. In the resulting geometry matrix, each row is a scan, with the number of columns equal to the number of scans in the analysis. A principal component analysis was conducted on the resulting matrix. For computational efficiency, the matrix was divided into 10 submatrices, principal component analysis (PCA) conducted on each, and the results recombined. Linear regression analysis was conducted to predict the principal component scores as a function of overall body dimensions, such as stature, body weight, and erect sitting height. To reduce the correlation of the predictors, body mass index (BMI), computed as body weight in kilograms divided by stature in meters squared, was substituted for body weight, and the ratio of sitting height to stature was used in place of sitting height.



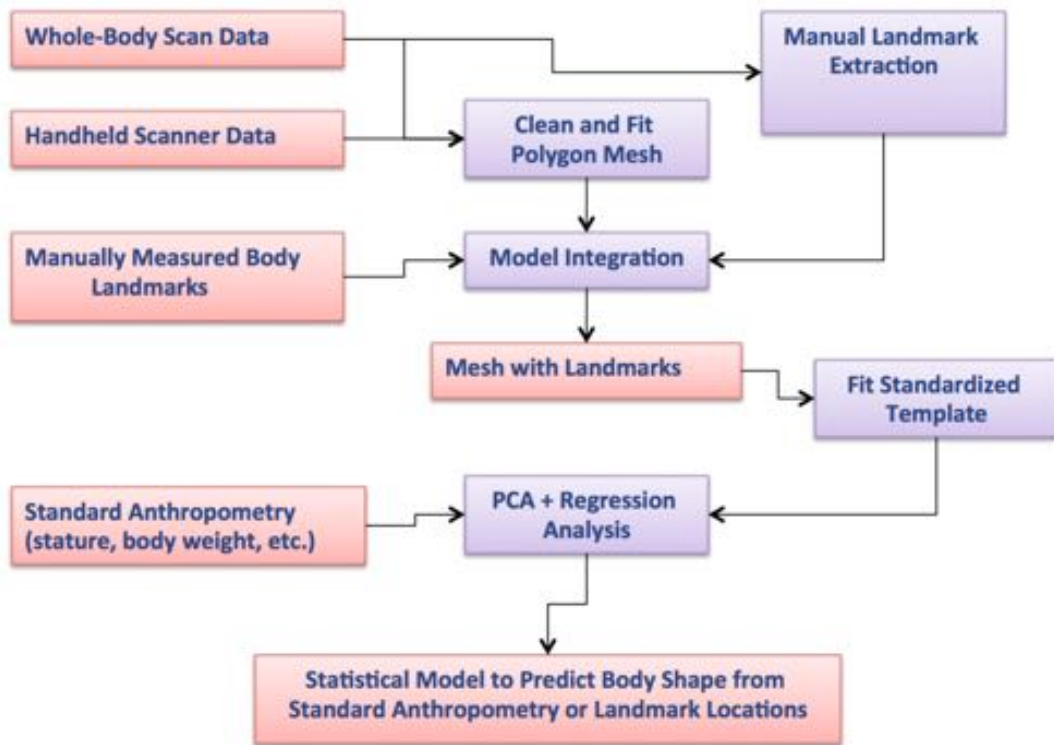


Figure 30. Schematic of scan data processing.



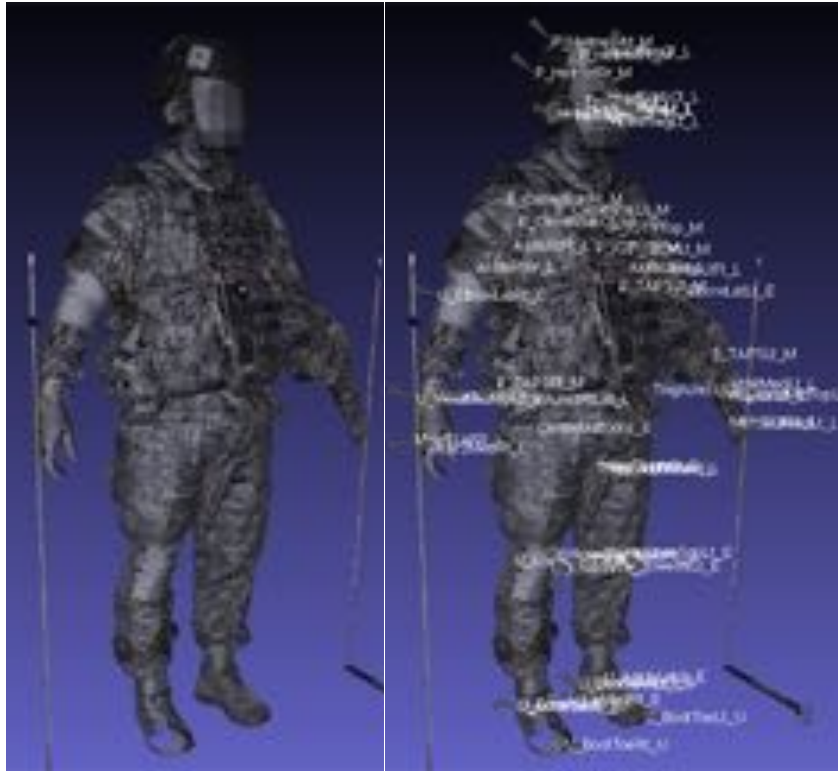


Figure 31. Example of digitizing points in Meshlab on gray scale of scan of an encumbered soldier.

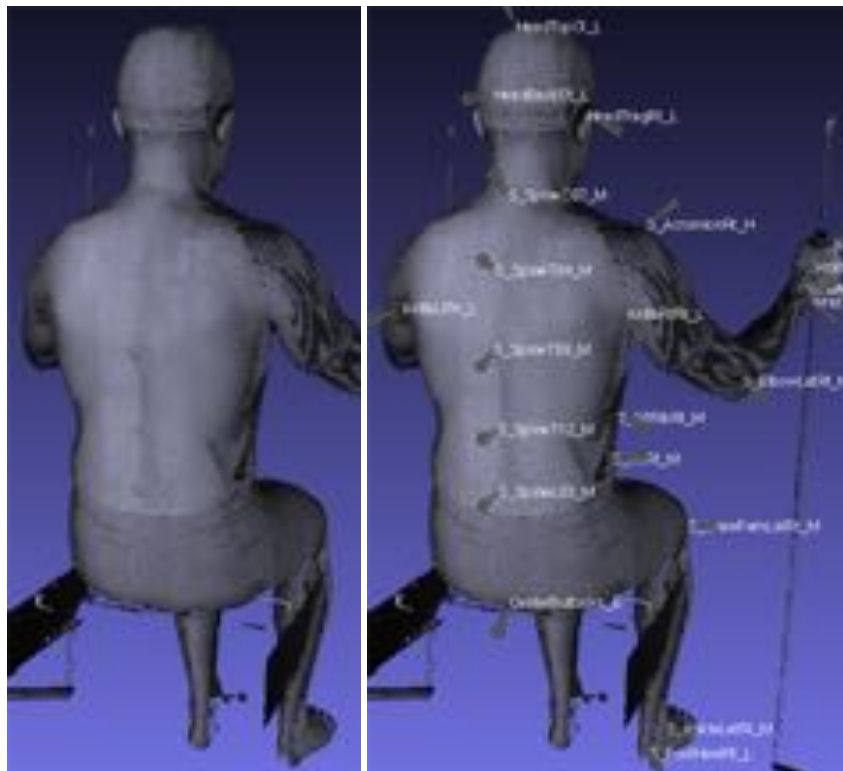


Figure 32. Example of digitizing points on gray scale of scan of soldier in scanwear.

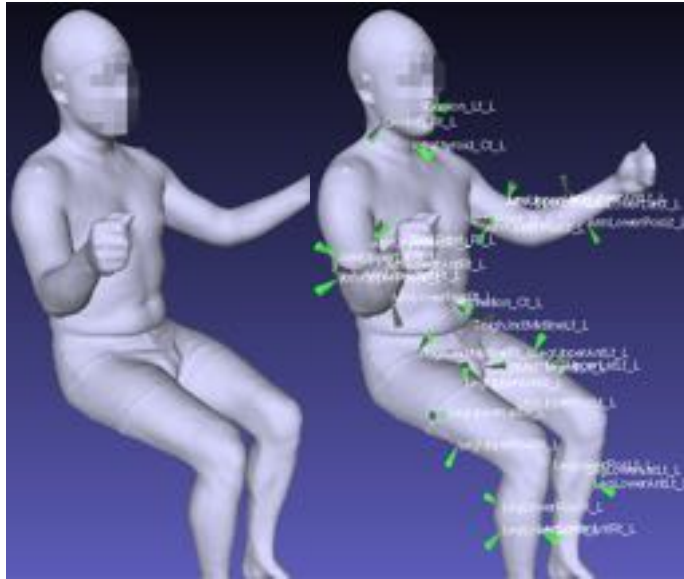


Figure 33. Example of digitizing points on avatar of a scan of soldier wearing scan wear.

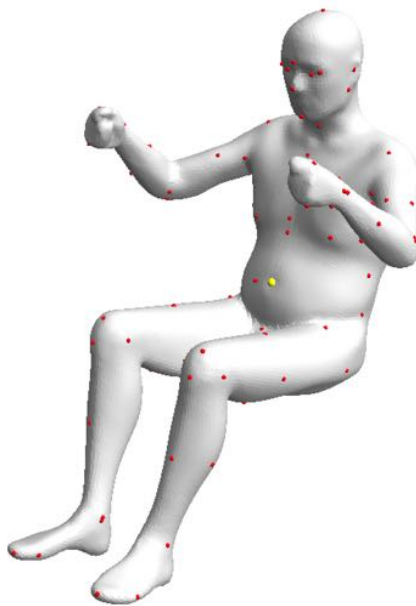


Figure 34. The template for seated scans, showing 137 landmarks, 34038 vertices, and 68072 polygons.

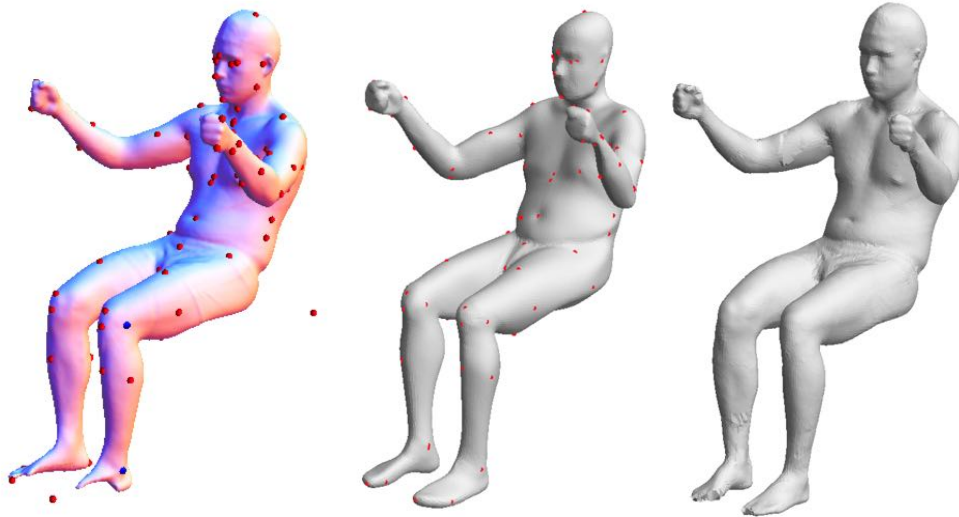


Figure 35. Template fitting for seated scans. Scanned mesh with landmarks (left), landmark-morphed template (center), and fitted scan (right).

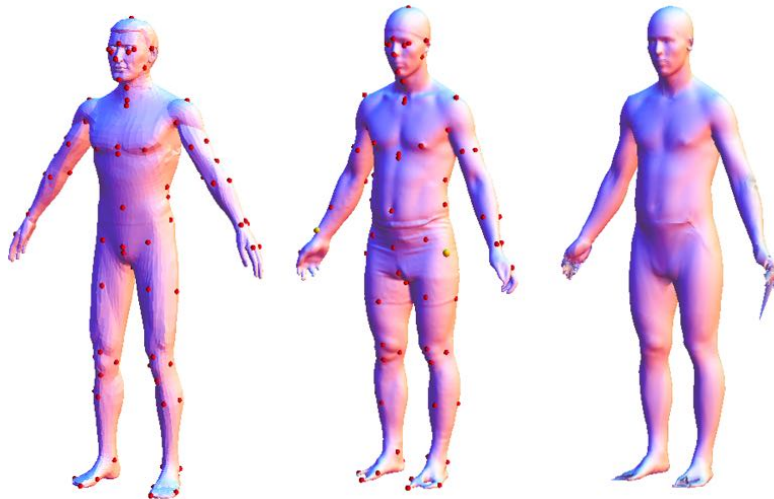


Figure 36. Template fitting for standing scans showing template based on Jack human figure model (left), sample scan (center), and the template fit to the scan (right). Anomalies at the hands and feet are due to limitations of the scan data.

## RESULTS

## Standard Anthropometry

Tables 14 through 18 present summary statistics of standard anthropometric measures for the male and female samples, divided into drivers and crew. Detailed tables for standard anthropometry are in Appendix F. Note that because this is a convenience sample, the data are not representative of the Army or any meaningful subpopulation. However, Tables 14-18 demonstrate that the sample spans a wide range of body size.

Table 14  
Summary Statistics for Standard Anthropometry, Female Drivers (N=26)

Measurements*	Percentiles					Mean	SD
	5th	25th	50th	75th	95th		
Acromial (Biacromial) Breadth	343	356	372	384	396	371	18
Acromion (Acromial) Height, Sitting	503	531	549	577	593	550	30
Acromion-Radiale Length	289	304	312	322	343	313	17
Age (yr)	20	21	23	25	30	24	4
Bicristal Breadth	235	246	254	265	291	257	18
Bideltoid Breadth	420	434	463	473	494	461	33
Bispinous Breadth	197	222	231	244	273	232	22
BMI (kg/m <sup>2</sup> )	21	23	24	26	28	25	4
Buttock-Knee Length	575	585	597	616	637	601	26
Buttock-Popliteal Length	490	496	505	526	544	512	25
Cervicale Height	1318	1363	1398	1419	1506	1402	62
Chest Breadth	241	249	259	272	283	261	20
Chest Circumference	839	892	949	986	1075	950	92
Chest Depth, on Scapula	216	235	249	265	288	249	26
Chest Depth, on Spine	163	170	187	209	226	192	27
Erect Sitting Height	797	827	851	868	905	849	33
Eye Height, Sitting	685	715	726	753	787	732	31
Foot Breadth, Horizontal	83	88	91	94	100	91	5
Foot Length	228	240	246	257	267	248	14
Forearm-Forearm Breadth	452	470	502	522	561	505	47
Forearm-Hand Length	411	425	437	459	485	443	26
Hand Breadth	70	76	78	80	85	78	5
Hand Length	162	171	181	185	196	179	11
Head Breadth	136	144	148	152	156	147	6
Head Length	179	188	193	197	204	192	7
Height of Chest (Chest Height)	1113	1159	1185	1220	1292	1191	59
Height of Hip Circumference (Buttock Height)	788	812	833	864	912	842	48
Hip Circumference (Buttock Circumference)	967	1006	1035	1070	1103	1042	57
Knee Height, Sitting	480	505	520	528	556	519	31
Maximum Hip Breadth, Sitting	352	369	378	399	414	385	27
Popliteal Height	401	415	426	436	460	427	25
Radiale-Stylian Length	221	233	239	257	272	243	18
Stature Without Boots	1547	1588	1632	1648	1743	1634	66
Stature With Boots	1577	1629	1671	1683	1788	1670	66
Tragion-Top of Head	119	124	128	134	137	128	6
Waist Circumference (Omphalion)	732	819	868	916	1025	879	106
Waist Height (Omphalion)	907	951	970	997	1070	978	59
Weight (kg)	57	62	68	74	77	69	10

\* mm unless noted

## UNCLASSIFIED

Table 15  
Summary Statistics for Standard Anthropometry, Female Crew (N=27)

Measurements*	Percentiles					Mean	SD
	5th	25th	50th	75th	95th		
Acromial (Biacromial) Breadth	339	350	365	371	384	362	15
Acromion (Acromial) Height, Sitting	499	511	542	577	606	547	36
Acromion-Radiale Length	281	302	307	317	329	307	15
Age (yr)	19	22	25	26	31	24	4
Bicristal Breadth	219	242	250	260	278	250	19
Bideltoid Breadth	417	438	445	455	488	445	22
Bispinous Breadth	197	208	227	244	265	227	24
BMI (kg/m <sup>2</sup> )	21	21	24	26	27	24	2
Buttock-Knee Length	546	575	589	612	629	592	27
Buttock-Popliteal Length	460	488	499	524	541	503	26
Cervicale Height	1281	1360	1388	1430	1473	1388	59
Chest Breadth	237	247	254	262	272	254	13
Chest Circumference	829	860	884	974	1061	919	80
Chest Depth, on Scapula	203	219	232	263	281	238	27
Chest Depth, on Spine	161	169	180	200	211	184	17
Erect Sitting Height	786	804	841	873	906	843	41
Eye Height, Sitting	668	695	718	762	789	727	41
Foot Breadth, Horizontal	82	89	91	95	100	91	5
Foot Length	225	237	248	256	268	248	13
Forearm-Forearm Breadth	431	468	490	514	542	490	36
Forearm-Hand Length	413	427	441	461	471	443	20
Hand Breadth	72	76	78	82	85	79	4
Hand Length	165	171	176	185	192	178	9
Head Breadth	142	144	145	149	152	146	3
Head Length	181	185	188	193	201	189	6
Height of Chest (Chest Height)	1078	1143	1177	1217	1252	1176	56
Height of Hip Circumference (Buttock Height)	767	814	828	859	885	831	37
Hip Circumference (Buttock Circumference)	933	969	1020	1070	1104	1019	70
Knee Height, Sitting	474	498	513	531	547	514	23
Maximum Hip Breadth, Sitting	337	358	373	394	425	377	30
Popliteal Height	383	412	428	436	456	424	21
Radiale-Stylian Length	226	235	242	254	260	243	12
Stature Without Boots	1502	1586	1619	1670	1716	1619	66
Stature With Boots	1533	1620	1653	1696	1753	1654	65
Tragion-Top of Head	118	124	127	130	142	127	7
Waist Circumference (Omphalion)	727	759	815	907	986	838	90
Waist Height (Omphalion)	899	935	972	1005	1026	968	44
Weight (kg)	55	59	62	70	83	65	9

\* mm unless noted

UNCLASSIFIED

## UNCLASSIFIED

Table 16  
Summary Statistics for Standard Anthropometry, All Female Soldiers (N=53)

Measurements*	Percentiles					Mean	SD
	5th	25th	50th	75th	95th		
Acromial (Biacromial) Breadth	339	353	367	378	392	367	17
Acromion (Acromial) Height, Sitting	500	526	549	578	595	549	33
Acromion-Radiale Length	282	302	309	318	333	310	16
Age (yr)	19	21	24	26	30	24	4
Bicristal Breadth	225	245	252	262	287	254	18
Bideltoid Breadth	420	437	446	468	494	453	29
Bispinous Breadth	195	214	229	246	267	229	23
BMI (kg/m <sup>2</sup> )	21	22	24	26	28	24	3
Buttock-Knee Length	563	580	593	615	637	596	27
Buttock-Popliteal Length	470	494	501	527	543	508	26
Cervicale Height	1292	1360	1394	1422	1497	1395	60
Chest Breadth	238	247	254	265	280	258	17
Chest Circumference	832	870	918	975	1066	934	86
Chest Depth, on Scapula	210	221	239	265	287	243	27
Chest Depth, on Spine	161	170	185	204	219	188	23
Erect Sitting Height	791	821	845	869	909	846	37
Eye Height, Sitting	675	698	725	755	791	729	36
Foot Breadth, Horizontal	83	88	91	95	100	91	5
Foot Length	227	240	247	257	268	248	13
Forearm-Forearm Breadth	448	468	494	519	554	497	42
Forearm-Hand Length	411	426	438	460	477	443	23
Hand Breadth	71	76	78	82	85	78	4
Hand Length	164	171	180	185	194	178	10
Head Breadth	141	144	146	149	153	146	5
Head Length	180	186	190	195	202	191	7
Height of Chest (Chest Height)	1081	1152	1180	1220	1274	1183	57
Height of Hip Circumference (Buttock Height)	771	813	832	863	889	836	42
Hip Circumference (Buttock Circumference)	951	975	1023	1070	1106	1030	64
Knee Height, Sitting	476	503	517	530	553	516	27
Maximum Hip Breadth, Sitting	337	363	376	398	422	381	29
Popliteal Height	385	414	426	436	459	426	23
Radiale-Stylian Length	224	233	241	254	268	243	15
Stature Without Boots	1509	1588	1624	1659	1733	1627	66
Stature With Boots	1549	1624	1660	1693	1774	1662	66
Tragion-Top of Head	119	124	127	132	140	128	7
Waist Circumference (Omphalion)	728	778	853	912	992	858	99
Waist Height (Omphalion)	901	940	972	1003	1055	973	52
Weight (kg)	55	59	66	72	81	67	10

\* mm unless noted

UNCLASSIFIED



## UNCLASSIFIED

Table 17  
 Summary Statistics for Standard Anthropometry, Male Drivers (N=129)

Measurements*	Percentiles					Mean	SD
	5th	25th	50th	75th	95th		
Acromial (Biacromial) Breadth	379	393	405	421	437	407	18
Acromion (Acromial) Height, Sitting	544	574	592	612	638	592	28
Acromion-Radiale Length	307	322	330	340	363	332	17
Age (yr)	19	21	24	27	35	25	5
Bicristal Breadth	244	260	275	293	310	277	21
Bideltoid Breadth	448	484	496	518	546	500	30
Bispinous Breadth	211	227	241	254	270	240	18
BMI (kg/m <sup>2</sup> )	20	23	26	28	32	26	4
Buttock-Knee Length	570	600	615	634	670	618	28
Buttock-Popliteal Length	482	502	517	533	570	520	25
Cervicale Height	1418	1471	1508	1536	1610	1507	58
Chest Breadth	265	283	296	312	337	298	22
Chest Circumference	898	983	1043	1090	1182	1041	87
Chest Depth, on Scapula	207	237	252	272	293	253	27
Chest Depth, on Spine	174	200	215	233	255	215	25
Erect Sitting Height	863	894	915	937	978	915	33
Eye Height, Sitting	749	772	795	814	855	795	31
Foot Breadth, Horizontal	93	97	100	104	110	101	5
Foot Length	248	262	269	275	293	269	13
Forearm-Forearm Breadth	492	534	563	599	652	567	49
Forearm-Hand Length	445	464	478	488	525	479	23
Hand Breadth	80	85	88	91	95	88	5
Hand Length	179	186	192	199	213	193	10
Head Breadth	144	149	153	157	163	153	6
Head Length	187	195	200	204	208	199	7
Height of Chest (Chest Height)	1207	1250	1280	1314	1370	1284	52
Height of Hip Circumference (Buttock Height)	821	859	884	908	976	887	46
Hip Circumference (Buttock Circumference)	924	982	1043	1087	1157	1042	75
Knee Height, Sitting	513	534	552	571	600	553	27
Maximum Hip Breadth, Sitting	325	343	364	385	413	365	28
Popliteal Height	426	440	455	470	508	458	23
Radiale-Stylian Length	242	253	261	271	292	262	16
Stature Without Boots	1648	1710	1752	1784	1860	1749	63
Stature With Boots	1694	1752	1794	1821	1891	1789	61
Tragion-Top of Head	121	128	132	135	140	131	6
Waist Circumference (Omphalion)	750	826	915	983	1043	906	104
Waist Height (Omphalion)	976	1016	1046	1075	1132	1047	48
Weight (kg)	61	73	83	90	103	82	13

\* mm unless noted

UNCLASSIFIED

## UNCLASSIFIED

Table 18  
 Summary Statistics for Standard Anthropometry, Male Crew (N=128)

Measurements*	Percentiles					Mean	SD
	5th	25th	50th	75th	95th		
Acromial (Biacromial) Breadth	378	396	406	418	436	407	18
Acromion (Acromial) Height, Sitting	550	576	591	618	652	597	30
Acromion-Radiale Length	305	320	333	345	369	334	19
Age (yr)	19	21	23	28	36	25	6
Bicristal Breadth	244	262	277	294	315	278	23
Bideltoid Breadth	460	481	500	516	546	500	28
Bispinous Breadth	207	227	242	256	272	241	20
BMI (kg/m <sup>2</sup> )	20	23	25	27	33	26	4
Buttock-Knee Length	576	598	618	645	683	622	33
Buttock-Popliteal Length	483	503	522	546	580	524	30
Cervicale Height	1421	1471	1511	1558	1623	1515	65
Chest Breadth	264	280	296	312	333	297	22
Chest Circumference	901	977	1035	1086	1174	1036	85
Chest Depth, on Scapula	213	236	252	270	293	254	26
Chest Depth, on Spine	180	195	214	233	256	215	26
Erect Sitting Height	862	895	919	942	976	920	35
Eye Height, Sitting	743	778	801	820	851	800	33
Foot Breadth, Horizontal	94	99	101	105	110	102	5
Foot Length	252	262	270	280	295	272	13
Forearm-Forearm Breadth	484	534	563	595	635	564	46
Forearm-Hand Length	448	466	479	498	529	482	24
Hand Breadth	83	86	89	91	95	89	4
Hand Length	181	188	194	200	212	195	10
Head Breadth	144	149	153	157	162	153	6
Head Length	186	194	198	203	209	198	7
Height of Chest (Chest Height)	1207	1245	1293	1334	1397	1293	60
Height of Hip Circumference (Buttock Height)	817	858	887	920	989	893	51
Hip Circumference (Buttock Circumference)	930	989	1042	1084	1192	1045	79
Knee Height, Sitting	512	538	550	576	609	557	31
Maximum Hip Breadth, Sitting	326	348	363	381	423	367	30
Popliteal Height	421	443	457	477	507	461	27
Radiale-Stylian Length	239	250	262	273	295	263	17
Stature Without Boots	1654	1704	1760	1805	1878	1758	70
Stature With Boots	1696	1744	1799	1846	1915	1798	70
Tragion-Top of Head	121	127	130	134	139	130	5
Waist Circumference (Omphalion)	765	834	913	971	1097	912	109
Waist Height (Omphalion)	970	1020	1050	1092	1158	1055	54
Weight (kg)	65	72	82	91	108	83	14

\* mm unless noted

UNCLASSIFIED

## UNCLASSIFIED

Table 19  
Summary Statistics for Standard Anthropometry, All Male Soldiers (N=257)

Measurements*	Percentiles					Mean	SD
	5th	25th	50th	75th	95th		
Acromial (Biacromial) Breadth	377	394	406	420	436	407	18
Acromion (Acromial) Height, Sitting	550	575	592	615	647	595	29
Acromion-Radiale Length	306	320	331	344	366	333	18
Age (yr)	19	21	23	27	35	25	6
Bicristal Breadth	244	261	276	293	313	277	22
Bideltoid Breadth	456	482	497	517	547	500	29
Bispinous Breadth	208	227	241	255	271	240	19
BMI (kg/m <sup>2</sup> )	20	23	26	28	32	26	4
Buttock-Knee Length	571	599	616	639	676	620	31
Buttock-Popliteal Length	483	502	520	541	573	522	28
Cervicale Height	1419	1471	1510	1548	1614	1511	62
Chest Breadth	264	282	296	312	333	298	22
Chest Circumference	899	980	1036	1089	1179	1038	86
Chest Depth, on Scapula	212	236	252	270	293	253	26
Chest Depth, on Spine	175	197	214	233	255	215	26
Erect Sitting Height	862	894	919	938	977	918	34
Eye Height, Sitting	746	776	798	818	854	798	32
Foot Breadth, Horizontal	93	98	101	105	110	101	5
Foot Length	251	262	270	278	293	271	13
Forearm-Forearm Breadth	486	534	563	598	648	565	47
Forearm-Hand Length	446	465	478	494	528	480	24
Hand Breadth	82	85	88	91	95	88	4
Hand Length	180	187	193	200	213	194	10
Head Breadth	144	149	153	157	162	153	6
Head Length	187	194	199	203	208	199	7
Height of Chest (Chest Height)	1207	1247	1284	1322	1393	1288	56
Height of Hip Circumference (Buttock Height)	819	858	885	915	982	890	48
Hip Circumference (Buttock Circumference)	925	985	1043	1087	1180	1043	77
Knee Height, Sitting	513	536	551	574	607	555	29
Maximum Hip Breadth, Sitting	326	344	363	384	418	366	29
Popliteal Height	425	442	455	474	508	459	25
Radiale-Styilion Length	240	251	262	272	294	263	16
Stature Without Boots	1654	1705	1755	1797	1866	1754	66
Stature With Boots	1694	1747	1796	1836	1903	1794	65
Tragion-Top of Head	121	127	131	135	140	131	6
Waist Circumference (Omphalion)	755	830	913	980	1069	909	106
Waist Height (Omphalion)	971	1016	1048	1080	1154	1051	51
Weight (kg)	64	73	82	91	104	83	13

\* mm unless noted

UNCLASSIFIED

Table 20 compares selected statistics for men and women in the sample to the results of the ANSUR 88 (Gordon et al. 1989) and the ANSUR II Pilot (A2P) Survey (Paquette et al. 2009). For men, the sample is very similar to the A2P distributions, but fewer heavy and short-stature men. For women, the means and medians are similar to the comparison populations, but the tail percentiles deviate more. Overall, the comparison indicates that the current sample spans a large percentage of the body dimensions of the Army populations represented by these comparison studies.

Table 20  
Comparison of Summary Anthropometry Statistics to Previous Army Studies (Men)

Measure	Stature (mm)	Body Weight (kg)	Erect Sitting Height (mm)
<b>Seated Soldier</b>			
5 <sup>th</sup> ile	1653	64	861
50 <sup>th</sup> ile	1755	82	919
95 <sup>th</sup> ile	1870	108	978
Mean	1754	83	918
SD	66	13	34
<b>Delta re ANSUR 88</b>			
5 <sup>th</sup> ile	6	2	7
50 <sup>th</sup> ile	0	5	5
95 <sup>th</sup> ile	4	10	6
Mean	-2	4	4
SD	-1	2	-2
<b>Delta re A2P</b>			
5 <sup>th</sup> ile	10	0	3
50 <sup>th</sup> ile	0	-2	1
95 <sup>th</sup> ile	-2	-7	-2
Mean	-2	-3	-1
SD	-4	-1	-3

\* Negative values indicate that measure for current sample is lower than in the comparison study.

UNCLASSIFIED

Table 21  
Comparison of Summary Anthropometry Statistics to Previous Army Studies (Women)

Measure	Stature (mm)	Body Weight (kg)	Erect Sitting Height (mm)
<b>Seated Soldier</b>			
5 <sup>th</sup> percentile	1506	54	788
50 <sup>th</sup> percentile	1624	66	845
95 <sup>th</sup> percentile	1740	86	911
Mean	1627	67	846
SD	66	10	37
<b>Delta re ANSUR 88*</b>			
5 <sup>th</sup> percentile	-22	5	-8
50 <sup>th</sup> percentile	-3	5	-6
95 <sup>th</sup> percentile	27	9	1
Mean	-3	5	-6
SD	2	1	2
<b>Delta re A2P*</b>			
5 <sup>th</sup> percentile	-15	3	-11
50 <sup>th</sup> percentile	-7	-2	-14
95 <sup>th</sup> percentile	10	-7	-7
Mean	-3	-2	-14
SD	2	-3	2

\* Negative values indicate that measure for current sample is lower than in the comparison study.

**Soldier Demographics**

The median male soldier age was 23 years (5<sup>th</sup> and 95<sup>th</sup> percentiles: 19, 35). For female soldiers, the 5<sup>th</sup>, 50<sup>th</sup>, and 95<sup>th</sup> percentiles were 19, 24, and 30 years. All soldiers were enlisted. Table 22 shows the distribution of rank. Table 23 shows the distribution of race reported by the soldiers.

Table 22  
Soldier Rank

	PVT	PV2	PFC	SPC	CPL	SGT	SSG
Male	5	18	61	143	3	23	4
Female		3	13	33		4	

UNCLASSIFIED

UNCLASSIFIED

Table 23  
Soldier Self-Reported Race

Category	Male (%)	Female (%)
Asian/Pacific Islander	9 (3.5)	1 (1.9)
Black, Not of Hispanic Origin	38 (14.9)	23 (43.4)
Hispanic	39 (15.3)	10 (18.9)
More than one	18 (7.1)	7 (13.2)
Native American	4 (1.6)	0 (0)
White, Not of Hispanic Origin	147 (57.6)	12 (22.6)

Among men, 27 identified their branch as Combat Service Support, 142 as Combat Support, and 88 as Combat Arms. Two were Army Reserve and 255 were Regular Army. Among women, 10 were Combat Service Support, 41 Combat Support, and 2 Command Arms. All women were Regular Army.

**Driver Postures**

*Regression Models*

The design of the study was such that the effects of the package dimensions (seat height and steering wheel position) could be evaluated in the ACU garb conditions across five packages. The effects of garb were evaluated only at the middle package condition (D05). The goal of the analysis was to quantify the effects of soldier body dimensions and the independent experimental variables on a set of measures of posture and position.

In each case, a series of exploratory analyses were conducted to identify the factors that had significant and important effects. In general, an effect was considered statistically significant if the associated p-value was less than 0.01. An effect was considered important if the adjusted R<sup>2</sup> value increased by 0.02 or more when the factor was included. An additional consideration was the development of interpretable and parsimonious prediction models. For example, although a variety of body dimensions correlated with stature could produce similar prediction values, evaluated using adjusted R<sup>2</sup>, stature is preferred because it is more generally available to describe vehicle occupant populations.

The fore-aft and vertical steering wheel position measures (L11 and H17) are correlated in the experiment design, because the neutral or driver-preferred steering wheel position is further forward when the wheel is higher. To improve model interpretation and the stability of the regression coefficients, L11 was recorded as L11<sub>rel</sub> (relative) using the relation

$$L11_{rel} = L11 - (888.75 - 0.75 H17)$$

L11<sub>rel</sub> takes on values of -75, 0, and 75 mm.



Table 24 shows regression models predicting driver posture and position variables along with the coefficient of determination adjusted for the number of predictors ( $R^2_{adj}$ ) and the root mean square error (RMSE = residual standard deviation). Table 25 lists regression models predicting torso segment orientations. Table 26 illustrates the relative importance of the effects by showing the effect on the dependent measures of varying the predictor over the typical application range.

As expected, drivers with greater stature sat more rearward and with their eyes higher than shorter drivers. Higher steering-wheel position relative to AHP (or, equivalently, higher nominal seat height) was associated with more-forward seat positions. Steering wheel positions that were more forward relative to the pedal produced seat positions further forward and slightly higher, while also causing more upright torso posture. Hip location with respect to seat H-point was essentially constant in ACU conditions, including with respect to driver attributes.

Driver seat back angle was weakly predicted by L11. Seat back angle can also be predicted from HipEyeAngle:

$$\text{Seat Back Angle (deg)} = 17.1 + 0.373 \text{ HipEyeAngle}, R^2_{adj} = 0.21, \text{RMSE} = 2.9$$

The seat back angle data showed a strong tendency for drivers to leave the seat back at the starting angle (17 degrees), which was chosen to be close to the expected mean. The driver-selected seat back angle was within one degree of the starting position in 46 percent of the ACU trials.

Table 24  
Regression Models\* Predicting Driver Posture and Position Variables in ACU

Dependent Measure	Constant	H17†	L11 <sub>rel</sub> ††	Stature	ln(BMI)	SH/S	$R^2_{adj}$	RMSE
Seat Position X	1014	-0.780	0.487	0.310	62.2	-923	0.75	30.3
Seat Position Z	-252	0.990	-0.089	-0.037			0.80	20.8
Seat Back Angle	18.4		0.0095				0.03	3.1
HipEyeAngle	25.9		0.008	-0.013			0.07	3.9
HipEyeDistance	-686			0.402		1239	0.77	17.0
HipReAHPX	1056	-0.773	0.519	0.331	43.7	-1007	0.74	32.4
HipReAHPZ	-441	1.03	-0.075		27.7		0.78	23.0
HipReHPtX	43.3				-20.1		0.01	22.2
HipReHPtZ	-128	0.038			28.7		0.15	10.8
EyeReAHPX	1281	-0.802	0.603	0.212		-660	0.59	45.1
EyeReAHPZ	-981	1.03		0.370		1227	0.78	28.0
EyeReHipX	262		0.084	-0.130			0.05	44.2
EyeReHipZ	-680			0.407		1208	0.76	17.3
EyeReHPtX	345		0.116	-0.108	-44.0		0.08	40.1
EyeReHPtZ	-816			0.411	29.0	1262	0.77	17.3

\* Assemble the linear function by multiplying each predictor by the associated slope and adding the constant.

† To use H30 as a predictor, use H30 + 312 mm for H17.

††  $L11_{rel} = L11 - (888.75 - 0.75 H17)$

Table 25  
Regression Models\* Predicting Driver Torso Segment Posture in ACU

Dependent Measure	Constant	HipEye Angle	ln(BMI)	Sitting Height/ Stature	R <sup>2</sup> <sub>adj</sub>	RMSE
HeadSegmentAngle	-30.5	0.641	--	59.2	0.21	5.4
NeckSegmentAngle	2.2	1.01	5.64	-53.4	0.39	5.0
ThoraxSegmentAngle	26.2	1.19	--	-64.4	0.54	4.3
AbdomenSegmentAngle	-51.3	0.603	--	153.6	0.10	9.7
PelvisSegmentAngle	35.8	1.07	16.8	-83.7	0.28	7.6

\* Assemble the linear function by multiplying each predictor by the associated slope and adding the constant.

Table 26  
Driver Posture Factor Effects (Range)\*

Dependent Measure	H17 (100 mm)	L11 <sub>rel</sub> (150 mm)	Stature (350 mm)	ln(BMI) (0.56 ln kg/m <sup>2</sup> )	SH/S (0.04 mm/mm)
Seat Position X	-78	73	109	35	-37
Seat Position Z	99	-13	-13	--	--
HipEyeAngle	--	1	-5	--	--
HipEyeDistance	--	--	141	--	50
HipReAHPX	-77	78	116	24	-40
HipReAHPZ	103	-11	0	16	0
HipReHPtX	--	--	--	-11	--
HipReHPtZ	4	--	--	16	--
EyeReAHPX	-80	90	74	--	-26
EyeReAHPZ	103	--	130	--	49
EyeReHipX	--	13	-46	--	--
EyeReHipZ	--	--	142	--	48
EyeReHPtX	--	17	-38	-25	--
EyeReHPtZ	--	--	144	16	50

\* Effect slopes in Table 24 multiplied by the applicable range estimates.

### Garb Effects

The effects of garb level were evaluated in the center package condition (D05). The experiment design allowed consideration of the main effects of driver covariates as well as potential

interactions between garb level and driver covariates. However, potential interactions between garb and package variables were not investigated.

The regression analysis demonstrated significant effects of garb level on several posture variables, as shown in Table 27. All coefficients for PPE and ENC in Table 27 are significant ( $p < 0.01$ ) differences relative to ACU. Note that PPE and ENC are not necessarily significantly different even if both coefficients appear.

The addition of PPE shifted seat position aft by an average of 21 mm. Adding ENC increased the rearward shift by an additional 34 mm. At the ACU level, the drivers' hip location was an average of 24 mm forward of the seat H-point. With the addition of PPE, the hip shifted forward an additional 23 mm. Adding ENC increased the forward shift relative to ACU to 47 mm. The position of the hips relative to the AHP was not significantly changed by the addition of PPE, indicating that the rearward seat shift accommodated the more-forward position on the seat. With ENC, the hip locations were an average of 18 mm further rearward, possibly because of interference between encumbrance and the steering wheel. The HipEyeAngle was more upright with the addition of PPE and even more upright with ENC. The HipToEyeDistance was an average of 12 mm larger with PPE or ENC, suggesting that the body armor reduced lumbar spine flexion slightly. Consequently, the eye location with respect to the H-point was also higher by an average of 13 mm. The more-upright torso posture resulted in the drivers' eye locations being an average of 36 mm further forward with PPE and a similar 39 mm with ENC. Compared to ACU, driver-selected seat back angle was not significantly different in PPE trials, but increased an average of 2.6 degrees for ENC trials.

Table 27  
Driver Garb Effects Relative to ACU

Dependent Measure (mm/deg)	ACU	PPE*	ENC*
Seat Position X	698	20.8	64.7
Seat Position Z	418	-2.5	-7.5
Seat Back Angle (deg)			
HipEyeAngle (deg)	3.6	-2.9	-4.9
HipEyeDistance	656	12	12
HipReAHPX	674	--	17.6
HipReAHPZ	412	--	--
HipReHPtX†	-24.3	-23	-47
HipReHPtZ	--	--	--
EyeReAHPX	715	-36	-39
EyeReAHPZ	1065	--	--
EyeReHipX	41.5	-33	-56
EyeReHipZ	653	13	13
EyeReHPtX	17.1	-56.3	-103
EyeReHPtZ	648	13	13

\* Deltas re ACU

† Negative = forward.

### *Combining Driver, Package, and Garb Effects*

The regression results in Tables 24-27 can be combined to predict driving postures for a wide range of conditions. The package data are needed as input to the model. H17 and L11 describe the steering wheel position. H17 can be calculated from H30 by adding 312 mm. The driver is characterized by stature, ln(BMI), and ratio of sitting height to stature. If sitting height is not available, the mean ratio from this sample of 0.523 can be used. Using the coefficients in Table 24, the expected driver-selected seat position (H-point location), hip location, and eye location can be calculated. Garb effects are added using the offsets in Table 27. Eye location can be obtained either by using the hip-eye vector angle and distance or calculated directly relative to AHP. If a particular vehicle has substantial limitations in seat track adjustment range, calculating the eye location relative to seat H-point allows that effect to be taken into account. If detailed torso posture is needed, the body segment angles are calculated from hip-eye angle and driver attributes using the coefficients in Table 25.

## **Crew Postures**

### *Regression Models*

Landmark data from the crew trials were analyzed using regression analysis in a manner similar to the analysis of the driver data. Detailed torso posture data were gathered in conditions C01,

C02, C05, and C07 at the ACU garb level. Table 28 shows the available trials in each condition and garb level, which reflects the experiment design and missing trials in some conditions.

At the PPE and ENC garb levels, only conditions C01 and C05 were used. At the ACU level, the data allow evaluations of the potential interaction of the recline effect (back angle 10 degrees vs. 0 degrees, combined with cushion angle at 5 degrees vs. 0 degrees) and seat height (350 and 450 mm).

Table 28  
Crew Trials Used for Torso Posture Analysis

Condition	Back Angle (deg)	Cushion Angle (deg)	Seat Height (H30)	ACU (N)	PPE (N)	ENC (N)
C01	0	0	450	121	89	87
C02	0	0	350	79	0	0
C05	10	5	450	96	47	47
C07	10	5	350	80	0	0

Table 29 lists the results of regression analyses on the primary posture variables at the ACU garb level. Table 30 lists coefficients for predictions of torso segment orientation along with the coefficient of determination adjusted for the number of predictors ( $R^2_{adj}$ ) and the root mean square error (RMSE = residual standard deviation). Because the seat position and seat back angle are fixed, no models are presented for those variables.

Seat height (H30) had small effects on the amount of torso slump, resulting in slightly increased hip-to-eye distances and higher eye locations relative to H-point at the higher seat height. Raising the seat 100 mm raised the eyes approximately 110 mm, due to less lumbar spine flexion. Table 30 suggests that this effect was mainly due to a more upright pelvis orientation.

Seat back angle affected the fore-aft position of the hip with respect to the H-point and, as expected, altered torso recline. Increasing the seat back angle changed the angle of the hip-to-eye vector by about half as much. Greater stature was associated with more-upright torso recline and eyes further forward relative to the hips and H-point. Higher body mass index resulted in hips further forward on the seat and eyes further rearward. As expected, greater stature and a greater ratio of sitting height to stature was associated with higher eye locations.

UNCLASSIFIED

Table 29  
Regression Models\* Predicting Crew Posture and Position Variables

Dependent Measure	Constant	H30	A40	Stature	ln(BMI)	SH/S	R <sup>2</sup> <sub>adj</sub>	RMSE
HipReHPtX	185	--	1.73	--	-66.1	--	0.27	20.5
HipReHPtZ	-98	--	--	--	26.6	--	0.08	12.4
HipEyeAngle	4.6	--	0.540	-0.0059	--	--	0.45	3.0
HipEyeDistance	-672	0.101	-1.11	0.361	--	1292	0.75	18.7
EyeReHipX	-53		6.32	-0.090	43.6	--	0.47	34.6
EyeReHipZ	-654	0.097	-0.749	0.354	--	1276	0.73	19.3
EyeReHPtX	173		8.05	-0.117	-20.8	--	0.68	28.5
EyeReHPtZ	-802	0.082	-0.675	0.393	--	1418	0.79	18.1

\* Assemble the linear function by multiplying each predictor by the associated slope and adding the constant.

Table 30 shows that torso segment angles were only modestly affected by body size, after taking into account torso recline (HipEyeAngle). Pelvis orientations were slightly more upright at higher seat heights, but the RMSE is large relative to the effect.

Table 30  
Regression Models\* Predicting Crew Torso Segment Posture in ACU

Dependent Measure	Constant	HipEye Angle	H30	Stature	ln(BMI)	Sitting Height/ Stature	R <sup>2</sup> <sub>adj</sub>	RMSE
HeadSegmentAngle	-55	0.334	--	0.012	--	70.4	0.07	5.9
NeckSegmentAngle	-2.7	0.637	--	--	--	--	0.24	4.6
ThoraxSegmentAngle	-5.9	1.32	--	--	--	--	0.53	5.0
AbdomenSegmentAngle	74.0	1.03	--	--	-17.3	--	0.15	10.5
PelvisSegmentAngle	9.8	0.791	-0.042	--	19.1	--	0.17	10.7

\* Assemble the linear function by multiplying each predictor by the associated slope and adding the constant.

For purposes of torso posture prediction, the angle of the side-view vector from the head/neck joint to the mid-tracion landmark was used. The angle of this vector from vertical is equal to the head segment angle minus 27 degrees.

*Segment Lengths*

The lengths of the torso segments can be estimated using the regression results in Table 31. Note that due to the nature of regression models, the sum of segment lengths will be less than the expected total of the segment lengths except at the mean.

UNCLASSIFIED



Table 31  
Regression Models\* Predicting Torso Segment Lengths (mm)

Dependent Measure	Constant	Stature	Sitting Height/ Stature	R <sup>2</sup> <sub>adj</sub>	RMSE
HeadSegmentLength	31	0.0193	36.3	0.09	4.8
Head/Neck Joint to Mid-Tragion	16	0.0055	--	0.09	1.5
NeckSegmentLength	-110	0.0762	193.6	0.30	9.7
ThoraxSegmentLength	-364	0.1943	625.5	0.48	17.4
AbdomenSegmentLength	-207	0.0803	435.1	0.20	16.2
PelvisSegmentLength	19.9	0.0338	50.6	0.29	4.3

\* Assemble the linear function by multiplying each predictor by the associated slope and adding the constant.

### *Lower-Extremity Postures*

Thigh segment angle with respect to horizontal and included knee angle (smaller angles indicate greater knee flexion) were calculated for each crew condition. Thigh segment angle was significantly affected by both seating environment variables and soldier attributes.

$$\text{ThighSegmentAngle (deg)} = 61 + 4.9 \text{ FP} - 0.126 \text{ H30} - 0.358 \text{ A40} + 0.0286 \text{ Stature} - 77.7 \text{ SHS}, \\ R^2_{\text{adj}} = 0.84, \text{ RMSE} = 2.9$$

where FP = 1 when the simulated “foot protection” was in place, zero otherwise. Taller subjects and those with shorter torsos per stature had higher thigh angles due to longer lower extremities. Thigh angles were lower at the higher seat height and with the more-reclined seat back angle.

Knee angle was affected by a similar set of variables, but also showed an effect of garb, due to the garb shifting the hips forward on the seat.

$$\text{Knee Angle (deg)} = 92.4 + 15.6 \text{ FP} + 0.094 \text{ H30} + 0.655 \text{ A40} - 0.067 \text{ Stature} - 5.76 \ln(\text{BMI}) + \\ 148 \text{ SHS} + \text{G}, R^2_{\text{adj}} = 0.86, \text{ RMSE} = 4.6.$$

The lateral spacing of the feet was not constrained by the subject instructions or the design of the apparatus, except that the foot-protection block was 380 mm wide. Because only the right foot location was recorded, foot spacing was estimated by doubling the lateral position of the right heel with respect to the C7 spine landmark, used to represent the midline of the body. The data were approximately normally distributed with a mean of 282 mm and standard deviation of 62 mm.

### *Head and Helmet Height*

The top-most point on the head and on the helmet, when worn, were recorded during each torso posture measurement in the crew seat. The height of these landmarks above the seat H-point is a useful indicator of headroom clearance requirements.

Top of Head re HPt Z (mm) =  $-679 - 0.547 A40 + 0.417 \text{ Stature} + 54 H + 1394 \text{ SHS}$ ,  $R^2_{\text{adj}} = 0.89$ , RMSE = 16,

where H is 1 for the PPE and ENC conditions when the helmet was worn, zero otherwise. Body dimensions are the primary predictors, but increased recline angle is associated with a lower head position, as expected.

### *Garb Effects*

Table 32 shows the effects of garb level on posture variables using data from conditions C01 and C05. The study design allows the evaluation of potential interactions between recline (0- vs. 10-degree A40) and garb level. A significant ( $p < 0.001$ ) interaction between garb level and A40 was observed for HipEyeAngle and EyeReHipX, indicating that the ENC level reduced torso recline more in the 10-degree A40 condition than with the vertical seat back. However, the net effect of including the interaction was small (approximately one degree for HipEyeAngle at  $A40 = 10^\circ$ ) and the improvement in the  $R^2$  value for the regression model was only 0.03. Consequently, interactions between A40 and garb level were neglected, and garb effects on crew postures were modeled as constant offsets from the ACU values, as shown in Table 32.

Garb level had minimal effect on torso segment orientations, except through its effect on overall torso recline (as measured by HipEyeAngle). Consequently, the models in Table 30 can be used for PPE and ENC conditions after adjusting the HipEyeAngle per Table 32. For example, the predicted HipEyeAngle for a soldier wearing PPE is equal to the predicted value for ACU minus 1.9 degrees.

Table 32  
Crew Garb Effects Relative to ACU (mm)

Dependent Measure (mm/deg)	PPE*	ENC*
HipReHPtX†	-29	-72
HipReHPtZ	--	--
HipEyeAngle (deg)	-1.9	-3.4
HipEyeDistance	--	--
EyeReHipX	-23	-41
EyeReHipZ	--	--
EyeReHPtX	-52	-113
EyeReHPtZ	--	--

\* Deltas re ACU

† Negative = forward for all values in the table.

## **Body Shape Data and Modeling**

### *Data Overview*





























A total of 8207 whole-body scans were gathered and processed in the study. Figure 37 illustrates some of the scans, illustrating the range of postures. Appendix D lists the entire set of landmarks digitized on each scan. Tables 33 and 34 list the number of scans successfully gathered in each condition. Several conditions shown in italics in the tables were dropped early in the program due to time constraints; only a few scans are available in each of those conditions. As shown in Figure 37, scan quality was generally high, except that feet were not scanned well due to the limitations of the equipment. Scan quality in the hand area was also poor, due to the resolution of the scanner. Torso scan quality was generally very good, with some shadowing in the under-arm, inner thigh, and crotch, leading to less accuracy in those regions.



Figure 37. Examples of scan data.

UNCLASSIFIED

Table 33  
Male/Female Counts per Scan Condition
















Posture	Scanwear	ACU	PPE	ENC	Total
L1					
	250 / 52	254 / 53	246 / 49	243 / 44	1191
L2					
	136 / 33	<i>9 / 2*</i>	<i>7 / 1</i>	<i>3 / 0</i>	191
R1					
	136 / 33	135 / 32	133 / 30	128 / 27	654
R2					
	134 / 33	132 / 32	131 / 30	0 / 0	492
R3					
	135 / 33	133 / 32	129 / 30	0 / 0	492
T1					
	135 / 33	133 / 33	130 / 30	128 / 28	650
T2					
	250 / 52	254 / 53	245 / 47	244 / 45	1190
T3					
	135 / 33	<i>8 / 2</i>	<i>4 / 0</i>	<i>3 / 0</i>	185
T4					
	135 / 33	135 / 32	128 / 29	128 / 27	647

\*Conditions in *italics* were dropped from the matrix early in the program due to time constraints.

UNCLASSIFIED

UNCLASSIFIED

Table 34  
Male/Female Counts per Scan Condition

Posture	Scanwear	ACU	PPE	ENC	Total
A1					
	135 / 33	0 / 0	6 / 1*	0 / 0	175
A2 (max)					
	134 / 33*	0 / 0	7 / 1	0 / 0	175
A3					
	134 / 33	0 / 0	6 / 1	0 / 0	174
A4 (max)					
	136 / 33	119 / 23	133 / 31	0 / 0	475
A5 (max)					
	135 / 33	0 / 0	130 / 30	0 / 0	328
V1					
	135 / 33	8 / 2	6 / 1	4 / 0	189
V2 (max)					
	135 / 33	134 / 33	128 / 31	0 / 0	494
V3					
	135 / 33	133 / 33	0 / 0	0 / 0	334
V4					
	134 / 33	4 / 0	0 / 0	0 / 0	171

\*Conditions in *italics* were dropped from the matrix early in the program due to time constraints.

UNCLASSIFIED



*Standing Body Shape*

A standing body shape model was constructed using data from 213 men in the ST2 condition. Each scan was fit using a template based on the Jack human figure model, as described in the Methods section. The regression analysis predicts body shape, surface landmark locations, and joint center locations as a function of the 11 standard anthropometric variables listed in Table 35. A second regression predicted the final nine variables from the first three variables, enabling a model with only three inputs.

Figure 38 shows examples of output from the model, demonstrating the range of body sizes and shapes the model is capable of generating. Figure 39 shows the range of body shape that can be obtained by holding stature at 1755 mm and BMI constant at 30 kg/m<sup>2</sup> (threshold obesity) while manipulating chest, waist, and hip circumference. These illustrations demonstrate that the model is capable of representing a large range of male body shapes.

Table 35  
Anthropometric Inputs to the Standing Body Shape Model

Stature*	BMI*
Sitting Height / Stature*	Biacromial Breadth
Knee Height Sitting	Forearm-Hand Length
Hip Breadth Sitting	Head Circumference
Chest Circumference	Waist Circumference Omphalion
Hip Circumference at Buttocks	

\* Used for concise model.

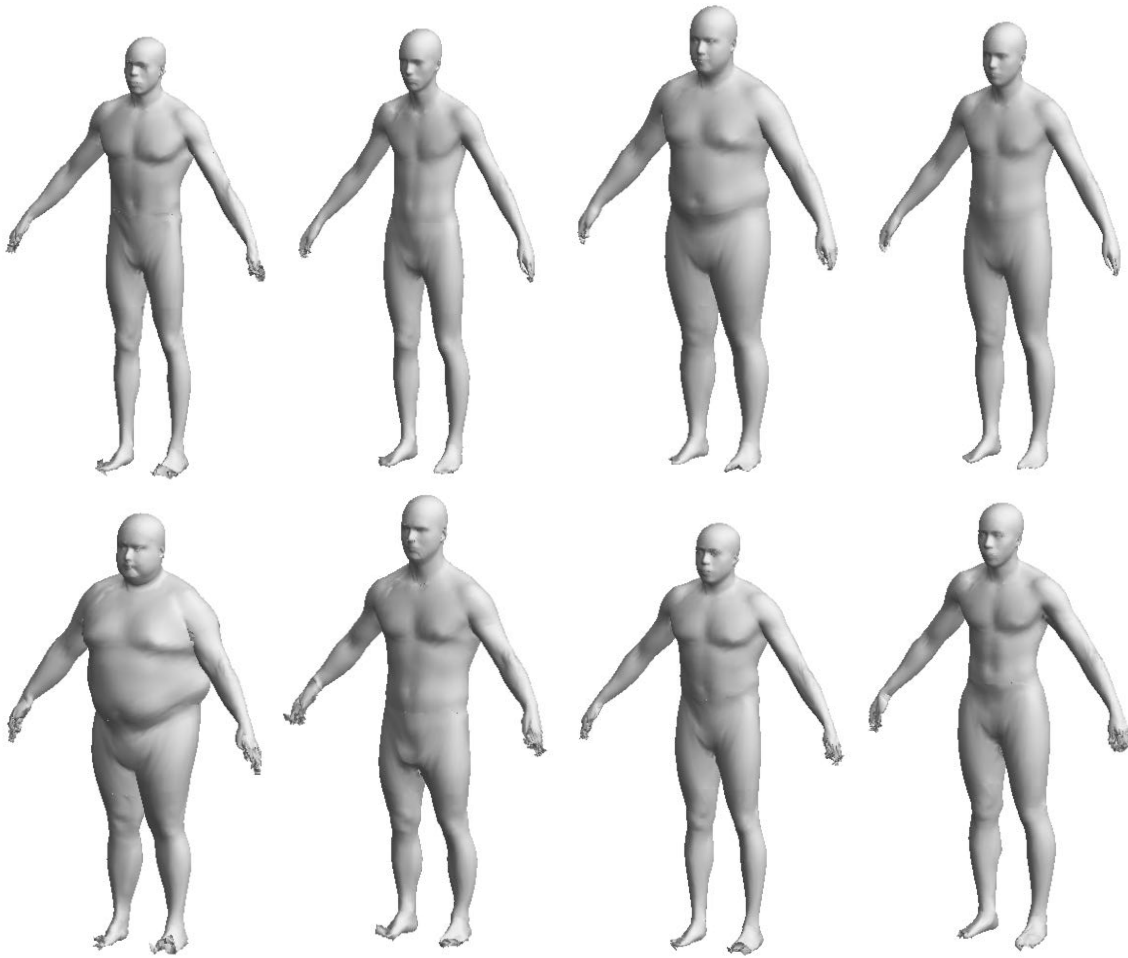


Figure 38. Illustration of body shapes produced by manipulating stature, BMI, and ratio of sitting height to stature in the male standing body shape model.

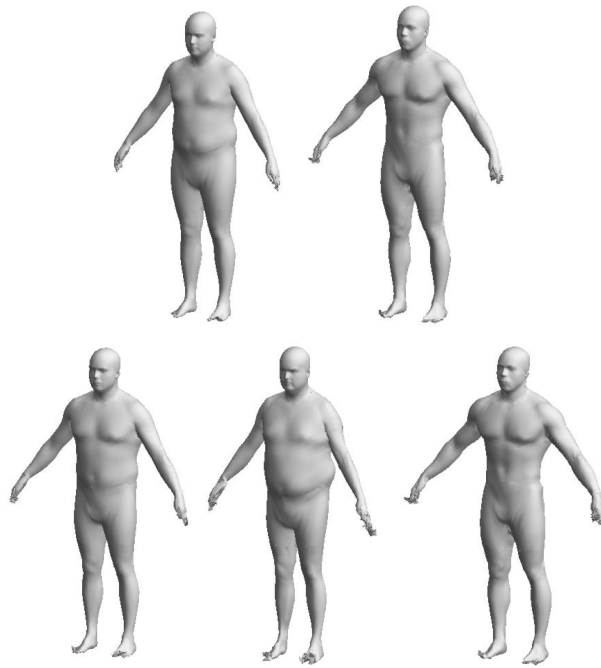


Figure 39. Illustration of a range of body shape while holding stature = 1755 mm and BMI = 30 kg/m<sup>2</sup> in the male standing body shape model.

Figure 40 shows the body shape obtained by entering the median values for stature, body weight, and sitting height from the ANSUR II Pilot Study (Paquette et al. 2009). Tables 36 and 37 list the surface landmark and joint location predictions for this midsize male figure. Note that the coordinate system has the Z axis vertical. The orientations of other axes are arbitrary. Note that these coordinates have not been rationalized; for example, left-right points that are homologous do not necessarily have the same z value, and points nominally on the midline of the body are not aligned.

UNCLASSIFIED

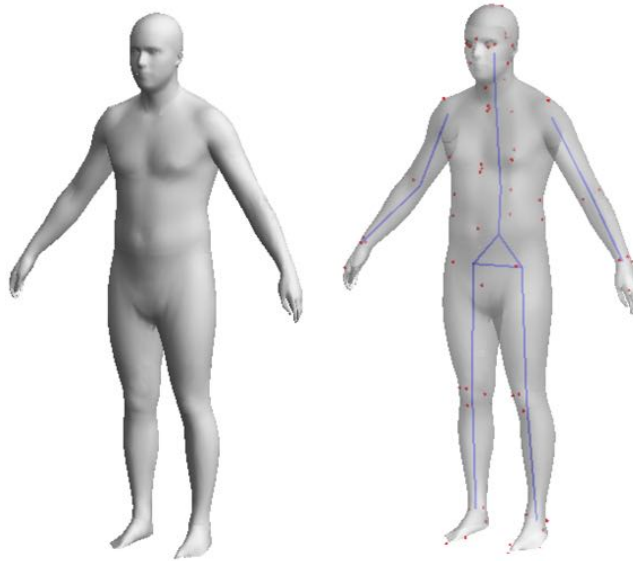


Figure 40. Midsize male with stature = 1755 mm, body weight = 82.3 kg, sitting height = 918 mm (median male values from Paquette et al. 2009). The image on the right shows surface landmarks and internal joint center location predictions.

UNCLASSIFIED

## UNCLASSIFIED

Table 36  
 Predicted Standing Surface Landmark Locations for Midsize Male\*

Landmark	X	Y	Z	Landmark	X	Y	Z
BackOfHead_Ct_L	-191	-41	1038	Suprapatella_Rt_L	-190	111	-99
TopOfHead_Ct_L	-267	7	1138	Infrapatella_Rt_L	-169	103	-161
Tragion_Rt_L	-196	93	1015	Heel_Rt_L	-62	10	-591
EyeCorner_Rt_L	-268	125	1024	Toe_Ct_Rt_L	-247	198	-601
EyeCenter_Rt_L	-287	118	1014	FemoralEpiCon_Med_Lt_M	-257	-26	-119
Glabella_Ct_L	-321	108	1041	Suprapatella_Lt_L	-323	-26	-100
EyeCenter_Lt_L	-330	73	1014	Infrapatella_Lt_L	-312	-45	-159
EyeCorner_Lt_L	-335	53	1024	Malleolus_Lat_Lt_M	-274	-135	-545
Tragion_Lt_L	-301	-15	1016	Heel_Lt_L	-213	-144	-591
Acromion_Ant_Rt_H	-107	158	844	Toe_Ct_Lt_L	-404	37	-602
HumeralEpiCon_Lat_Rt_M	49	221	566	Gonion_Lt_L	-307	2	962
Wrist_Lat_Rt_L	104	373	357	Infrathyroid_Ct_L	-275	64	885
Wrist_Med_Rt_L	57	398	361	Gonion_Rt_L	-215	99	961
WristMidTop_Rt_M	83	385	374	BustPoint_Rt_L	-226	170	664
HandMetCarp2_Med_Rt_L	70	452	278	Omphalion_Ct_L	-312	104	442
Acromion_Ant_Lt_H	-364	-112	846	ThighJn_CtMidline_Rt_L	-197	155	321
HumeralEpiCon_Lat_Lt_M	-429	-261	564	CrotchMidThighHt_Ct_L	-295	87	256
HumeralEpiCon_Med_Lt_M	-398	-217	531	ThighJn_CtMidline_Lt_L	-357	-7	323
Wrist_Lat_Lt_L	-580	-314	354	TopOfHeadOnMesh	-243	31	1138
Wrist_Med_Lt_L	-604	-266	364	BackOfHeadOnMesh	-242	38	1137
WristMidTop_Lt_M	-593	-295	372	TopOfHeadReHardSeat	-181	-31	1038
HandMetCarp5_Lat_Lt_L	-602	-327	266	BackOfHeadReHardSeat	-182	-30	1052
HandMetCarp2_Med_Lt_L	-659	-276	277	Suprasternale_RB	-255	47	818
SpineC07_Ct_M	-184	-25	905	Substernale_RB	-298	86	632
SpineT04_Ct_M	-149	-61	797	AcromionOffsetRt	-101	153	841
SpineT08_Ct_M	-138	-71	672	AcromionOffsetLt	-359	-117	843
SpineT12_Ct_M	-154	-54	543	ShoulderJntRt	-91	140	788
SpineL03_Ct_M	-155	-50	463	ShoulderJntLt	-349	-130	790
Acromion_Ant_Rt_M	-107	158	844	Heel_Rt_Calc	-62	10	-588
Acromion_Ant_Lt_M	-364	-112	846	MetaTars1_Med_Rt_Calc	-216	126	-592
Suprasternale_Ct_L	-264	53	827	MetaTars5_Lat_Rt_Calc	-128	171	-603
Suprasternale_Ct_M	-272	59	811	Toe_Ct_Rt_Calc	-246	199	-601
Substernale_Ct_L	-308	95	621	Malleolus_Lat_Rt_Calc	-68	72	-540
Substernale_Ct_M	-304	90	645	Malleolus_Med_Rt_Calc	-130	39	-522
Iliocrystal_Rt_M	-108	130	460	MetaTars1_Med_Lt_Calc	-331	9	-595
Rib10_Lt_M	-333	-93	527	MetaTars5_Lat_Lt_Calc	-374	-79	-604
Iliocrystal_Lt_M	-334	-102	465	Toe_Ct_Lt_Calc	-404	38	-602
FemoralEpiCon_Lat_Rt_M	-122	115	-111	Malleolus_Lat_Lt_Calc	-274	-138	-543
FemoralEpiCon_Med_Rt_M	-183	47	-123	Malleolus_Med_Lt_Calc	-242	-76	-526

\* Coordinate system is arbitrary with z axis vertical.

UNCLASSIFIED

Table 37  
 Predicted Standing Joint Center Locations for Midsize Male\*

Joint Name	X	Y	Z
ElbowJntRt	30	202	547
ElbowJntLt	-408	-241	545
WristJntRt	88	390	358
WristJntLt	-585	-281	358
KneeJntRt	-153	81	-116
KneeJntLt	-292	-61	-118
AnkleJntRt	-99	56	-531
AnkleJntLt	-248	-109	-545
HeadNeckJnt	-243	26	991
C7T1Jnt	-227	20	865
T12L1Jnt_RB	-203	-5	551
L5S1Jnt_FitLower	-212	5	406
HipJntRt	-159	76	306
HipJntLt	-283	-50	306

\* Coordinate system is arbitrary with z axis vertical.

### *Seated Body Shape*

A seated body shape model was constructed using methods similar to those employed for the standing data. A total 338 scans from 126 men in scanwear postures L1, SR1, R2, and R3 were used. The model was parameterized by stature, BMI, ratio of erect sitting height to stature, and two torso posture variables: recline and flexion. Torso recline was parameterized by the angle of the vector from the L3 to C7 surface landmarks with respect to vertical. Flexion (of the lumbar spine) was parameterized by the angle of the vector from L3 to T12 relative to the vector for T12 to C7.

Figure 41 illustrates the effect of anthropometric variables in the seated body shape model. Stature and BMI were exercised over the 5<sup>th</sup> - to 95<sup>th</sup>-percentile values in the data. Figure 42 shows a range of postures achievable with the model, and Figure 43 shows a set of randomly generated figures spanning a large range of the input variables.

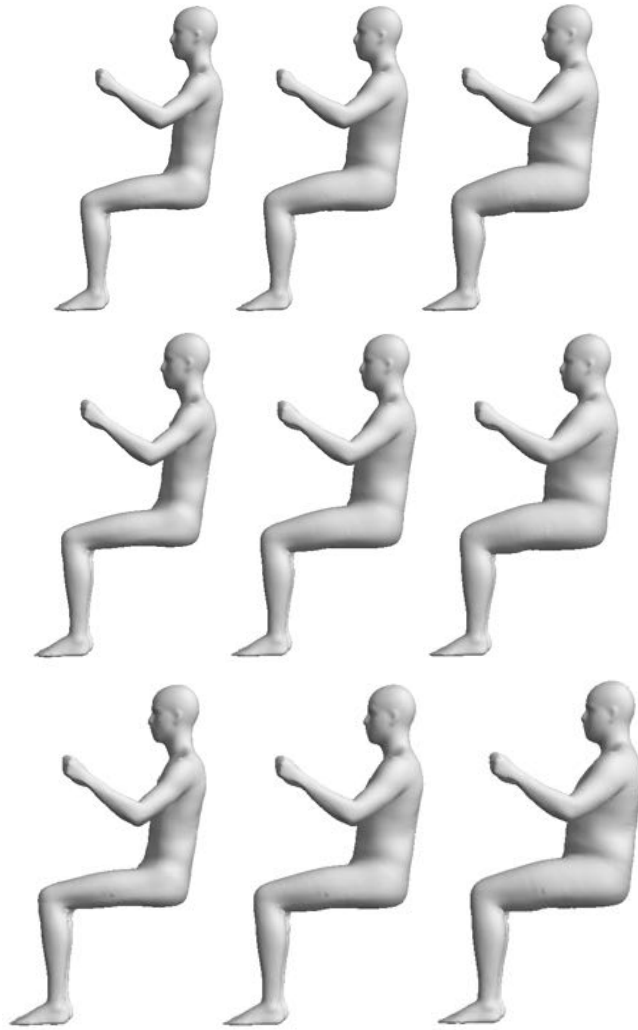


Figure 41. Anthropometric effects in the seated body shape model. The columns from left to right are 5<sup>th</sup>, 50<sup>th</sup>, and 95<sup>th</sup>-percentile BMI from Table 19. The rows from top to bottom are 5<sup>th</sup>, 50<sup>th</sup>, and 95<sup>th</sup>-percentile statures from Table 19.



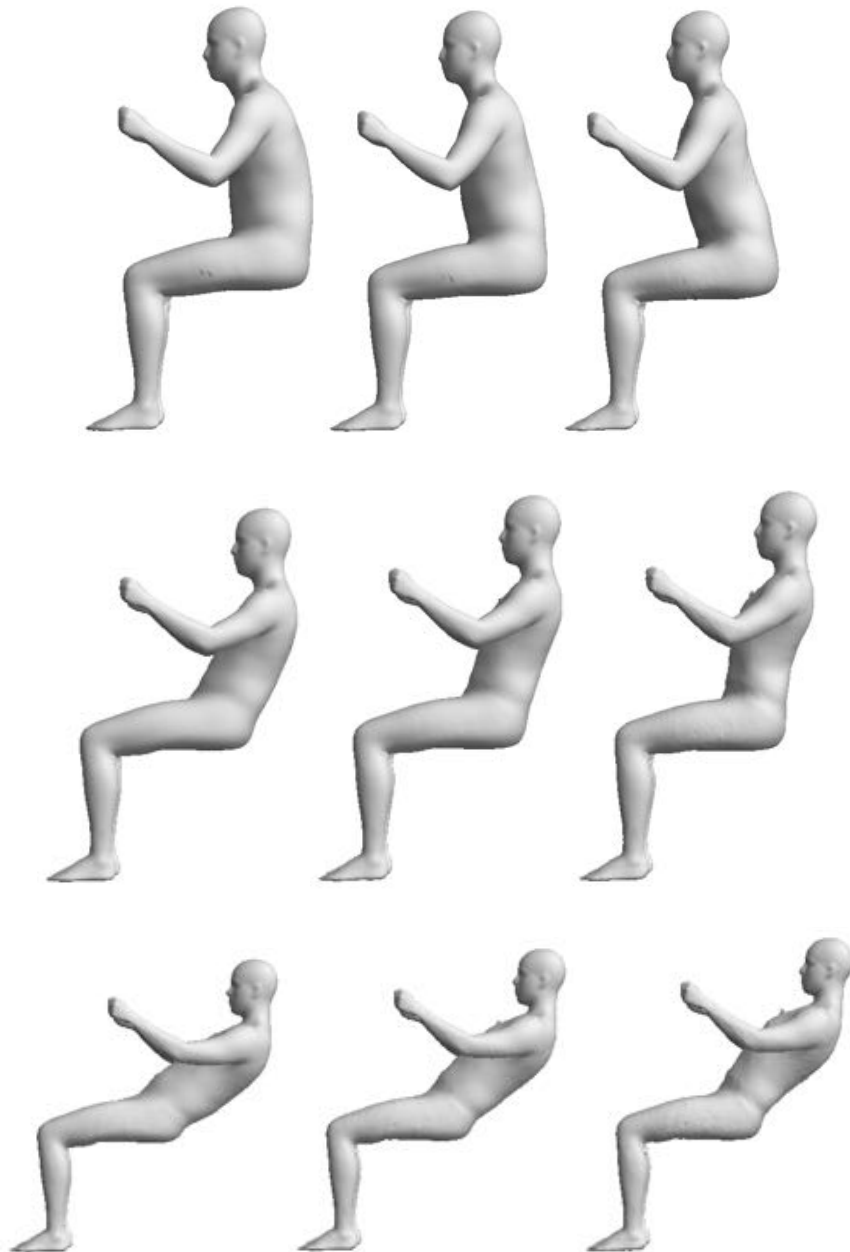


Figure 42. Posture effects in the seated body shape model. The columns from left to right show a range of lumbar spine flexion. The rows from top to bottom show a range of recline.

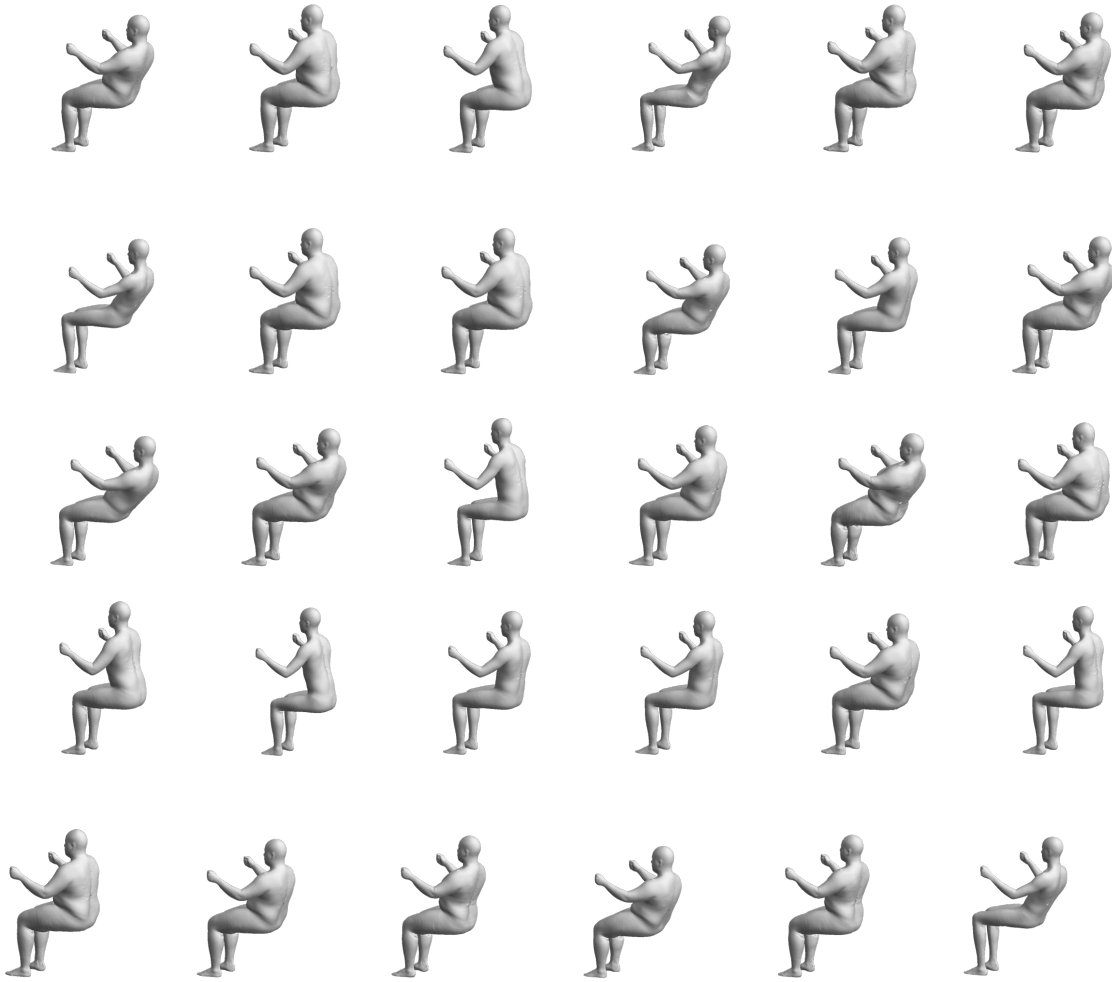


Figure 43. A range of postures and body shapes generated by the seated body shape model.

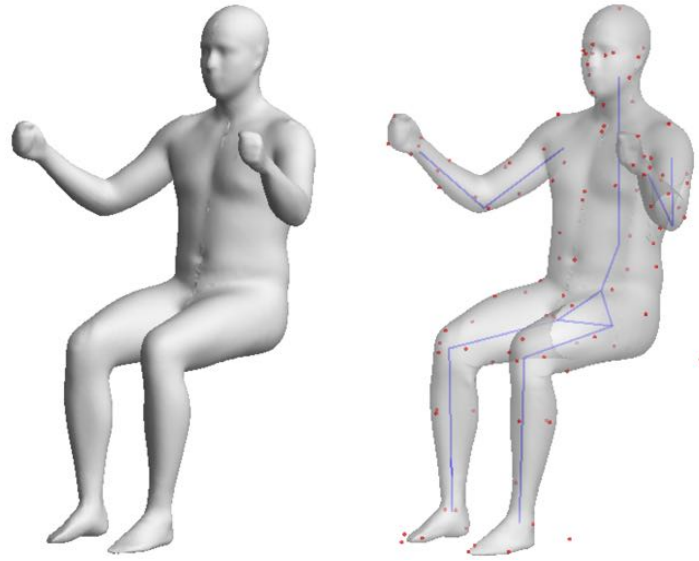


Figure 44. Midsize male model with stature = 1755 mm, body weight = 82.3 kg, sitting height = 918 mm (median male values from Paquette et al. 2009) and recline and lumbar flexion values set to zero (see text for definitions). The image on the right shows surface landmarks and internal joint center location predictions.

## UNCLASSIFIED

Table 38  
 Predicted Seated Landmark Locations for Midsize Male\*

Landmark	X	Y	Z	Landmark	X	Y	Z
BackOfHead_Ct_L	233	-22	665	Rib10_Rt_M	124	149	166
TopOfHead_Ct_L	146	-1	769	Iliocristal_Rt_M	135	156	98
Tragion_Rt_L	137	74	646	Rib10_Lt_M	119	-159	163
EyeCorner_Rt_L	61	50	656	Iliocristal_Lt_M	128	-166	101
EyeCenter_Rt_L	50	33	649	FemoralEpiCon_Lat_Rt_M	-350	175	-103
Glabella_Ct_L	35	1	676	FemoralEpiCon_Med_Rt_M	-361	81	-109
EyeCenter_Lt_L	49	-32	649	Suprapatella_Rt_L	-378	136	-65
EyeCorner_Lt_L	60	-49	657	Infrapatella_Rt_L	-403	138	-121
Tragion_Lt_L	134	-76	647	Malleolus_Lat_Rt_M	-333	149	-536
Acromion_Ant_Rt_H	132	175	479	Malleolus_Med_Lt_M	-318	-65	-444
HumeralEpiCon_Lat_Rt_M	2	342	251	Malleolus_Med_Rt_M	-354	99	-530
HumeralEpiCon_Med_Rt_M	-24	278	226	Heel_Rt_L	-278	119	-587
Wrist_Lat_Rt_L	-227	387	370	MetaTars1_Med_Rt_L	-486	105	-593
Wrist_Med_Rt_L	-212	366	414	MetaTars5_Lat_Rt_L	-432	205	-599
WristMidTop_Rt_M	-202	382	390	Toe_Ct_Rt_L	-538	132	-602
HandMetCarp5_Lat_Rt_L	-303	406	398	FemoralEpiCon_Lat_Lt_M	-355	-165	-107
HandMetCarp2_Med_Rt_L	-284	402	470	FemoralEpiCon_Med_Lt_M	-367	-64	-104
Acromion_Ant_Lt_H	131	-186	478	Suprapatella_Lt_L	-388	-120	-64
HumeralEpiCon_Lat_Lt_M	-10	-346	251	Infrapatella_Lt_L	-411	-121	-118
HumeralEpiCon_Med_Lt_M	-32	-286	220	Malleolus_Lat_Lt_M	-336	-136	-542
Wrist_Lat_Lt_L	-243	-377	372	Heel_Lt_L	-216	-169	-588
Wrist_Med_Lt_L	-222	-359	416	MetaTars1_Med_Lt_L	-500	-75	-591
WristMidTop_Lt_M	-219	-376	389	MetaTars5_Lat_Lt_L	-469	-162	-600
HandMetCarp5_Lat_Lt_L	-316	-394	400	Toe_Ct_Lt_L	-548	-93	-600
HandMetCarp2_Med_Lt_L	-297	-391	472	InnerThigh_Ct_E	-95	1	-29
SpineC07_Ct_M	218	-5	522	ThighJnct_Lat_Rt_L	8	169	13
SpineT04_Ct_M	248	-6	405	ThighJnct_Med_Rt_L	-102	17	-30
SpineT08_Ct_M	249	-8	287	ThighJnct_Med_Lt_L	-107	-13	-32
SpineT12_Ct_M	224	-10	166	ThighJnct_Lat_Lt_L	-142	-329	6
SpineL03_Ct_M	217	-10	77	Axilla_Ant_Lt_L	64	-180	390
Acromion_Ant_Rt_M	132	175	478	Axilla_Ant_Rt_L	69	171	389
Acromion_Ant_Lt_M	131	-185	478	Axilla_Pos_Rt_L	199	198	347
Suprasternale_Ct_L	96	-3	460	Axilla_Pos_Lt_L	194	-206	346
Suprasternale_Ct_M	86	-4	447	CenterButtocks_E	182	-1	-127
Substernale_Ct_L	11	-3	269	Chin_Tip_Ct_L	38	-2	550
Substernale_Ct_M	19	-4	291	Nose_Tip_Ct_L	15	1	624

\* Coordinate system is arbitrary with z axis vertical.

UNCLASSIFIED

Table 39  
 Predicted Seated Joint Center Locations for Midsize Male\*

Joint	X	Y	Z
HeadNeckJnt	160.1	2.4	586.3
C7T1Jnt	171.9	3.4	458.9
T12L1Jnt	188.7	-0.8	147.5
L5S1Jnt	118.9	2.3	24.6
HipJntRt	54.4	93.0	-57.8
HipJntLt	48.8	-88.7	-57.2
ShoulderJntRt	161.9	178.0	386.5
ShoulderJntLt	163.9	-177.9	386.6
ElbowJntRt	-1.9	309.4	224.5
ElbowJntLt	-7.5	-306.6	226.6
WristJntRt	-198.8	378.3	373.4
WristJntLt	-212.4	-368.6	370.2
KneeJntRt	-368.9	129.6	-111.3
KneeJntLt	-372.7	-116.1	-111.9
AnkleJntRt	-339.6	121.3	-537.3
AnkleJntLt	-345.6	-101.0	-541.0

\* Coordinate system is arbitrary with z axis vertical.

### *Effects of PPE and ENC*

The effects of PPE and body-borne gear on space claim for the seated soldier are important for the design of seats and vehicle interiors. An examination of the scan data showed that the greatest increase in space requirements for both PPE and ENC conditions is observed in the waist area. After considering a range of alternative calculations, a fairly simple method to quantify the encumbered dimensions was adopted.

Analyses were conducted using ACU, PPE, and ENC scans from the L1 condition, which provided good scan access to the front and lateral areas of the torso. A horizontal plane was established 50 mm above a lateral target digitized on the outer ammo pouches of the ENC kit, chosen because this height was at or close to the maximum breadth. Figure 45 shows this plane location on an example scan. Points on the scan within 25 mm of this plane were extracted and the most-lateral, most-forward, and most-rearward points were identified. The fore-aft distance between the most-forward and most-rearward points was calculated as the abdomen area depth, and the lateral distance between the most-lateral points on the right and left sides was calculated as the abdomen area width. Similar calculations were then performed using the ACU and PPE conditions using the plane height for each subject identified in the ENC scan. In this way, the abdomen area dimensions were measured at approximately the same location at each garb level.

Figure 46 shows abdomen area depth and breadth measures at three garb levels. Not surprisingly, adding PPE and ENC increased the abdomen area dimensions significantly, with the largest change observed in the transition from PPE to ENC.



Figure 45. Abdomen area plane used to quantify depth and breadth.

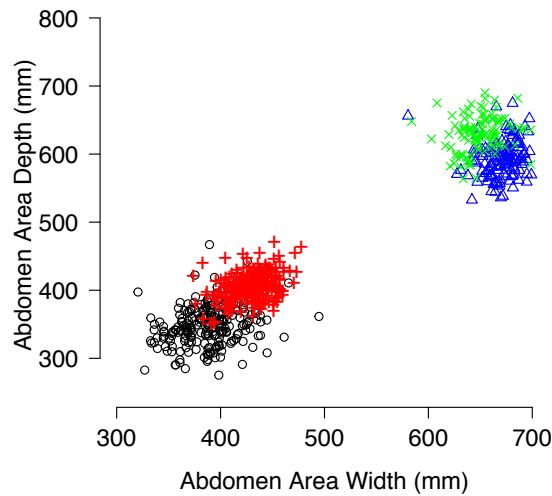


Figure 46. Abdomen area dimensions for ACU (o), PPE (+), ENC-Rifleman ( $\Delta$ ), and ENC-SAW (x) conditions. See text for measurement definitions.

Figure 47 shows that abdomen area depth was significantly related to BMI across all garb levels, with no interaction. That is, higher BMI was associated with the same increase in abdomen area depth regardless of garb level. Relative to the ACU level, the mean abdomen area depth of 349 mm was increased by 56 mm with the addition of PPE, by 244 mm with the addition of ENC-Rifleman, and by 281 mm by ENC-SAW. The lack of interaction with body size means that the effects of encumbrance on abdomen area depth are effectively constant across individuals, and hence can be evaluated on a small number of individuals rather than requiring a large and diverse sample.

Figure 48 shows abdomen area breadth as a function of BMI and garb level. The effect of BMI is negligible for ENC-Rifleman and minimal for ENC-SAW, but otherwise is similar to the effects on abdomen area depth. Relative to the ACU level, the mean abdomen area breadth of 389 mm was increased by 41 mm with the addition of PPE, by 281 mm with the addition of ENC-Rifleman, and by 260 mm by ENC-SAW. The results show that the lateral space claim requirements at the ENC levels are essentially independent of body size, and hence can be assessed accurately using individuals of any size wearing the gear. Depth measures are dependent on subject BMI, but the difference in measures between ACU and ENC conditions is independent of body size.

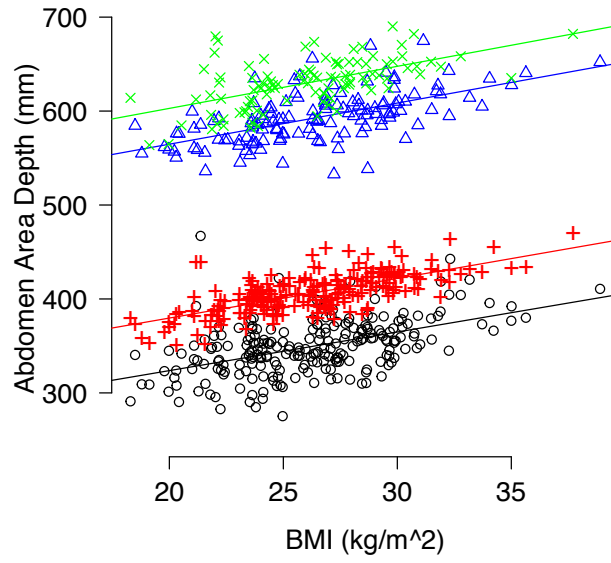


Figure 47. Abdomen area depth as a function of BMI and garb level for ACU (o), PPE (+), ENC-Rifleman ( $\Delta$ ), and ENC-SAW (x) conditions.

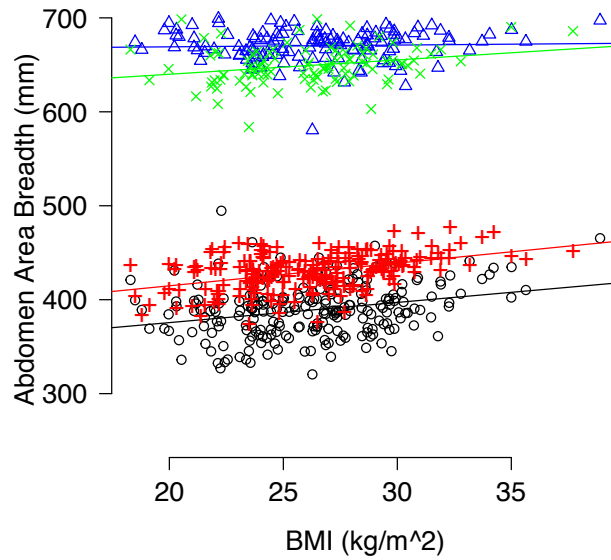


Figure 48. Abdomen area breadth as a function of BMI and garb level for ACU (o), PPE (+), ENC-Rifleman ( $\Delta$ ), and ENC-SAW (x) conditions.



## APPLICATIONS

### **Posture Prediction for Human Figure Models**

This report presents the first detailed, empirical posture-prediction model based on soldier postures in realistic military seating scenarios. The study conditions were selected to be complementary to previous studies at UMTRI covering passenger cars, light trucks, and commercial trucks and buses. The combined data and posture-prediction models now cover the feasible range of conventional driver layouts with a steering wheel, pedals, and adjustable seat.

The application of these results to driver posture prediction is straightforward, following the Cascade Prediction Model approach presented by Reed et al. (2002). This approach prioritizes the accurate prediction of seat position, hip location, and eye location, with the remainder of the posture predicted from those results. The input variables are the vehicle package dimensions and the reference anthropometry for the human figure model (stature, BMI, and erect sitting height). Garb level is also an input to the new model. The seat position (height and fore-aft location of the translated seat H-point) is predicted first, followed by hip location relative to H-point. Next, eye location is predicted relative to hip location. Torso segment orientations are predicted from the hip-eye vector angle, and finally lower and upper extremity postures are predicted by inverse kinematics. For squad postures, the approach is similar, except that seat position is not predicted.

As with previous vehicle occupant posture-prediction models developed at UMTRI, we expect these results to be easily implemented in commercial human modeling software packages, such as the Jack Occupant Packaging Toolkit from Siemens and the Vehicle Occupant Accommodation Tool from Dassault Systemes. These implementations will make the posture prediction readily accessible to the Army and its contractors and suppliers. UMTRI will also make a spreadsheet available that constitutes the reference implementation of the posture prediction models for use in verification of the commercial tools as well as additional applications, such as posturing manikins in CAD software.

### **Vehicle Accommodation Models**

The posture-prediction models were developed to be readily adapted to the development of vehicle accommodation tools. Work is currently underway in a separate project to create a seating accommodation model, eyellipse, and other population accommodation models using these results. The methods are based on Reed et al. (2005), which uses normal-distribution approximations along with the linear posture models to obtain predictions of population distributions of key variables. We expect that these tools will also be readily implemented in commercial software systems.

### **Creation of 3D Body Shapes**

The body shape models presented in this report are the first available based on U.S. Soldier body shapes that encompass both seated and standing postures. The standing body shape model is already being implemented in the Jack human figure modeling software for use by the Army. Both the male standing and seated models, as well as female body shape models created by merging these data with those from other UMTRI studies, will be made available for commercial

software implementation. Importantly, the methods used to perform the template fitting and conduct the shape analysis can be readily implemented with expanded datasets or with alternative templates, such as those from other commercial manikin systems. The body shape models are expected to have a wide range of applications ranging from seat design assessment to the evaluation of body armor and clothing. The data have been used to create anthropometric specifications for a midsize-male Warrior Injury Assessment Manikin (WIAMan) intended for use in physical testing to assess occupant protection in underbody blast events (Reed 2013).

### **Spatial Effects of Body Armor and Encumbrance**

This report presents the first analysis of the effects of body armor and encumbrance on posture and space claim for seated soldiers. These data and analysis results will be widely used for vehicle interior design, and particularly for the design of seats and restraint systems that interact closely with body armor and encumbrance. The results can be applied in several ways. The findings regarding increase in abdomen area width and depth can be used to design vehicle interior layout and seat dimensions. The effects on posture can be used via human posture prediction and population accommodation modeling. Finally, the scan data themselves can be used as examples for assessing restraint designs and routing.

## DISCUSSION

### **Innovation in Methods**

This study is the first systematic examination of soldier postures in realistic vehicle seating environments, and the first to assess the effects of body armor and encumbrance on seated postures. The basic posture-measurement methods have been applied before in a range of UMTRI studies, but this study is the first to use detailed hardseat measurements to interpret posture data obtained from sitters wearing garb that restricts access to anterior torso landmarks. This necessitated new methods for constructing subject-specific skeletal linkages and fitting them to data from seating trials.

The methods also represented considerable innovation in body scanning techniques, notably in the recording of many seated postures; previous studies have recorded only one or a few seated postures. Of particular interest, this is the first study of adults to have gathered body shape data from a large number of individuals in a wide range of supported seated postures relevant for vehicle and seat design. Moreover, the scan data include body armor and two levels of encumbrance, providing a rich data source for modeling soldier body shape and space claim.

### **Posture Data and Models**

The posture prediction models in this report are the first available obtained from soldiers and the first from any population spanning this important range of vehicle packages at the high end of the SAE Class-A range (passenger cars and light trucks) and the low end of the SAE Class-B range (commercial trucks and buses). Based on the success and widespread use of previous UMTRI posture-prediction models for drivers and passengers, we expect widespread use of the new models. Importantly, they can be applied to military vehicle design with confidence that they accurately reflect the unique attributes and experiences of soldiers as well as the effects of soldier-specific garb and gear.

As noted above, the posture-prediction models will be adapted to develop accommodation models that predict population distributions of key variables, such as eye location, rather than the postures of particular individuals. This provides key flexibility for laying out seat tracks, assessing interior and exterior vision, and providing sufficient headroom and knee clearance. Another ongoing study will couple seated reach capability, difficulty, and kinematics data to the static predictions given in the current work.

### **Body Shape Data and Models**

This project developed the first body shape models of seated soldiers and the first body shape models for supported seated postures based on large numbers of subjects and postures. Previous work (Reed et al. 2008) used morphing techniques to alter unsupported postures to approximate supported postures, but the current methods are based on more-relevant scans and a wide range of postures.

## Limitations

As with any empirical study, this work has a number of important limitations. The soldiers who volunteered were a convenience sample. As documented above, the anthropometric distributions are remarkably similar to the most recent data available for the Army, particularly for men, but this population should not be assumed to represent the Army or any subset of interest. Reweighting or modeling will always need to be done to apply the current results.

Postures were measured in short-duration, static conditions with no ride motion, in minimal seating mockups. The driver mockup included a simulated headliner, but the positioning was such that no headroom interference was produced. Any effects of exterior vision restriction are also not represented, although previous UMTRI research has shown that these are of secondary importance (Reed et al. 2000, Reed 2006). No actual driving task was simulated; steering wheel efforts, shifter actuation, clutching, and reaching to other controls might alter drivers' posture and position.

In the driver mockup, a fairly large percentage of soldiers left the seat back angle at the original setting. Although this angle was chosen as the mean expected angle in advance of the study, it's likely that some fraction of these drivers would have chosen a different angle in a more relaxed or longer-duration situation. However, it's likely that as a group their mean angles would be similar. As noted above, the back angle and hip-eye angle analyses were not meaningfully different when the non-adjusters were excluded. Importantly, the seat height and seat fore-aft adjustment data did not show evidence of non-adjustment behavior. The seat position and back angle data in the driver mockup were free of censoring, meaning that it's reasonable to assume that all drivers were able to select a comfortable posture.

The driver and crew mockups used particular seats that may have affected the postures beyond the controlled variables, such as crew seat back angle. The driver seat, a typical commercial truck seat, had modest bolstering; a seat with more prominent bolsters might have produced a larger effect of body armor and encumbrance. The crew seat had no bolsters, and in fact was deliberately chosen as the least featured among several considered. However, unlike in some current crew/squad seats, no relief for the hydration pack was provided. If present, a relief feature would likely have reduced the effects of the encumbered conditions on torso posture and fore-aft hip location. The crew seat was equipped with a five-point harness, but there was no evidence that the harness affected posture, since it was donned after the soldier was seated. The crew conditions did not consider the effects of substantial foot position restrictions, such as limiting the feet to a narrow area. The statistically significant effect of seat height on pelvis orientation suggests that much-lower or much-higher effective seat heights produced by foot position restriction might affect torso posture.

The crew posture prediction models include effects of seat back angle that may not extrapolate well beyond the 0-to-10-degree range studied. In particular, the effect of seat back angle on thorax orientation in this range is opposite in sign to that observed in previous studies examining

seat back angles between 20 and 30 degrees, where the thorax lags behind the seat back as the angle increases. Consequently, care should be taken in extrapolating to more-reclined seat back angles. Also, seat cushion angle was fully correlated with seat back angle across the conditions, so the data do not provide independent information on the effects of seat cushion angle.

The scanning conditions were chosen and carefully controlled to obtain a wide range of postures and body shapes. However, the unnatural situation of being in a scanner with only small supports means that the scanned postures should not be interpreted directly as likely or typical seated postures. Rather, the postures obtained in the vehicle seat mockups can be used with statistical models based on the scan data to obtain good predictions of the body shapes of seated soldiers.

### **Future Work**

The rich data set gathered in this study will provide the foundation for a wide range of future research and applications. In addition to the follow-on studies on accommodation modeling and reach that are already underway, additional analyses of both the seated posture and body shape data could be undertaken.

Primary consideration should be given to developing more advanced and more complete models of body shape. For example, the two models presented above are based on only 5 of the postures measured in the study. The data include extensive information on the patterns of body shape change with shoulder and spine movement that could be exploited to develop more complex shape models useful for improving the design of a wide range of garments and protective equipment. The scan data from soldiers with body armor and encumbrance could also be analyzed more completely than in the current report. In particular, a library of encumbered shapes could be created as a virtual assessment panel to assess seat and restraint systems.

Given the current body of knowledge, smaller studies could be conducted to extend the data in important ways. For example, a focused study could examine the effects of a wider range of squad seating conditions, including novel seat designs that provide relief for gear or support for body armor.

The current study measured only 53 women. This sample was large enough to state with confidence that no important posture differences are likely between men and women in these conditions after accounting for overall body size, but the data are insufficient to develop female body shape models. A larger sample of female soldiers in the scanner conditions would be valuable for creating a parallel to the male body shape models presented above. Such models would be particularly valuable for developing body armor specifically tailored to female anatomy.

**REFERENCES**

- Allen, B., Curless, B., and Popovic, Z. (2003). The space of human body shapes: reconstruction and parameterization from range scans. *Proceedings of the 2003 International Conference on Computer Graphics and Interactive Techniques (SIGGRAPH)*. San Diego, CA.
- Bennink, H.E., Korbeeck, J.M., Janssen, B.J., and Romenij, B.M. (2006). Warping a neuro-anatomy atlas on 3D MRI data with radial basis functions. *Proceedings of the 2006 International Conference on Biomedical Engineering*. pp. 214-218.
- Bush T.R., and Gutowski P.E. (2003). An approach for hip joint center calculation for use in seated postures. *Journal of Biomechanics*, 36:1739–43.
- Carr, J.C., Beatson, R.K., Cherrie, J.B., Mitchell, T.J., Fright, W.R., McCallum, B.C., and Evans, T.R. (2001). Reconstruction and representation of 3D objects with radial basis functions. *SIGGRAPH 01: Proceedings of the 28th Annual Conference on Computer Graphics and Interactive Techniques*. ACM.
- Chaffin, D.B. (2003). *Digital Human Modeling for Vehicle and Workplace Design*. SAE International, Warrendale, PA.
- Dempster, W.T. (1955). Space requirements of the seated operator: Geometrical, kinematic, and mechanical aspects of the body with special reference to the limbs. WADC Technical Report No. 55-159. Wright-Patterson Air Force Base, OH: Wright Air Development Center.
- Flanagan, C.A.C., Manary, M.A., Schneider, L.W., and Reed, M.P. (1998). An improved seating accommodation model with applications to different user populations. Technical Paper No. 980651. Warrendale, PA: Society of Automotive Engineers, Inc.
- Gordon, C. C., Churchill, T., Clauser, C.E., Bradtmiller, B., McConville, J.T., Tebbetts, I., and R. A. Walker, (1989). *1988 Anthropometric Survey of U.S. Army Personnel: Methods and Summary Statistics*, Final Report. Technical Report NATICK/TR-89/027, U.S. Army Natick Research, Development and Engineering Center, Natick, MA.
- Hotzman, J., Gordon, C.C., Bradtmiller, B., Corner, B.D., Mucher, M., Kristensen, S., Paquette, S., and Blackwell, C.L. (2011). *Measurer's Handbook: U.S. Army and Marine Corps Anthropometric Surveys*. Technical Report NATICK/TR-11/017. U.S. Army Natick Soldier RD&E Center.
- Manary, M.A., Flanagan, C.A.C., Reed, M.P., and Schneider, L.W. (1998). Development of an improved driver eye position model. *SAE Transactions: Journal of Passenger Cars*, 107(6): 43-50.
- Meldrum, J.F. (1965). *Automobile driver eye position*. Technical Paper 650464. Warrendale, PA: Society of Automotive Engineers, Inc.

- Paquette, S., Gordon, C., and Bradtmiller, B. (2009). Anthropometric Survey (ANSUR) II Pilot Study: Methods and Summary Statistics. Technical Report NATICK/TR-09/014. U.S. Army Natick Soldier Research, Development, and Engineering Center, Natick, MA.
- Parkinson, M.B., Reed, M.P., Kokkolaras, M., and Papalambros, P.Y. (2005). Robust truck cabin layout optimization using advanced driver variance models. *Proceedings of 2005 ASME Design Engineering Technical Conference*. ASME, New York.
- Parkinson, M.B. and Reed, M.P. (2006). Optimizing vehicle occupant packaging. *SAE Transactions: Journal of Passenger Cars – Mechanical Systems*, 115: 890-901.
- Parkinson, M.B., Reed, M.P., Kokkolaras, M., Papalambros, P.Y. (2007). Optimizing truck cab layout for driver accommodation. *Journal of Mechanical Design*, 129(11):1110-1117.
- Reed, M.P., Manary, M.A., and Schneider, L.W. (1999). Methods for measuring and representing automobile occupant posture. Technical Paper 990959. Society of Automotive Engineers, Warrendale, PA.
- Reed, M.P., Manary, M.A., and Schneider, L.W. (2000). The effects of forward vision restriction on automobile driver posture. *Transportation Human Factors*, 2(2). 173-179.
- Reed, M.P., Manary, M.A., Flannagan, C.A.C., and Schneider, L.W. (2002). A statistical method for predicting automobile driving posture. *Human Factors*, 44 (4): 557-568.
- Reed, M.P. (2005). Development of a New Eyellipse and Seating Accommodation Model for Trucks and Buses. Technical Report UMTRI-2005-30. University of Michigan Transportation Research Institute, Ann Arbor, MI.
- Reed, M.P. (2006). Accommodation Models for Truck Driver Knee Clearance, Abdomen Clearance, and Shifter Location. Technical Report UMTRI-2006-30. University of Michigan Transportation Research Institute, Ann Arbor, MI.
- Reed, M.P. and Parkinson, M.B. (2008). Modeling variability in torso shape for chair and seat design. DETC2008-49483. *Proceedings of the ASME Design Engineering Technical Conferences*. ASME, New York.
- Reed, M.P. (2011). An eyellipse for rear seats with fixed seat back angles. Technical Paper 2011-01-0596. *SAE International Journal of Passenger Cars– Mechanical Systems*.
- Reed, M.P. (2013). Development of Anthropometric Specifications for the Warrior Injury Assessment Manikin (WIAMan). UMTRI Technical Report 2013-38. University of Michigan Transportation Research Institute, Ann Arbor, MI.
- Robinette, K., Blackwell, S., Daanen, H. and Boehmer, M. (2002) *Civilian American and European Surface Anthropometry Resource (CAESAR), Final Report, Vol. 1*. United States Air Force Research Laboratory, Wright-Patterson Air Force Base, OH.
- SAE International (2012). *SAE Handbook*. SAE International, Warrendale, PA.

UNCLASSIFIED

Seidl, A. (1997). RAMSIS - a new CAD-tool for ergonomic analysis of vehicles developed for the German automotive industry. Technical Paper 970088. Warrendale, PA: Society of Automotive Engineers, Inc.

UNCLASSIFIED



UNCLASSIFIED

## **APPENDIX A CONSENT FORM**

### **The University of Michigan Transportation Research Institute Informed Consent for Experimental Procedure Soldier-Centered Vehicle Seating Design Tools based on Measurement and Modeling of Soldiers**

This study is funded by the U.S. Army. The purpose of this study is to obtain data on human body dimensions, postures, and body shapes. The data will be used to improve the design of Army vehicles to make them safer and more comfortable for soldiers. Representatives of the Army may review your research records from this study.

The investigators will take measurements of your body that describe your body proportions and size. Your seating posture and position will be recorded using a digital coordinate measurement device as you sit in 10 to 20 vehicle seat conditions as a driver or passenger. You will be measured while wearing minimal clothing provided to you (shorts for men, shorts and a sports bra for women), wearing your uniform, and wearing your uniform with body armor and other protective equipment. The testing will require 2 to 3 hours.

The investigator will touch points on your body to record their locations with a measurement probe. Measurement points include landmarks on the head, chest, pelvis, and extremities. You have observed a demonstration of the measurement point locations and agree that it is acceptable for the experimenter to touch those locations.

Your body surface shape will be recorded using a laser scanner. The laser light is similar to the light used in supermarket checkout machines. The laser light causes no discomfort and is not harmful to the skin or eyes. You will need to remain still in a seated or standing position for about 15 seconds during each measurement. Approximately 20 to 30 measurements will be taken with the scanner.

Photographs will be taken during testing to document your posture. Your face will be obscured in any photographs used in publications or presentations.

Your participation in this study is voluntary and conditional on review of your physical qualifications relative to experimental design criteria. If you choose not to participate, no data will be obtained from you.

The Transportation Research Institute is a research organization and, as such, your records and personal information may be reviewed by research staff. The data gathered in this study will be used in scientific publications and presentations only in coded form not identifying you. The data obtained will be retained indefinitely for analysis.

The researchers have taken steps to minimize the risks of this study. Even so, you may still experience some risks related to your participation, even when the researchers are careful to avoid them. These risks include injury due to exertion when performing the requested tasks. Minor skin irritation may occur due to the paint used to identify body landmarks. Please tell the researchers about any concerns or problems you have during the study. By signing this form, you do not give up your right to seek payment if you are harmed as a result of being in this study.

If significant new knowledge is obtained during the course of this research, which may relate to your willingness to continue participation, you will be informed of this knowledge. The person listed below may be contacted for more information about any aspect of this study. If you have questions about your rights as a research participant, or wish to obtain information, ask questions or discuss any concerns about this study with someone other than the researcher(s), please contact the University of Michigan

Health Sciences and Behavioral Sciences Institutional Review Board, 540 E Liberty St., Ste 202 Ann Arbor, MI 48104-2210, (734) 936-0933 [toll free, (866) 936-0933], irbhsbs@umich.edu.

UNCLASSIFIED



**APPENDIX B  
DEMOGRAPHICS FORM**

Subject Number: \_\_\_\_\_

Date: \_\_\_\_\_

1. What is your gender?  Male  Female

2. What is your current rank / grade?

- | Enlisted                         | Warrant Officer              | Officer                       |
|----------------------------------|------------------------------|-------------------------------|
| <input type="checkbox"/> Private | <input type="checkbox"/> W01 | <input type="checkbox"/> 2LT  |
| <input type="checkbox"/> PV2     | <input type="checkbox"/> CW2 | <input type="checkbox"/> 1LT  |
| <input type="checkbox"/> PFC     | <input type="checkbox"/> CW3 | <input type="checkbox"/> CAPT |
| <input type="checkbox"/> CPL     | <input type="checkbox"/> CW4 | <input type="checkbox"/> MAJ  |
| <input type="checkbox"/> SPC     | <input type="checkbox"/> CW5 | <input type="checkbox"/> LTC  |
| <input type="checkbox"/> SGT     |                              | <input type="checkbox"/> COL  |
| <input type="checkbox"/> SSG     |                              | <input type="checkbox"/> BG   |
| <input type="checkbox"/> SFC     |                              | <input type="checkbox"/> MG   |
| <input type="checkbox"/> MSG     |                              | <input type="checkbox"/> LTG  |
| <input type="checkbox"/> 1SG     |                              | <input type="checkbox"/> GEN  |
| <input type="checkbox"/> SGM     |                              |                               |
| <input type="checkbox"/> CSM     |                              |                               |
| <input type="checkbox"/> SMA     |                              |                               |

3. Component:  Regular Army  Army Reserve  Army Nat'l Guard

4. Branch you are in:

- Combat Arms  Combat Service Support  
 Combat Support (CSS incl: Med, Vet, Dental, JAG, Chaplain,  
- - -)

5. Please identify your user identification code (UIC) by number:  
(ex: WJM5BO, W1D1AA, W6DW04)

\_\_\_\_\_

6. Please identify your primary military occupational specialty (MOS):  
(ex: 11B; 19D; 79R; 13B; 15P; 25X; 38B; 68A)

\_\_\_\_\_

UNCLASSIFIED

Subject Number: \_\_\_\_\_

Date: \_\_\_\_\_

7. Your Population Subgroup: (please mark all that apply)

White, not of Hispanic Origin

Black, not of Hispanic Origin

Hispanic (please mark all that apply)

Mexican

Latin American: \_\_\_\_\_

Puerto Rican

Other Hispanic: \_\_\_\_\_

Cuban

Asian or Pacific Islander (please mark all that apply)

Chinese

Japanese

Korean

Vietnamese

Filipino

Samoan

Guamanian/Chamorro

Melanesian

Micronesian

Polynesian

Other Pacific Islander: \_\_\_\_\_

Other Asian: \_\_\_\_\_

Native American (please mark all that apply)

Eskimo

Aleut

U.S./Canadian Tribe(s): \_\_\_\_\_

Other (please mark all that apply)

East / Asian Indian

Arab or Middle Eastern

Caribbean Islander

Other: \_\_\_\_\_

8. What group do you usually select on military questionnaires?

<input type="checkbox"/>	<input type="checkbox"/>	<input type="checkbox"/>	<input type="checkbox"/>	<input type="checkbox"/>	<input type="checkbox"/>	<input type="checkbox"/>
White	Black	Hispanic	Asian	Native Hawaiian/ Pacific Islander	Amer. Indian/ Alaskan Native	Other

\_\_\_\_\_

9. Age: \_\_\_\_\_

10. Birthdate: (mm/dd/yyyy) \_\_\_\_\_ / \_\_\_\_\_ / \_\_\_\_\_

## **APPENDIX C SUBJECT INTERACTION SCRIPTS**

### **Introduction Script**

Thank you for volunteering today. Over the next two hours, you will be participating in a scientific study investigating the shapes and sizes of soldiers' bodies.

We will start by measuring the size of your body with a set of rulers called anthropometers (*photo*). An investigator will touch your head, arms, legs, hips, lower back and chest.

We will measure the outside surface of your body with a scanning machine (*photo*). The machine uses a red laser light that is similar to the one used at the checkout of a grocery store. The laser is safe for eyes. The scanner does not produce X-rays, and it is not like the scanners at the airport that can see through clothes. The scanner can only record the outside of your body and clothing. Each scan takes 12 seconds, during which time you will have to stand or sit very still.

We will record the position of your body using a Faro Arm (*photo*) while you sit in different vehicle seats. An investigator will take the rounded tip of the arm and touch it to points on your body. A computer records the location of the tip. You will need to sit very still while we take these measurements.

We will also put marks on your skin with a pen, ink stamp and body paint. These marks help us take measurements. Please do not remove the marks until after we are finished with the study.

For some of the measurement you will wear your uniform, for others you will wear special testing clothing. The testing clothes include bicycle shorts (sports bra) and a swim cap.

## Driver Station Instruction Script

**Overview:** At this station we will ask you to sit in this driver seat, and then we will record your posture using this measurement arm.

*If they have not been introduced to the arm:* I will feel for the location of a bone, then touch that location with this tip and press a button. The amount of rotation at each of these joints tells the computer where in space this tip is. It is similar to a mouse on a computer. I will record points on your head, neck, chest, hips, arms and legs.

Please sit very still while we take the measurements otherwise we will have to start the measurements over. We will ask you to stand up at times so that we can make adjustments to the setup.

### ***In the First Condition:***

Please have a seat.

This is a simple seat but I am required to show you how the controls work.

When you turn this lever the seat back recline changes. Please try it out.

When you press this button the seat moves forward or backward. Please try it out.

When you press this button the seat moves up or down. Please try it out.

Please adjust the seat to a comfortable position for driving, as though you were going to be driving for a long time.

Please sit as though you were driving with your hands on the steering wheel and your right foot on the accelerator and your left foot flat on the floor.

*If they naturally sit centered left-right, in a symmetrical posture with the left foot flat on the floor and hands near the 2 and 10 position proceed to next instruction. Otherwise -*

- *If they are not centered left-right ask them to do so being sure to use the terms left and right, otherwise they might change their hip position forward-backward. For example say- Please move your rear-end left (or right) so that you are lined up with the seat.*
- *If their hands are in a different position or their feet are in some odd position, ask them to move their hands to 10 and 2, or place the left foot flat on the floor.*
- *If they say that this is how they usually or prefer to sit, say - I understand, but for this study we ask that everyone sit in a more standard driving position*
- *Further explanation if needed - We are not measuring your personal preference in this study, but rather how the different shapes and sizes of soldiers fit in seats and reach vehicle components.*

Relax your shoulders and look forward as though you are looking down the road. This is the position that I will need you to “freeze” in while I take measurements. Please stay frozen until I tell you to “unfreeze”. I may move your hands so that I can reach points on your body, but please keep the rest of your body frozen.

**After finishing measurements:**

Now please be very careful as you step out to the left. Stand on the floor facing away from the seat while I set up the next condition.

Please return to the seat. I have moved the seat, so you’ll need to adjust it again to get to your preferred position. Be sure to adjust the seat back angle, and adjust it forward and backward and up and down until you reach a comfortable posture.

## **Crew Station Instruction Script**

**Overview:** At this station we will ask you to sit in this crew seat, and then we will record the position of your body using this measurement arm.

*If they have not been introduced to the arm:* I will feel for the location of a bone, then touch that location with this tip and press a button. The amount of rotation at each of these joints tells the computer where in space this tip is. It is similar to a mouse on a computer. I will record points on your head, neck, chest, hips, arms and legs.

Please sit very still while we take the measurements otherwise we will have to start the measurements over. We will ask you to stand up at times so that we can make adjustments to the seat.

### ***For Each Condition:***

Please have a seat, then put on and tighten the 5-point harness.

*If they have not tightened the harness, remind them to do so.*

*If they say that they do not use the harness normally, say – I understand, but for this study we ask that you please wear it anyway.*

*If they naturally sit centered left-right, in a symmetrical posture with legs uncrossed, proceed to next instruction. Otherwise -*

- *If they are not centered left-right ask them to do so being sure to use the terms left and right, otherwise they might change their hip position forward-backward. For example say- Please move your rear-end left (or right) so that you are lined up with the seat.*
- *If their legs or ankles are crossed ask them to uncross them. If they say that this is how they usually or prefer to sit say - I understand, but for this study we ask that everyone sit with their legs and ankles uncrossed.*
- *Further explanation if needed - We are not measuring your personal preference in this study, but rather how soldiers or different shapes and sizes fit in seats.*

Please rest your palms on your thighs with your elbows at your sides.

Relax your shoulders and look straight ahead.

This is the position that I will need you to “freeze” in while I take measurements. Please stay frozen until I tell you to “unfreeze”. I may move your hands to reach your hips, but please keep the rest of your body frozen.



UNCLASSIFIED

**APPENDIX D  
POINTS DIGITIZED ON SCANS**

UNCLASSIFIED

Table D1  
Points Digitized on All Scans

Point Name	Body Part	Type of Point	Anatomical Reference	Additional Description	Point to Digitize
Mcar2MedLt_L	Arm	Landmark	Metacarpal 2 Medial Left	Knuckle – grip axis, index side	On landmark
Mcar2MedRt_L	Arm	Landmark	Metacarpal 2 Medial Right	Knuckle – grip axis, index side	On landmark
Mcar5LatLt_L	Arm	Landmark	Metacarpal 5 Lateral Left	Knuckle – grip axis, pinky side	On landmark
Mcar5LatRt_L	Arm	Landmark	Metacarpal 5 Lateral Right	Knuckle – grip axis, pinky side	On landmark
WristLatLt_L	Arm	Landmark	Ulnar Styloid	Styloid process on ulna (pinky side) lateral point on the wrist “bump”	On landmark
WristLatRt_L	Arm	Landmark	Ulnar Styloid	Styloid process on ulna (pinky side) lateral point on wrist “bump”	
WristMedLt_L	Arm	Landmark	Radial Styloid	Styloid process on radius (thumb side) – opposite of wrist “bump”	On landmark
WristMedRt_L	Arm	Landmark	Radial Styloid	Styloid process on radius (thumb side) – opposite of wrist “bump”	
EyeCenLt_L	Head	Landmark	Orbit at pupil center	Point on orbit below the eye at the same lateral position as the pupil when looking straight forward	On landmark
EyeCenRt_L	Head	Landmark	Orbit at Pupil Center	Point on orbit below the eye at the same lateral position as the pupil when looking straight forward	On landmark
EyeCorLt_L	Head	Landmark	Ectoorbitale	Point on orbit nearest the corner of eye	On landmark
EyeCorRt_L	Head	Landmark	Ectoorbitale	Point on orbit nearest the corner of eye	On landmark
HeadBackCt_L	Head	Landmark	Opistion	Most posterior point on head or helmet	On landmark
HeadGlabCt_L	Head	Landmark	Glabella	Smooth elevation of the frontal bone just above the bridge of the nose, between eyebrows	On landmark
HeadTopCt_L	Head	Landmark	Vertex	Most superior point on head or helmet	On landmark
HeadTragLt_L	Head	Landmark	Tragion	Notch just above the tragus of the ear	On landmark
HeadTragRt_L	Head	Landmark	Tragion	Notch just above the tragus of the ear	On landmark
CenterButtocks_E	Torso	Estimate		Most posterior midline point on the buttocks	Center of Estimate
InnerThighCt_E	Torso	Estimate		Most inferior midline point on torso – mid crotch point	Center of Estimate
AxillaLtFt_L	Torso	Land/Est	Axilla Left Front	Armpit Front	On landmark
AxillaLtRr_L	Torso	Land/Est	Axilla Left Rear	Armpit Rear	On landmark
AxillaRtFt_L	Torso	Land/Est	Axilla Right Front	Armpit Front	On landmark
AxillaRtRr_L	Torso	Land/Est	Axilla Right Rear	Armpit Rear	On landmark
ThighJnctLtLat_L	Torso	Land/Est	Thigh Junction Left Lateral	Thigh – abdominal junction, lateral point (defining a line)	On landmark
ThighJnctLtMed_L	Torso	Land/Est	Thigh Junction Left Medial	Thigh – abdominal junction, medial point (defining a line)	On landmark
ThighJnctRtLat_L	Torso	Land/Est	Thigh Junction Right Lateral	Thigh – abdominal junction, lateral point (defining a line)	On landmark
ThighJnctRtMed_L	Torso	Land/Est	Thigh Junction Right Medial	Thigh – abdominal junction, medial point (defining a line)	On landmark
WristMidTopLt_M	Arm	Stamp Marker		On the back of the wrist slightly proximal to the cross section plane of the ulnar styloid.	Proximal, nearest Ulnar Styloid

## UNCLASSIFIED

Point Name	Body Part	Type of Point	Anatomical Reference	Additional Description	Point to Digitize
WristMidTopRt_M	Arm	Stamp Marker		On the back of the wrist slightly proximal to the cross section plane of the ulnar styloid.	Proximal, nearest Ulnar Styloid

Table D2  
Landmarks Digitized on Scans with Scanwear

Point Name	Body Part	Type of Point	Anatomical Reference	Additional Description	Point to Digitize
FootMtar5LatLt_L	Leg	Landmark	Fifth Meta-tarsophalangeal Protrusion		On landmark
FootToe1Lt_L	Leg	Landmark	Longest Tibiale		On landmark
FootMtar1MedLt_L	Leg	Landmark	First meta-tarsophalangeal protrusion		On landmark
FootMtar1MedRt_L	Leg	Landmark	First Meta-tarsophalangeal Protrusion		On landmark
FootToe1Rt_L	Leg	Landmark	Longest tibiale		On landmark
FootMtar5LatRt_L	Leg	Landmark	Fifth Meta-tarsophalangeal Protrusion		On landmark
KneeSupLt_L	Leg	Landmark	Suprapatella	Most proximal point on left patella	On landmark
KneeInfLt_L	Leg	Landmark	Infrapatella	Most distal point on left patella	On landmark
KneeSupRt_L	Leg	Landmark	Suprapatella	Most proximal point on right patella	On landmark
KneeInfRt_L	Leg	Landmark	Infrapatella	Most distal point on right patella	On landmark
FootHeelRt_L	Leg	Landmark	Pternion	Most posterior point on right heel	On landmark
FootHeelLt_L	Leg	Landmark	Pternion	Most posterior point on left heel	On landmark
SternSupCt_L	Torso	Landmark	Suprasternale	Anterior surface of jugular notch	On landmark
SternSubCt_L	Torso	Landmark	Substernale		On landmark

UNCLASSIFIED

Table D3  
Markers Digitized on Scans with Scanwear

Point Name	Body Part	Type of Point	Anatomical Reference	Additional Description	Point to Digitize
ElbowLatRt_M	Arm	Stamp Marker	Humeral Epicondyle, Lateral	Lateral epicondyle (marker with elbow bent 90°)	Proximal, extensor surface
ElbowMedRt_M	Arm	Stamp Marker	Humeral epicondyle, medial	Medial epicondyle (marker with elbow bent 90°)	Proximal, extensor surface
ElbowMedLt_M	Arm	Stamp Marker	Humeral Epicondyle, Medial	Medial epicondyle (marker with elbow bent 90°)	Proximal, extensor surface
ElbowLatLt_M	Arm	Stamp Marker	Humeral epicondyle, lateral	Lateral epicondyle (marker with elbow bent 90°)	Proximal, extensor surface
KneeFemLatLt_M	Leg	Stamp Marker	Femoral Epicondyle, Lateral		Proximal, flexor surface
AnkleLatLt_M	Leg	Stamp Marker	Malleolous, Medial		Proximal, plantar flexion surface side
AnkleMedRt_M	Leg	Stamp Marker	Malleolous, Medial		Proximal, plantar flexion surface side
KneeFemMedRt_M	Leg	Stamp Marker	Femoral Epicondyle, Medial		Proximal, flexor surface
KneeFemMedLt_M	Leg	Stamp Marker	Femoral Epicondyle, Medial		Proximal, flexor surface
KneeFemLatRt_M	Leg	Stamp Marker	Femoral Epicondyle, Lateral		Proximal, flexor surface
AnkleLatRt_M	Leg	Stamp Marker	Malleolous, Lateral		Proximal, plantar flexion surface side
AnkleMedLt_M	Leg	Stamp Marker	Malleolous, Medial		Proximal, plantar flexion surface side
SpineC07_M	Torso	Stamp Marker	Cervicale	Spinous process of the 7 <sup>th</sup> cervical vertebra	Center
SpineT04_M	Torso	Stamp Marker	T4	Spinous process of 4 <sup>th</sup> thoracic vertebra	Center
SpineT08_M	Torso	Stamp Marker	T8	Spinous process of 8 <sup>th</sup> thoracic vertebra	Center
SpineT12_M	Torso	Stamp Marker	T12	Spinous process of 12 <sup>th</sup> thoracic vertebra	Center
SpineL03_M	Torso	Stamp Marker	L3	Spinous process of 3 <sup>rd</sup> lumbar vertebra	Center
10RibRt_M	Torso	Stamp Marker	Tenth Rib, Lateral	Most lateral point on the 10 <sup>th</sup> rib	Superior-Posterior
IlioRt_M	Torso	Stamp Marker	Iliocristale	Iliocristale (most superior lateral point on pelvis when standing)	Superior-Posterior
ChestUpper_M	Torso	Stamp Marker		Body midline, about one thumb's width down from suprasternal, (or about mid-manubrium)	Superior, Soldier's Left
ChestLower_M	Torso	Stamp Marker		Body midline, first flat, boney surface on sternum body above belly	Superior, Soldier's Left
10RibLt_M	Torso	Stamp Marker	Tenth Rib, Lateral	Most lateral point on the 10 <sup>th</sup> rib	Superior-Posterior
IlioLt_M	Torso	Stamp Marker	Iliocristale	Iliocristale (most superior lateral point on pelvis when standing)	Superior-Posterior
AcromionLt_H	Torso	Hemisphere	Acromion	Center of hemisphere on most anterior point on the acromion	Center of hemisphere

## UNCLASSIFIED

<b>Point Name</b>	<b>Body Part</b>	<b>Type of Point</b>	<b>Anatomical Reference</b>	<b>Additional Description</b>	<b>Point to Digitize</b>
AcromionRt_H	Torso	Hemi-sphere	Acromion	Center of hemisphere on most anterior point on the acromion	Center of hemisphere

Table D4  
Landmarks and Markers Digitized on Scans with Uniform

Point Name	Body Part	Type of Point	Anatomical Reference	Additional Description	Point to Digitize
ElbowLatLt_E	Arm	Estimate		Estimate of lateral elbow	Center of Estimate
WristMidTopLt_E	Arm	Estimate		On the back of the wrist slightly proximal to the cross section plane of the ulnar styloid.	Proximal, nearest Ulnar Styloid
WristMidTopRt_E	Arm	Estimate		On the back of the wrist slightly proximal to the cross section plane of the ulnar styloid.	Proximal, nearest Ulnar Styloid
AnkleLatRt_E	Leg	Estimate	Malleolous, Lateral	Estimate of lateral ankle on boot	Center of estimate
AnkleMedLt_E	Leg	Estimate	Malleolous, Medial	Estimate of medial ankle on boot	Center of estimate
KneeSupLt_E	Leg	Estimate		Estimate of suprapatella	Center of Estimate
KneeInfLt_E	Leg	Estimate		Estimate of infrapatella	Center of Estimate
AnkleMedRt_E	Leg	Estimate	Malleolous, Medial	Estimate of medial ankle on boot	Center of estimate
AnkleLatLt_E	Leg	Estimate	Malleolous, Lateral	Estimate of lateral ankle on boot	Center of estimate
BootHeelRt_U	Leg	Landmark		Bottom edge of sole at midline	
BootHeelLt_U	Leg	Landmark		Bottom edge of sole at midline	
BootToeRt_U	Leg	Landmark		Bottom edge of sole, longest shoe point	
BootToeLt_U	Leg	Landmark		Bottom edge of sole, longest shoe point	
CollarPtC7_E	Torso	Estimate		Estimate of C7 when clothed	Center of Estimate
ElbowLatRt_C	Arm	Velcro marker	Humeral Epicondyle, Lateral	Lateral epicondyle marked with elbow in scan position	Center of marker
ElbowMedRt_C	Arm	Velcro marker	Humeral Epicondyle, Medial	Medial epicondyle marked with elbow in scan position	Center of marker
KneeFemLatRt_C	Leg	Velcro marker	Femoral Epicondyle, Lateral	Lateral condyle marked with the knee in scan position	Center of marker
KneeSupRt_C	Leg	Velcro marker	Suprapatella	Most proximal point on patella marked in scan position	Center of marker
KneeInfRt_C	Leg	Velcro marker	Infrapatella	Most distal point on patella marked in scan position	Center of marker
KneeFemMedRt_C	Leg	Velcro marker	Femoral Epicondyle, Medial	Medial condyle marked with the knee in scan position	Center of marker

## UNCLASSIFIED

Table D5  
Points Digitized on Scans with PPE

Point Name	Body Part	Type of Point	Additional Description	Corner of Marker
IOTVRt_M	PPE	Tape Marker	Vest marker	Superior-Posterior
IOTVTop_M	PPE	Tape Marker	Vest marker	Superior-Posterior
IOTVLt_M	PPE	Tape Marker	Vest marker	Superior-Posterior
HelmetFt_M	PPE	Tape Marker	Helmet marker _ most anterior	Superior-Posterior
HelmetMd_M	PPE	Tape Marker	Helmet marker – most superior in the middle	Superior-Posterior
HelmetRr_M	PPE	Tape Marker	Helmet marker – most posterior	Superior-Posterior

Table D6  
Points Digitized on Scans with Encumbrances

Point Name	Body Part	Type of Point	Additional Description	Corner of Marker
CamelBakRt_M	ENC	Tape Marker	Hydration backpack marker	Superior-Posterior
CamelBakCt_M	ENC	Tape Marker	Hydration backpack marker	Superior-Posterior
CamelBakLt_M	ENC	Tape Marker	Hydration backpack marker	Superior-Posterior
TAPSLt_M	ENC	Tape Marker	TAPS system marker	Superior-Posterior
TAPSCt_M	ENC	Tape Marker	TAPS system marker	Superior-Posterior
TAPSRt_M	ENC	Tape Marker	TAPS system marker	Superior-Posterior

UNCLASSIFIED

Table D7  
Points Digitized on Avatar

Point Name	Body Part	Additional Description for Investigators
Gonion Lt L	Head	Corner of jaw
Infrathyroid Ct L	Head	Adam's apple
Gonion Rt L	Head	Corner of jaw
BustPoint Rt L	Torso	Most anterior point on pectoral muscle or bust
BustPoint Lt L	Torso	Most anterior point on pectoral muscle or bust
Omphalion Ct L	Torso	Belly button (or center of belly button crease)
ArmUpper Ant Rt L	Arm	<p>Three points on each limb segment</p> <p>These points ring-around the middle of each segment on the anterior, posterior and lateral surfaces a determined in a neutral standing position. Nothing on the medial surface, as the inner thighs and inner arms usually do not scan well. Note: the anterior arm points will be pointing posterior when the shoulder is flexed (A1)- but still digitized the point on the biceps...etc.</p>
ArmUpper Lat Rt L	Arm	
ArmUpper Pos Rt L	Arm	
ArmLower Ant Rt L	Arm	
ArmLower Lat Rt L	Arm	
ArmLower Pos Rt L	Arm	
ArmLower Pos Lt L	Arm	
ArmLower Ant Lt L	Arm	
ArmUpper Ant Lt L	Arm	
ArmUpper Pos Lt L	Arm	
LegUpper Ant Lt L	Leg	
LegUpper Lat Lt L	Leg	
LegUpper Pos Lt L	Leg	
LegLower Ant Lt L	Leg	
LegLower Lat Lt L	Leg	
LegLower Pos Lt L	Leg	
LegLower Pos Rt L	Leg	
LegLower Lat Rt L	Leg	
LegLower Ant Rt L	Leg	
LegUpper Ant Rt L	Leg	
LegUpper Lat Rt L	Leg	
LegUpper Pos Rt L	Leg	
ThighJn CtMidline Rt L	Leg/Torso	On the top (anterior) midline of the thigh where it contacts the abdomen.
ThighJn CtMidline Lt L	Leg/Torso	On the top (anterior) midline of the thigh where it contacts the abdomen.
CrotchMidThighHt Ct L	Leg/Torso	Center of crotch at the mid-thigh height

Research assistants used Meshlab (V1.3.1) to extract landmark locations. A scan with grayscale texture and a template of the point names listed in Tables D1-D6 were imported into the program. Using a mouse the research assistant selected a name from the list and then digitized the corresponding point on the scan. Next the Avatar of the same scan was imported, and the points in Table D7 were digitized. The research assistants received training on how to locate the landmarks on the scan and only digitized the points that were visible leaving missing or obscured landmarks as uncollected. There were four types of landmarks: 1) markers attached to the soldier over a boney landmark or to track equipment, 2) boney landmarks that were visibly apparent but without a marker, 3) edges of a contour or 4) an estimates of anatomical planes or of landmarks covered by clothing. Tables D8-D11 list these types of landmarks and measures of reproducibility in locating them. Multiple researchers digitized a scan and then a standard deviation of the distances (both total distance and distance along 3 axes) of the points to the mean location was calculated. This process was repeated across multiple scans including standing and sitting postures and with soldiers wearing different levels of garb. The averages of the standard deviations are reported.



## UNCLASSIFIED

Table D8  
 Reproducibility Values for Landmarks with Markers Digitized on Scans

Point Names	Number of:			Average of Standard Deviations Across Scans (mm)			
	Points Collected	Scans Digitized	Postures Included	Total	Along Axis 1	Along Axis 2	Along Axis 3
10RibLt_M	151	23	6	1.0	1.6	0.9	1.6
10RibRt_M	150	23	6	1.0	1.7	0.9	1.6
AnkleLatLt_M	151	23	6	1.3	1.8	1.1	2.1
AnkleLatRt_M	151	23	6	1.3	1.8	2.5	1.1
AnkleMedLt_M	78	12	4	1.0	1.5	0.8	1.5
AnkleMedRt_M	82	13	5	2.8	3.2	5.5	3.5
ChestLower_M	152	23	6	1.4	2.1	2.3	1.6
ChestUpper_M	152	23	6	1.3	2.0	2.3	1.3
DiagPlatform_Ft_M	56	8	2	1.5	1.5	2.3	2.3
DiagPlatform_Rr_M	58	9	2	2.0	1.2	3.1	2.8
E_CamelBakCt_M	18	3	2	1.2	2.0	1.5	1.2
E_CamelBakLt_M	18	3	2	3.9	5.3	6.5	6.5
E_CamelBakRt_M	19	3	2	0.9	1.6	1.0	1.6
ElbowLatLt_M	152	23	6	1.5	2.1	1.4	2.5
ElbowLatRt_M	150	23	6	1.1	1.8	1.7	1.0
ElbowMedLt_M	100	15	4	1.6	2.3	1.7	3.0
ElbowMedRt_M	88	13	4	2.3	3.0	3.6	2.9
IlioLt_M	143	21	5	1.3	1.8	1.0	2.1
IlioRt_M	145	21	5	1.0	1.5	1.0	1.2
KneeFemLatLt_M	151	23	6	1.2	2.0	1.4	1.6
KneeFemLatRt_M	148	22	6	2.0	2.2	3.5	2.1
KneeFemMedLt_M	127	20	6	1.3	2.3	1.2	1.8
KneeFemMedRt_M	122	19	5	2.0	2.1	4.4	1.6
P_HelmetFt_M	38	6	4	1.2	2.3	1.1	1.3
P_HelmetMd_M	38	6	4	1.0	1.3	1.4	1.0
P_HelmetRr_M	38	6	4	1.1	1.8	1.4	0.9
P_IOTVlt_M	38	6	4	1.2	2.4	1.9	1.6
P_IOTVRt_M	38	6	4	1.0	1.9	1.2	1.6
P_IOTVTop_M	38	6	4	1.4	2.0	1.6	1.7
Seat_Lt_M	40	6	2	2.1	3.0	3.3	3.0
Seat_Rt_M	47	7	2	2.1	1.9	3.8	2.4
SpineC07_M	149	23	6	1.0	1.4	1.6	1.1
SpineL01_M	111	17	4	0.7	1.2	1.2	0.7
SpineL03_M	152	23	6	0.8	1.4	1.1	0.8
SpineT04_M	152	23	6	0.9	1.5	1.3	0.7
SpineT08_M	144	21	5	0.9	1.3	1.1	0.8
SpineT12_M	126	19	6	0.8	1.5	1.1	0.9
WristMidTopLt_M	146	23	6	1.6	2.6	2.2	2.0
WristMidTopRt_M	151	23	6	1.6	2.5	1.6	2.3
U_ElbowLatRt_C	51	9	6	1.7	1.9	3.2	2.1
U_ElbowMedRt_C	22	4	2	6.4	10.8	10.6	10.3
U_KneeFemLatRt_C	49	8	6	1.5	2.5	1.9	1.5
U_KneeFemMedRt_C	44	7	5	2.2	3.9	3.5	2.0
U_KneeInfRt_C	48	8	6	1.5	2.1	1.2	1.7
U_KneeSupRt_C	53	9	6	1.7	1.6	1.0	2.4
AcromionLt_H	152	23	6	1.7	1.9	3.0	2.5
AcromionRt_H	151	23	6	2.1	2.6	3.8	5.6

UNCLASSIFIED

## UNCLASSIFIED

Table D9  
 Reproducibility Values for Landmarks without Markers Digitized in Scans

Point Names	Number of:			Average of Standard Deviations Across Scans (mm)			
	Points Collected	Scans Digitized	Postures Included	Total	Along Axis 1	Along Axis 2	Along Axis 3
AxillaLtFt_L	205	32	12	5.6	11.0	6.4	6.6
AxillaLtRr_L	204	32	12	9.0	14.6	7.1	12.4
AxillaRtFt_L	205	32	12	7.4	12.1	6.1	7.5
AxillaRtRr_L	204	32	12	9.7	16.5	12.8	9.4
BustPoint_Lt_L	141	19	4	3.8	5.2	6.3	2.9
BustPoint_Rt_L	141	19	4	3.8	5.4	5.2	5.0
ChinTipCt_L	151	23	6	2.0	3.6	3.1	2.1
EyeCenLt_L	202	32	12	1.8	3.4	2.3	1.7
EyeCenRt_L	202	32	12	1.5	2.7	1.8	1.7
EyeCorLt_L	201	32	12	2.0	2.2	3.5	1.7
EyeCorRt_L	196	32	12	2.5	2.8	2.6	4.5
FootHeelLt_L	148	23	6	3.6	7.0	4.3	3.3
FootHeelRt_L	152	23	6	3.4	7.0	4.0	2.9
FootMtar1MedLt_L	136	22	6	3.9	7.9	4.2	6.0
FootMtar1MedRt_L	145	23	6	4.6	6.9	4.5	7.5
FootMtar5LatLt_L	135	21	6	4.2	3.5	4.7	6.6
FootMtar5LatRt_L	140	22	6	4.2	4.2	5.3	6.7
FootToe1Lt_L	146	22	6	1.9	3.1	2.9	2.1
FootToe1Rt_L	152	23	6	1.8	2.9	3.3	2.1
Gonion_Lt_L	141	19	4	5.3	7.5	4.9	9.5
Gonion_Rt_L	141	19	4	6.4	6.9	7.0	11.0
HeadBackCt_L	204	32	12	8.4	12.0	11.2	13.1
HeadGlabCt_L	205	32	12	1.5	3.0	1.4	1.1
HeadTopCt_L	185	32	12	9.0	5.7	15.6	17.1
HeadTragLt_L	184	30	12	3.7	7.2	4.4	5.0
HeadTragRt_L	193	32	12	3.9	7.7	5.1	5.8
Infrathyroid_Ct_L	141	19	4	5.0	7.4	4.6	7.2
KneeInfLt_L	152	23	6	8.2	13.3	10.3	5.3
KneeInfRt_L	152	23	6	8.3	14.6	9.5	6.1
KneeSupLt_L	151	23	6	5.0	6.3	10.0	4.5
KneeSupRt_L	152	23	6	7.5	7.4	12.8	8.4
Mcar2MedLt_L	186	29	9	2.3	3.4	3.2	3.2
Mcar2MedRt_L	204	32	12	2.5	3.9	3.7	3.4
Mcar5LatLt_L	185	29	9	2.4	4.1	3.3	2.8
Mcar5LatRt_L	199	31	11	2.9	4.4	3.5	3.4
NoseTipCt_L	149	22	5	1.3	2.3	1.5	1.1
Omphalion_Ct_L	135	19	4	3.2	6.0	2.8	2.7
SternSubCt_L	146	23	6	10.2	20.6	5.6	9.2
SternSupCt_L	152	23	6	3.4	6.4	2.7	3.0
WristLatLt_L	159	23	6	3.9	6.4	5.3	4.7
WristLatRt_L	159	23	6	4.8	6.0	6.9	5.3
WristMedLt_L	160	25	8	5.0	7.1	8.7	5.6
WristMedRt_L	158	25	8	5.6	7.8	7.8	5.8

UNCLASSIFIED

## UNCLASSIFIED

Table D10  
 Reproducibility Values for Contours Points Digitized on Scans

Point Names	Number of:			Average of Standard Deviations Across Scans (mm)			
	Points Collected	Scans Digitized	Postures Included	Total Distance	Along Axis 1	Along Axis 2	Along Axis 3
ArmLowerAntLt_L	141	19	4	7.3	13.1	9.5	7.7
ArmLowerAntRt_L	141	19	4	5.9	7.6	9.2	6.2
ArmLowerLatLt_L	141	19	4	6.9	12.2	7.6	11.9
ArmLowerLatRt_L	141	19	4	6.6	10.6	8.1	7.8
ArmLowerPosLt_L	141	19	4	7.4	11.4	13.1	8.0
ArmLowerPosRt_L	141	19	4	7.2	10.7	11.6	7.5
ArmUpperAntLt_L	141	19	4	7.2	10.9	10.6	6.3
ArmUpperAntRt_L	141	19	4	7.7	12.9	9.6	7.4
ArmUpperLatLt_L	141	18	3	6.6	12.7	5.7	10.6
ArmUpperLatRt_L	141	19	4	7.2	11.6	7.5	7.8
ArmUpperPosLt_L	141	19	4	7.5	11.8	11.0	8.8
ArmUpperPosRt_L	141	19	4	8.1	13.3	12.0	8.4
CrotchMidThighHtCt_L	141	19	4	10.7	21.4	9.6	14.3
LegLowerAntLt_L	141	19	4	9.8	23.8	9.9	6.2
LegLowerAntRt_L	141	19	4	7.9	16.2	6.3	4.1
LegLowerLatLt_L	141	19	4	12.2	25.3	13.2	7.0
LegLowerLatRt_L	141	19	4	8.7	19.0	3.6	8.2
LegLowerPosLt_L	141	19	4	11.9	26.7	12.9	4.8
LegLowerPosRt_L	141	19	4	8.1	16.3	6.4	5.0
LegUpperAntLt_L	135	19	4	11.2	11.4	15.9	8.1
LegUpperAntRt_L	138	19	4	13.2	20.0	19.3	12.0
LegUpperLatLt_L	141	19	4	9.6	14.9	10.2	11.3
LegUpperLatRt_L	141	19	4	13.9	24.0	17.4	15.9
LegUpperPosLt_L	135	19	4	9.4	12.3	15.1	9.8
LegUpperPosRt_L	136	19	4	13.9	20.4	21.3	12.3
ThighJnctLtLat_L	197	32	12	17.7	32.3	24.6	23.0
ThighJnctLtMed_L	189	32	12	13.8	30.2	16.5	17.0
ThighJnctMidlineLt_L	141	19	4	11.3	17.8	23.4	12.7
ThighJnctMidlineRt_L	141	19	4	11.4	16.5	14.8	16.3
ThighJnctRtLat_L	196	32	12	16.9	31.2	23.3	25.8
ThighJnctRtMed_L	188	32	12	14.1	30.0	17.1	17.3

UNCLASSIFIED

## UNCLASSIFIED

Table D11  
 Reproducibility Values for Estimated Landmarks Digitized on Scans

Point Names	Number of:			Average of Standard Deviations (mm)			
	Points Collected	Scans Digitized	Postures Included	Total	Along Axis 1	Along Axis 2	Along Axis 3
CenterButtocks_E	205	31	11	8.6	16.6	8.9	7.1
InnerThighCt_E	200	31	11	10.2	20.3	7.0	9.6
U_AnkleLatLt_E	52	9	6	7.4	14.5	8.9	5.7
U_AnkleLatRt_E	53	9	6	6.2	11.5	9.2	4.8
U_AnkleMedLt_E	36	7	6	9.8	17.9	14.9	7.9
U_AnkleMedRt_E	43	9	6	7.1	9.1	13.2	7.4
U_CollarPtC7_E	48	9	6	10.8	18.5	11.2	13.3
U_ElbowLatLt_E	53	9	6	9.3	15.1	9.5	15.2
U_KneeInfLt_E	53	9	6	5.0	12.6	3.7	5.6
U_KneeSupLt_E	53	9	6	5.0	10.0	4.1	7.0
U_WristMidTopLt_E	45	9	6	7.5	12.1	10.2	8.8
U_WristMidTopRt_E	43	9	6	5.2	12.5	11.0	6.1
CenterButtocks_E	205	31	11	8.6	16.6	8.9	7.1
InnerThighCt_E	200	31	11	10.2	20.3	7.0	9.6

UNCLASSIFIED

## APPENDIX E

### TECHNIQUES FOR MEASURING AND REPRESENTING POSTURE

#### HARD SEAT

##### Hard Seat Data Collection

The locations of body landmarks were measured using a FARO Arm coordinate digitizer while the soldiers sat in a specially designed laboratory “hard seat” that provides access to posterior landmarks on the spine and pelvis (Figure E1). Table E1-E3 list and define the landmarks which were recorded using measurement methods derived from those used in previous studies of automotive posture (Reed et al. 1999, Reed et al. 2005, Reed et al. 2006). Figures E2-E4 illustrate the locations of some of the key landmarks. Figure E1 shows a soldier being measured in the hard seat. The FARO Arm coordinate system was set with the X axis parallel to the sagittal plane of the seated soldier.

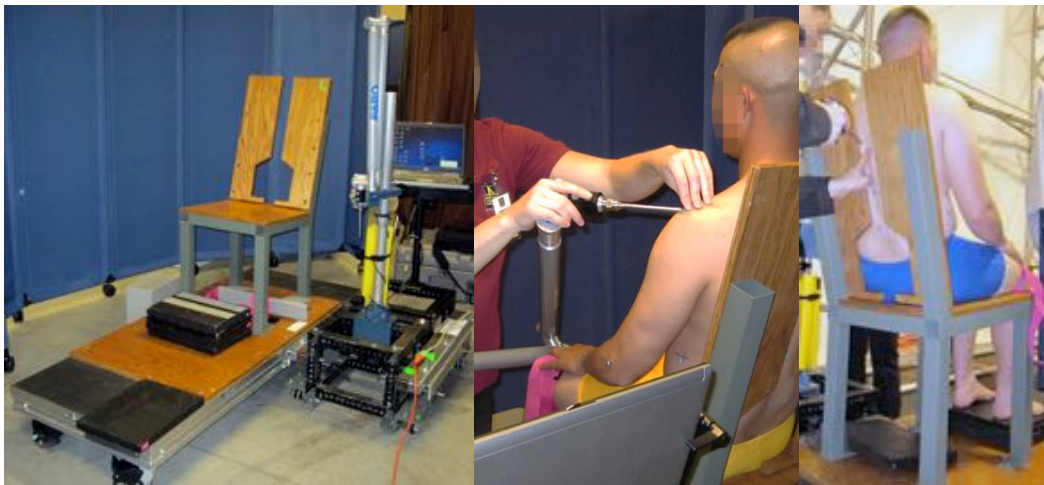


Figure E1. The hard seat with back cutaway to enable measurement of spine and back of the pelvis with a FARO Arm.

UNCLASSIFIED

Table E1  
List of Landmarks Digitized in Hard Seat

Back Of Head	Ulnar Styloid Process (L)
Top Of Head (Vertex)	Radial Styloid Process (L)
Tragion (L)	Lateral Femoral Epicondyle (L&R)
Ectoorbitale (L)	Medial Femoral Epicondyle (L&R)
Infraorbitale at Pupil Center (L)	Suprapatella (L&R)
Glabella	Infrapatella (L&R)
Suprasternale	Lateral Malleolus (L)
Substernale	Medial Malleolus (L)
C7, T4, T8, T12, L1- L5	Ball of Foot Medial (L)
Posterior Superior Iliac Spine (L&R*)	Toe (Longest Tibiale) (L)
Anterior Superior Iliac Spine (L&R)	Ball of Foot Lateral (L)
Acromion (L&R)	Heel (L)
Lateral Humeral Epicondyle (L)	
Medial Humeral Epicondyle (L)	

\* L and R = left and right

## UNCLASSIFIED

Table E2  
Definitions of Head and Trunk Landmarks Digitized in the Hard Seat

<b>Landmark</b>	<b>Definition</b>
Back Of Head	Undepressed skin surface point at the most posterior on the midsagittal plane of the head when head is in the Frankfurt horizontal. Hair is lightly compressed,
Top Of Head (Vertex)	Undepressed skin surface at the highest point on the midsagittal plane of the head when head is in the Frankfurt horizontal.
Tragion	Undepressed skin surface point obtained by palpating the most anterior margin of the cartilaginous notch just superior to the tragus of the ear
Ectoorbitale	Undepressed skin surface point located at the lateral junction of the upper and lower eyelids
Infraorbitale at Pupil Center	Undepressed skin surface point located at the lateral location of the pupil when the soldier is looking straight forward, obtained by palpating the inferior margin of the eye orbit (eye socket)
Glabella	Undepressed skin surface point obtained by palpating the most forward projection of the forehead in the midline at the level of the brow ridges.
Suprasternale (manubrium)	Undepressed skin surface point at the superior margin of the jugular notch of the manubrium on the midline of the sternum
Substernale (xyphoid process)	Depressed skin surface point at the inferior margin of the sternum on the midline
Cervicale (C7)	Depressed skin surface point at the most posterior aspect of the seventh cervical vertebra spinous process.
T4	Depressed skin surface point at the most posterior aspect of the fourth thoracic vertebra spinous process
T8	Depressed skin surface point at the most posterior aspect of the eighth thoracic vertebra spinous process
T12	Depressed skin surface point at the most posterior aspect of the twelfth thoracic vertebra spinous process
L1	Depressed skin surface point at the most posterior aspect of the first lumbar vertebra spinous process
L2	Depressed skin surface point at the most posterior aspect of the second lumbar vertebra spinous process
L3	Depressed skin surface point at the most posterior aspect of the third lumbar vertebra spinous process
L4	Depressed skin surface point at the most posterior aspect of the fourth lumbar vertebra spinous process
L5	Depressed skin surface point at the most posterior aspect of the fifth lumbar vertebra spinous process
Anterior Superior Iliac Spine (ASIS)	Depressed skin surface point at the anterior-superior iliac spine, located by palpating proximally on the midline of the anterior thigh surface until the anterior prominence of the iliac spine is reached
Posterior Superior Iliac Spine (ASIS)	Depressed skin surface point located by palpating posteriorly along the margin of the iliac spine until the most posterior prominence is located, adjacent to the sacrum

Table E3  
Definitions of Extremity Landmarks Digitized in the Hard Seat

Landmark	Definition
Acromion	Undepressed skin surface point obtained by palpating the most anterior–superior portion of the lateral margin of the acromial process of the scapula
Lateral Humeral Epicondyle	Undepressed skin surface point at the most lateral aspect of the humeral condyle (near elbow)
Medial Humeral Epicondyle	Undepressed skin surface point at the most medial aspect of the humeral condyle (near elbow)
Ulnar Styloid	A point on the surface of the skin obtained by palpating the most distal margin of the styloid process of the ulna
Radial Styloid Process	A point on the surface of the skin obtained by palpating the most distal margin of the styloid process of the radius
Lateral Femoral Condyle	Undepressed skin surface point at the most lateral aspect of the lateral femoral condyle.
Medial Femoral Condyle	Undepressed skin surface point at the most lateral aspect of the medial femoral condyle
Suprapatella	Undepressed skin surface point at the most proximal aspect of the sagittal midline of the patella
Infrapatella	Undepressed skin surface point at the most distal aspect of the sagittal midline of the patella
Lateral Malleolus	Undepressed skin surface point at the most lateral aspect of the malleolus of the fibula (outer ankle protrusion)
Medial Malleolus	Undepressed skin surface point at the most medial aspect of the malleolus of the tibia (outer ankle protrusion)
Lateral Ball of Foot	Point on the lateral aspect of the foot medial to the fifth metatarsal-phalangeal joint
Medial Ball of Foot	Point on the medial aspect of the foot medial to the first metatarsal-phalangeal joint
Heel (Pternion)	The most posterior point on the heel
Toe (Longest Tibiale)	

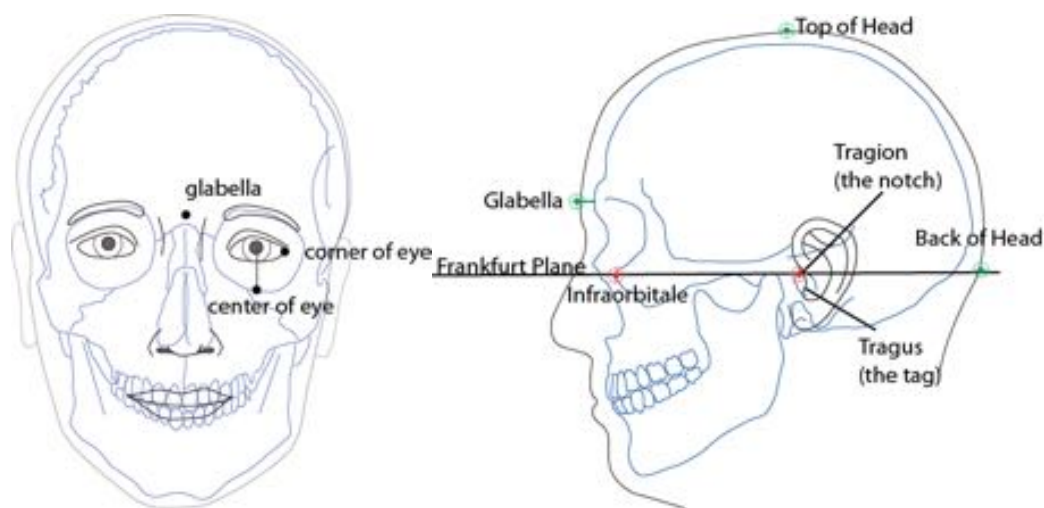


Figure E2. Illustration of head landmarks.



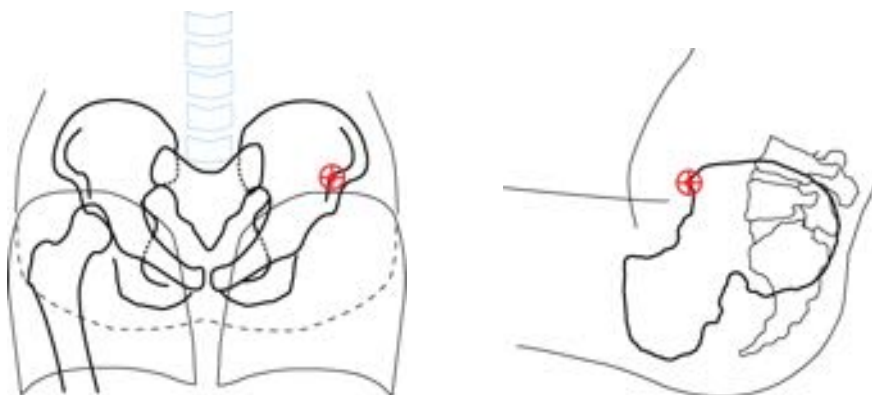


Figure E3. Illustration of ASIS landmark.

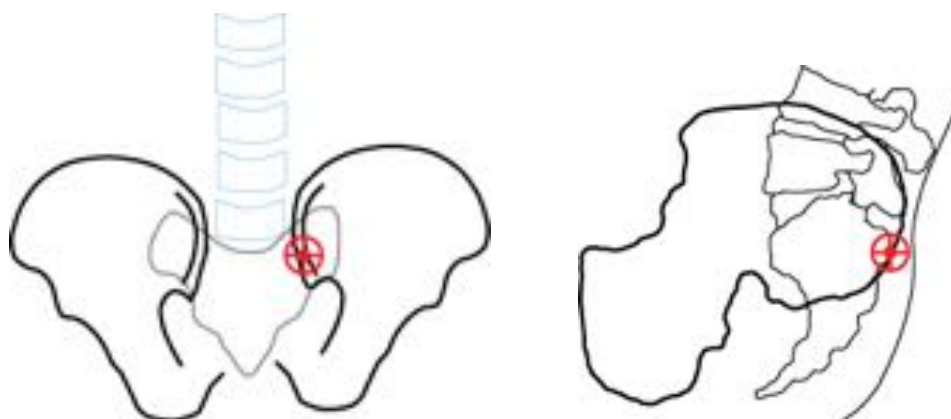


Figure E4. Illustration of PSIS landmark.

### Joint Centers in Hard Seat

The upper neck joint corresponds anatomically to the atlanto-occipital joint. Figure E5 shows the technique for calculating the location of the upper neck joint from the infraorbitale and trasion landmarks. In the sagittal plane, the upper neck joint center is located by rotating a vector from trasion to infraorbitale downward through 117 degrees. The vector length is 31 percent of the measured sagittal plane distance from trasion to infraorbitale. The lateral position for the upper neck joint was set at the sagittal midline of the head using the lateral coordinate of the digitized glabella.

The lower neck joint corresponds anatomically to the C7/T1 joint. The location of this joint is

calculated using the C7 and suprasternale surface landmarks, as shown in Figure E5. The vector from C7 to suprasternale is rotated upward 8 degrees and scaled to have a length equal to 55 percent of the measured sagittal-plane distance from C7 to suprasternale.

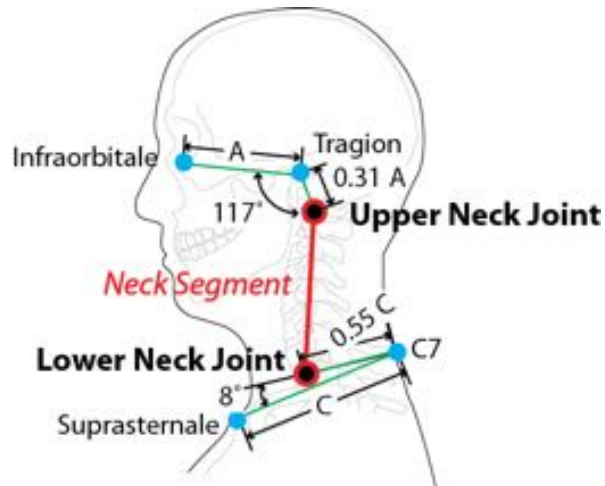


Figure E5. Calculation method for upper and lower neck joints.

The upper lumbar joint corresponds anatomically to the T12/L1 joint. With the soldier sitting in the reference hard seat, the locations of suprasternale, C7, T8, and T12 are recorded. The data from T8 and T12 are used to calculate the location of the upper lumbar joint as shown in Figure E6.

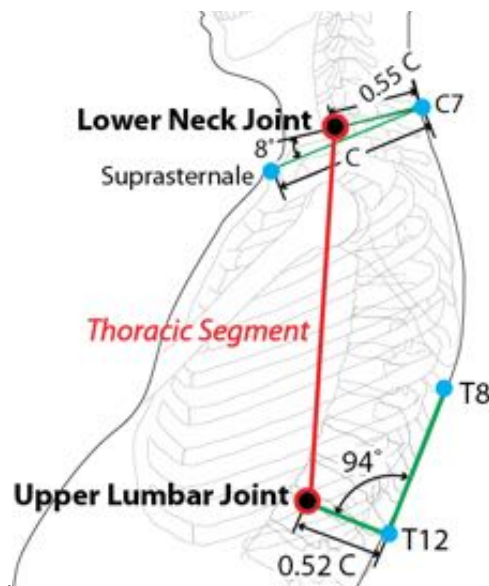


Figure E6. Calculation method for lower neck and upper lumbar joints.

The hip joint and lower lumbar joint locations are calculated using the two anterior-superior iliac spine (ASIS) landmarks and the two posterior-superior iliac spine (PSIS) landmarks. The hip joint locations are calculated individually, then averaged in the XZ plane to obtain a mean hip

joint location for use in calculating pelvis segment orientation (pelvis angle). The lower lumbar and hip joint locations are calculated in a pelvis-centered coordinate system, which is then transformed to the desired global coordinate system. The Y axis is defined by the vector connecting the left and right ASIS. The X axis is perpendicular to this line and points from the midpoint of the two ASIS to the midpoint of the two PSIS in the sagittal plane. The Z axis is mutually perpendicular to the X and Y axes. Note that the coordinate system is based on points on the bone, rather than surface landmarks with a flesh margins at the ASIS of 5 mm. An examination of the hardseat data showed that the PSIS landmark had been placed too superior on the ilia when compared to the PSIS and L5 for some subjects. In those cases, the PSIS points were moved down 50 mm below L5 along the seat back angle to match the average PSIS-L5 geometry found in other UMTRI studies.

Figure E7 illustrates how the locations of the hip and lower lumbar (L5/S1) joints were calculated in the pelvis coordinate system using vectors scaled with reference to pelvis dimensions defined by the bone landmark locations. The scaling factors are in Table E4. The reference dimensions were pelvis width (distance between right ASIS to left ASIS) and pelvis depth (distance between the mid point between the two ASIS points and the midpoint between the two PSIS points). These were measured represent on-bone dimensions (after the flesh margins were subtracted) and are shown in Figure E8.

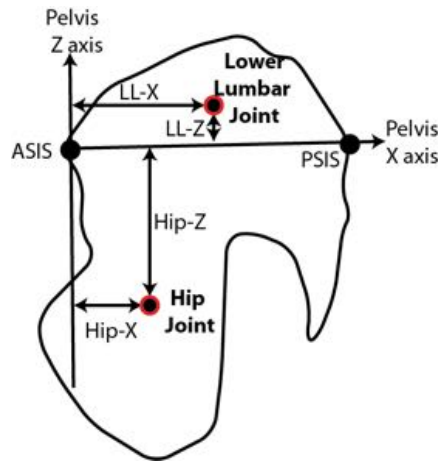


Figure E7. Illustration of the hip and lower lumbar joints in the XZ plane of the pelvis coordinate system (not to scale).

Table E4  
Joint Locations as a Function of Pelvis Depth and Width (Bispinous Breadth)

Joint	Axis	Function of Pelvis	Female		Male	
			Intercept	Slope	Intercept	Slope
Hip Joint Center	Hip-X	Depth	-13.6	0.3822	-11.1	0.3686
	Hip-Y	Width	-54.5	-0.1439	-56.8	-0.1372
	Hip-Z	Depth	-70.7	-0.0512	-74.3	-0.0606
Lower Lumbar Joint Center	LL-X	Depth	-42.8	0.8640	-51.6	0.8693
	LL-Y	Midline				
	LL-Z	Depth	4.6	0.0686	-2.6	0.1280

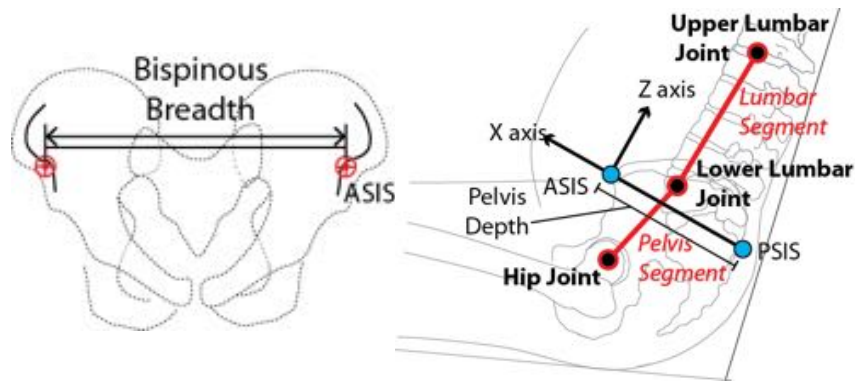


Figure E8. Illustration of dimensions used for scaling pelvis

The mean distance between the two ASIS points (pelvis width) calculated from the digitized ASIS points was 12.5 mm smaller than the mean bispinous breadth measured using anthropometers (bispinous breadth). Therefore the left and right ASIS landmarks were moved 6.25 mm laterally along the pelvis Y axis on each soldier.

The landmark and joint centers from the hard seat were used to locate the joint centers in the vehicle mockups in which not all of the landmarks were accessible. Figure E9 shows the landmarks, segments and joints relationships from the hard seat saved for use in the vehicle mockups.

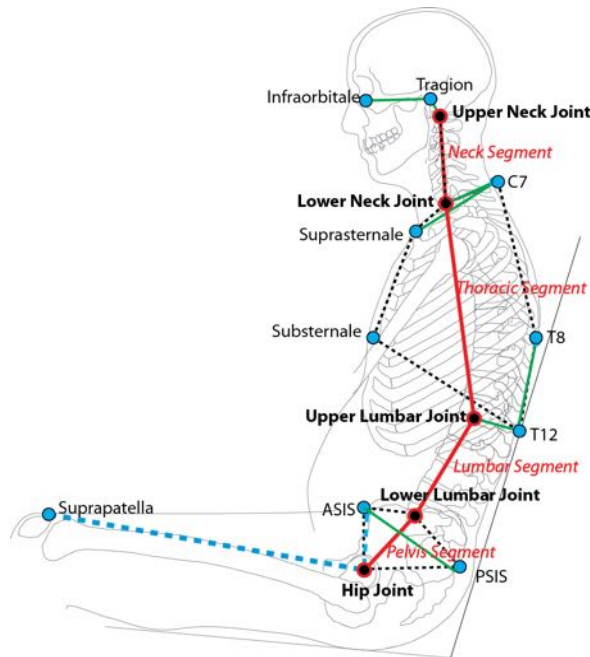


Figure E9. Creating a spine model for each soldier using landmarks digitized in the hard seat. Calculation methods for locating spine joints relative to digitized landmarks and setting up rigid body and fixed relationships between landmarks and joints (dashed lines)

## VEHICLE MOCKUP

### ACU

The upper and lower neck joints were located using the same digitized landmarks and methods as in the hard seat. The upper lumbar joint was considered part of the thorax rigid body, and located by using the geometry of the C7, suprasternale and substernale from the hard seat. Figure E10 shows the landmarks and linkage.

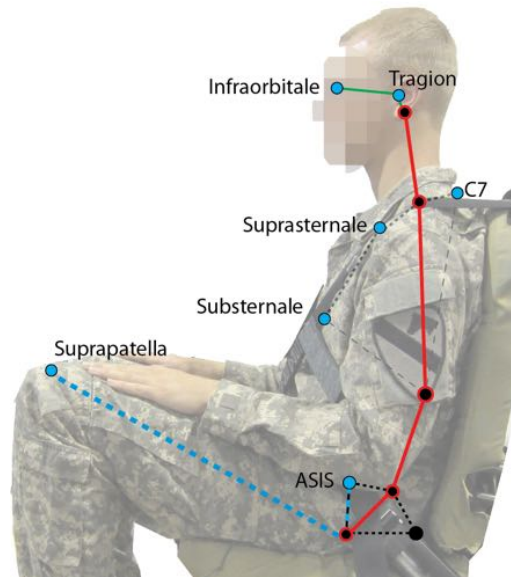


Figure E10. Soldier in ACU with the accessible landmarks (blue) used to locate joints and inaccessible landmarks (black).

In the vehicle seat the PSIS points were not accessible to the investigator therefore the lower lumbar (L5/S1) joint was located using a method similar to the one used by Bush and Gutowski 2003. The leg length (knee at suprapatella to hip joint) and the distance from the hips to the ASIS landmarks (Figure E11), which were measured in the hard seat, were used to solve for the left and right hip locations, whose relationship to the ASIS landmarks were used to solve for the PSIS landmarks and lower lumbar joint. Figure E11 illustrates the pelvis and leg, and Figure E12 illustrates the calculations used for locating the hip joint.

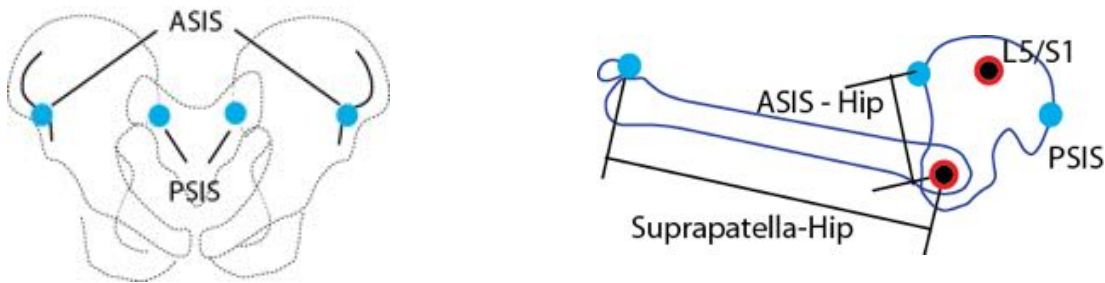


Figure E11. Fixed lengths calculated from knee and pelvis points recorded in the hard seat used to estimate hip location.



Figure E12. Digitizing knee and ASIS (in different postures) in vehicle seat and then using the knee-hip length and ASIS-hip length to calculate the hip joint location (left) and then using the ASIS and hip joint to calculate the lower lumbar joint and PSIS locations (right)

As illustrated in Figure E13, the ASIS bone location was found by applying a 5 mm flesh margin at a  $32^\circ$  angle to the digitized ASIS points (the mean orientation of the estimated bone ASIS-PSIS vector). A vector with a length equal to the hip-ASIS distance measured in the hard seat and perpendicular to the pelvis Y axis was constructed at point along the pelvis Y axis at the same Hip-Y distance from the midline as that for the soldier value in the hard seat. The point along the arc created by rotating the vector around the pelvis Y axis whose distance from the knee landmark was equal to the leg length in the hard seat, was the calculated hip joint location.

The lower lumbar joint and PSIS landmarks from the hard seat pelvis geometry were fitted to the vehicle seat with a least squares alignment between the ASISs and hip joints, now common points between the two seats.

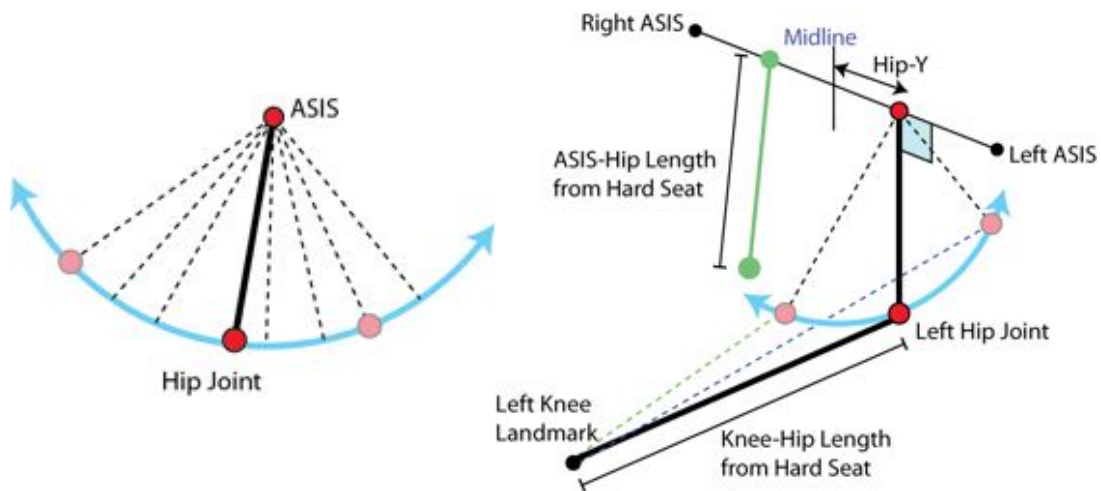


Figure E13. Method for locating one hip joint in vehicle mockup using the digitized ASIS and knee point landmarks with the geometry from hard seat from side (left) and oblique (right) viewpoints.



## PPE

When the soldiers were in PPE, the sternum and ASIS landmarks were not accessible for measurement. Therefore additional information from the hard seat spine linkage and from the seat geometry was used to fit the spine to the landmarks available.

### *Lower Neck Joint*

The points on the soldier's head needed to calculate the upper neck joint and C7 were accessible, but the suprasternale was not. The methods used to locate the lower neck joint are as follows. First a triangle was constructed in the sagittal plane at the soldier's midline. Two of the triangle lengths were set to the values from the hard seat: the length of neck segment and the distance from C7 to lower neck joint. The third side was set to a length from the trial: the distance from the C7 digitized landmark to the calculated upper neck joint location. The law of cosines was then used to solve for the included angle at C7. The vector from C7 to the upper neck joint was then scaled to the C7 to lower neck joint distance from the hard seat and rotated the included angle. Figure E14 illustrates this process.

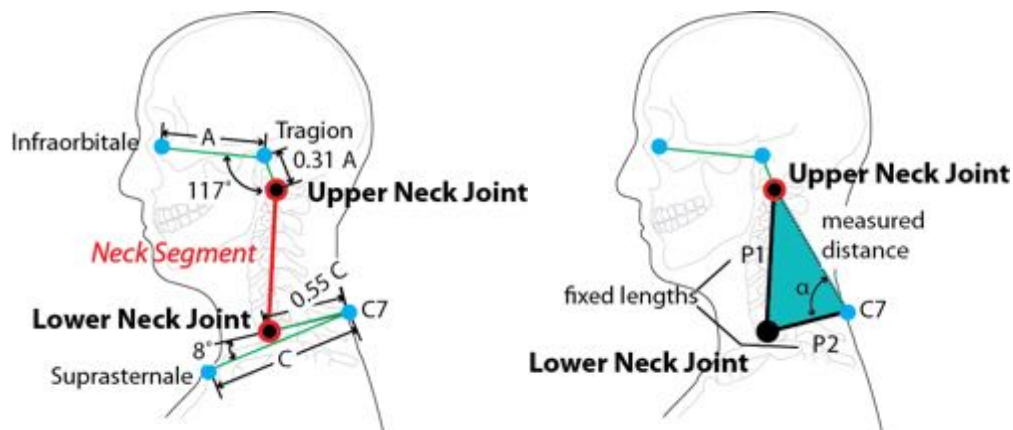


Figure E14. Using the fixed length of the neck segment and distance from C7 to lower neck joint to calculate the location of the lower neck joint using the Law of Cosines when only the head and C7 landmarks were available due to PPE covering the sternum.

The ASIS landmarks were not accessible with PPE therefore the pelvis Y axis could not be located using the same methods as in the uniform trials. Instead, a vector was constructed running parallel to the soldier's sagittal plane and located laterally relative the soldier's midline at the hip position (Hip-Y) measured in the hard seat. The vertical location of the vector was set relative to the seat H-point. The vertical offset of soldier's hip height above seat H-point (J826) when wearing ACU in the same vehicle condition was used to locate the vector above H-point. The hip was located at the point along the vector whose distance to the accessible knee point was equal to the leg length measured in the hard seat.

The upper and lower lumbar joints were located by taking the spine linkage for a soldier from the hard seat and overlaying it on the vehicle seat mockup so that the hip joints were aligned, and then rotating the entire linkage around the hip joint and included angles at the upper and lower lumbar joints, while keeping segment lengths constant, until the lower neck joint of the hard seat

linkage matched the location of that in the vehicle seat. The ASIS and PSIS landmarks from the hard seat pelvis geometry were fitted to the vehicle seat with a least squares alignment between the lower lumbar joint and hip joints, now common points between the two seats. Figure E15 illustrates the spine fitting method for conditions with PPE.

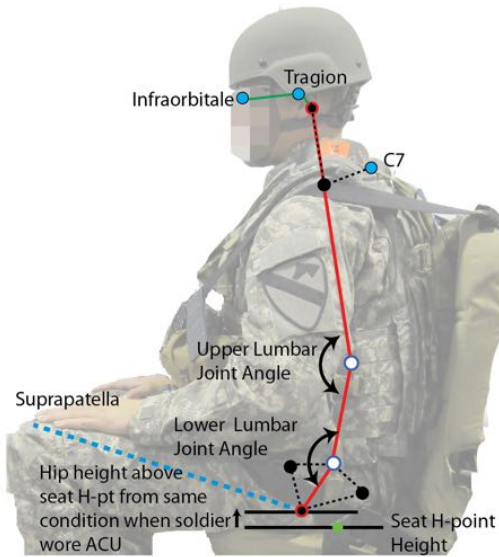


Figure E15. Fitting a soldier's hard seat spine model to the landmarks digitized in PPE conditions in which the ASIS landmarks and sternum were not accessible.



UNCLASSIFIED